CLEAN WATER WATER POLLUTION CONTROL RESEARCH SERIES • 1606 DLL 09/70

# DISPERSION IN HETEROGENEOUS NONUNIFORM ANISOTROPIC POROUS MEDIA

ENVIRONMENTAL PROTECTION AGENCY • WATER QUALITY OFFICE

## WATER POLLUTION CONTROL RESEARCH SERIES

The Water Pollution Control Research Series describes the results and progress in the control and abatement of pollution of our Nation's waters. They provide a central source of information on the research, development, and demonstration activities of the Water Quality Office, Environmental Protection Agency, through inhouse research and grants and contracts with Federal, State, and local agencies, research institutions, and industrial organizations.

Inquiries pertaining to the Water Pollution Control Research Reports should be directed to the Head, Project Reports System, Office of Research and Development, Water Quality Office, Environmental Protection Agency, Washington, D.C. 20242.

# DISPERSION IN HETEROGENEOUS NONUNIFORM ANISOTROPIC POROUS MEDIA

by

Robert A. Greenkorn

School of Chemical Engineering
Purdue University
Lafayette, Indiana 47907

for the

WATER QUALITY OFFICE

ENVIRONMENTAL PROTECTION AGENCY

Grant No. 16060 DLL (Formerly WP-101048-03)

September 1970

For sale by the Superintendent of Documents, U.S. Government Printing Office, Washington, D.C. 20402 - Price $1

## EPA Review Notice

This report has been reviewed by the Water Quality Office, EPA, and approved for publication. Approval does not signify that the contents necessarily reflect the views and policies of the Environmental Protection Agency, nor does mention of trade names or commercial products constitute endorsement or recommendation for use.

## ABSTRACT

The objective of this project is to study the theory and measurement of dispersion during miscible flow in heterogeneous nonuniform anisotropic porous media. An understanding of the dispersion phenomenon is necessary to predict flow of miscible fluids in non-homogeneous porous media. A significant literature review of dispersion in non-homogeneous porous media was accomplished. The continuum and statistical theories of flow in porous media were studied. A series of experiments in models of unconsolidated porous media were run to study the effects of heterogeneity, nonuniformity, and anisotropy on dispersion.

The non-homogeneities are defined in relation to permeability of the media and dispersion coefficients are correlated with respect to permeability. Tracer output curves from models were interpreted for dispersion. Dispersion changes significantly with permeability. When models of different permeability are connected, the dispersive effect is not reciprocal. Dispersion changes significantly with nonuniformity. Likewise there is a significant effect when models of different nonuniformity are interconnected (second-order heterogeneity). Anisotropy was included in two kinds of models (linear and radial) by packing alternate layers of beads causing flow through these layers at different angles. The usual dispersion model is not adequate for "block box" prediction of the tracer output curve for data on anisotropic shperes.

The results have immediate practical applicates, especially in tracing of contaminents in surface and subsurface flow such as movement of pesticides, fertilizers, acid mine drainage, feed-lot waste, etc. through the soil.



This report was submitted in fulfillment of project 16060DLL under the partial sponsorship of the Federal Water Pollution Control Administration.

Key words - Heterogeneous, nonuniform, anisotropic, porous media, dispersion, permeability.

CONTENTS

| | PAGE |
|---|---|
| Conclusions | vi |
| Recommendations | vii |
| Introduction | 1 |
| Theory | 10 |
| Dispersion During Flow in Linear Heterogeneous Porous Media | 18 |
| Dispersion During Flow in Nonuniform, Heterogeneous Porous Media | 32 |
| An Exploratory Study of Permeability and Dispersion Phenomena in Anisotropic Porous Media | 51 |
| Permeability and Dispersion During Flow in Linear Heterogeneous Anisotropic Porous Media | 61 |
| Appendices | |
| 1. Dispersion in Heterogeneous Nonuniform Anisotropic Porous Media | 78 |
| 2. On Dispersion in Laminar Flow Through Porous Media | 81 |
| 3. A Statistical Model of a Porous Medium with Nonuniform Pores | 82 |

FIGURES


| | | PAGE |
|---|---|---|
| 1 | DISPERSION AND FLOW | 2 |
| 2 | OBSERVED PERMEABILITY FOR UNIFORM MEDIA | 4 |
| 3 | OBSERVED PERNEABILITY FOR NONUNIFORM MEDIA | 5 |
| 4 | DESCRIPTION OF MODEL | 19 |
| 5 | DIAGRAM OF EQUIPMENT | 21 |
| 6 | k vs $d_{50}$ | 24 |
| 7 | DISPERSION COEFFICIENT VERSUS VELOCITY | 28 |
| 8 | $D/\nu$ vs $R_k$ | 30 |
| 9 | PLEXIGLAS MODEL -- SINGLE TUBE | 33 |
| 10 | EQUIPMENT SET-UP | 36 |
| 11 | SIZE DISTRIBUTION OF BEADS USED IN PACKING MODELS | 37 |
| 12 | DISPERSION COEFFICIENT VERSUS VELOCITY (SIX NON-UNIFORM MODELS) | 43 |
| 13 | DISPERSION COEFFICIENTS VERSUS VELOCITY (FIRST AND SECOND ORDER HETEROGENEITY) | 44,45,46 |
| 14 | $D/\nu$ vs $R_k$ (HOMOGENEOUS) | 47 |
| 15 | $D/\nu$ vs $R_k$ (HETEROGENEOUS) | 48 |
| 16 | D vs $\frac{v}{k}$ FOR VARIOUS S | 50 |
| 17 | MODEL SKETCH (DOUBLE FIGURE) | 52 |
| 18 | SKETCH OF APPARATUS | 54 |
| 19 | $\frac{1}{\sqrt{k}}$ vs angle | 57 |
| 20 | $1/\sqrt{D}$ vs angle | 60 |
| 21 | LENTH APPARATUS CORED AT 45° INTERVALS | 62 |
| 22 | DESCRIPTION OF MODELS | 63 |
| 23 | EQUIPMENT DIAGRAM | 65 |

| | | PAGE |
|---|---|---|
| 24 | BREAKTHROUGH CURVE | 66 |
| 25 | AVERAGE PERMEABILITY VERSUS FLOW RATE | 67 |
| 26 | $\sqrt{k}$ vs ANGLE | 69 |
| 27 | FLOW PATTERN IN MODEL | 72 |
| 28 | $\sqrt{D}$ vs ANGLE | 74 |

## TABLES


| No. | | PAGE |
|---|---|---|
| 1 | Model Properties | 23 |
| 2 | Velocity and Dispersion Coefficients | 26 |
| 3 | Porosities and Slopes of Bead Size Distribution | 38 |
| 4 | Permeability of Models | 40 |
| 5 | Permeability of Composite Models | 41 |
| 6 | Permeability of Anisotropic Model | 55 |
| 7 | Dispersion Coefficients | 59 |
| 8 | Dispersion Coefficients | 70 |
| 9 | Ratio of Longitudinal to Transverse Dispersion Coefficients | 79 |

## CONCLUSIONS

1. There is a significant effect on dispersion due to difference in average particle size or average permeability.

2. The exponent of the relation $D = a\ v^n$ is dependent upon heterogeneity.

3. It appears there is a difference in overall dispersion through a heterogeneous system depending on the arrangement of heterogeneities. (That is, permeabilities cannot be "lumped" into one average).

4. When determing average permeability of glass spheres based on bead diameter, a valve of d between $d_{10}$ and $d_{20}$ should be used.

5. There is a significant effect of nonuniformity on the dispersion coefficient even though the distributions have the same average permeability.

6. The parameter "a" in the expression $D = a\ v^n$ is dependent on the nonuniformity of the system (i.e. the slope of the log permeability distribution.)

7. Permeability in heterogeneous anisotropic porous media is dependent on the direction of flow.

8. Dispersion in anisotropic porous media is dependent on the direction of flow.

9. Both permeability and dispersion in 2 d porous media exhibit tensorial properties in that $1/\sqrt{k}$ and $1/\sqrt{D}$ versus angle plot as ellipses.

10. Both permeability and dispersion in 1-d anisotropic porous media exhibit tensorial properties in that $\sqrt{k}$ and $\sqrt{D}$ versus angle plot as ellipses.

11. We were unable to prove experimentally whether the permeability and dispersion tensors are symmetric.

12. At low velocity, the major directions of the permeability tensor and dispersion tensor are the same but as velocity increases the dispersion becomes a circle (i.e. principal values the same.) If one extrapolates the comparison to high flow rate, the major directions of the two tensors become orthoganol. The low velocity behavior (principal directions parallel) was observed in 1-d anisotropic models and the relation between relative valves of dispersion and velocity extrapolated to high flow velocities. The high velocity behavior (principle directions orthoganal) was observed in an exploratory 2-d study.

13. The "diffusion form" of the dispersion equation cannot be used for predicting concentration breakout in heterogeneous anisotropic porous media.

## RECOMMENDATIONS

1. Data in consolidated material media should be obtained.

2. The data should be used to develop a correlation - probably of the form

$$\frac{D_L}{D_T} = \frac{\lambda + 2\mu}{\lambda}$$

   where $\lambda$ and $\mu$ are determined from nonuniformity data, and $\lambda$ and $\mu$ are made dependent on angle and velocity.

3. More realistic models, such as the telegraph equation, where the effects of the media are distributed, should be studied both analytically and numerically.

4. A useable scheme for predicting flow in real media using the above should be developed.

## NOMENCLATURE

| Symbol | Explanation |
|---|---|
| $a$ | A proportionality constant |
| $A$ | Cross-sectional area of the porous medium |
| $b_0$, $b_1$, .. | Coefficients in regression equation |
| $C$ | Concentration of tracer |
| $C_0$ | Inlet tracer concentration |
| $\underline{C}$ | Dimensionless concentration, $C/C_0$ |
| $C'$ | Proportionality constant |
| $d$ | Parameter reflecting directional effect due to method of packing the porous medium |
| $d_{10}$ | Effective particle diameter used in permeability studies |
| $d_{50}$ | Average particle diameter |
| $d_{84}$, $d_{16}$ | Particle diameter of the 84% and 16% cumulative fractions |
| $D$ | Dispersion coefficient |
| $g$ | Gravitational constant |
| $h_1$, $h_2$ | Fluid heights in manometer tube |
| $k$ | Permeability |
| $K$ | Constant in Darcy's Law, dependent on properties of fluid and porous medium |
| $L$ | Length of porous medium |
| $n$ | Constant used to designate value of exponent |
| $n$ | Unit vector normal to flow |
| $p_L$, $p_0$ | Fluid pressures at top and bottom of porous medium |
| $P$ | Combination of static pressure and force of gravity |
| $Pe$ | Peclet number, $vL/D$ |
| $Q$ | Volumetric flow rate |

| | |
|---|---|
| $R_{d[10]}$ | Reynolds number based on $d_{10}$ |
| $R_{d[50]}$ | Reynolds number based on $d_{50}$ |
| Re | Reynolds number based on $\delta$ and u |
| $R_k$ | Reynolds number based on permeability |
| S | Slope of log-normal line describing the distribution of particle diameters |
| t | Time |
| v | Seepage velocity, Darcy Law velocity |
| v | Frontal velocity, $u/\phi$ |
| V | Volume of fluid displaced |
| $V_0$ | Value of one pore volume of a porous medium |
| V' | Volume of empty plexiglass tube |
| z | Vertical distance |
| $\alpha$ | Constant dependent on the pore system, coordinate axes |
| $\beta$ | Proportionality constant, coordinate axes |
| $\gamma$ | Coordinate axes |
| $\Gamma$ | Proportionality constant |
| $\delta$ | A diameter (average bead, pore, etc.) associated with the porous medium |
| $\eta$ | D/vz |
| $\theta$ | Number of pore volumes of a fluid displaced, $V/V_0$ |
| $\lambda_1$ | Major elliptical axes |
| $\lambda_2$ | Minor elliptical axes |
| $\mu$ | Fluid viscosity |
| $\nu$ | Kinematic viscosity of fluid |
| $\xi$ | vt/z |
| $\rho$ | Fluid density |

| | |
|---|---|
| $\phi$ | Porosity of porous medium |
| $\psi$ | Proportionality constant |
| $\Omega$ | Proportionality constant |

# INTRODUCTION

This report presents the results of a study of dispersion during flow in nonhomogeneous porous media. The theories of dispersion were reviewed, a statistical theory derived, and an experimental program of measuring dispersion completed. Since most real media are non-homogeneous, that is they are heterogeneous, nonuniform, and anisotropic it is necessary to understand the effects of these non-homogeneities when attempting to predict dispersion in such systems.

We start with definitions of dispersion and the non-homogeneities, heterogeneity, nonuniformity and anisotropy. After a brief literature review we derive the mathematical model we will use to interpret the tracer experiments, a brief discussion of certain statistical terms, the experimental techniques, and the results and interpretation of these results for a series of four experiments. The conclusion and recommendations presented earlier are from this interpretation.

Definitions. Dispersion, as considered here, is the macroscopic mixing caused by uneven cocurrent laminar flow in fixed beds of real media. The behavior of a traced fluid in one dimension is indicated schematically in Figure 1a with some boundary conditions. We imagine fluid flowing according to Darcy's Law

$$v_x = -\frac{k}{\mu}\frac{dp}{dx} \tag{1}$$

and further imagine we can mark a line of particles, the X's in the figure. As a result of velocity variation in path selection, this line spreads as flow progresses. If we plot the concentration of marked particles C (normalized by the input concentration $C_o$) versus throughput measured in multiples of total pore volume, we characteristically obtain a breakthrough curve as shown in Figure 1b. We usually apply a diffusion model to dispersion with such velocities such that there is no significant diffusion effect, so

$$\frac{\partial C}{\partial t} = D\frac{\partial^2 C}{\partial X^2} - v_x\frac{\partial C}{\partial x} \tag{2}$$

where D is called the dispersion coefficient. The approximate solution of this equation, with boundary conditions of Figure 1 is

$$\frac{C}{C_o} = \frac{1}{2}\left[1 - \mathrm{erf}\left\{\frac{L-v_x t}{2\sqrt{Dt}}\right\}\right] \tag{3}$$

where L is the length of the media. At a pore volume throughput equal to 1 for the idealized situation of Figure 1, the slope of this breakout curve gives the D in equation (2) which is given by

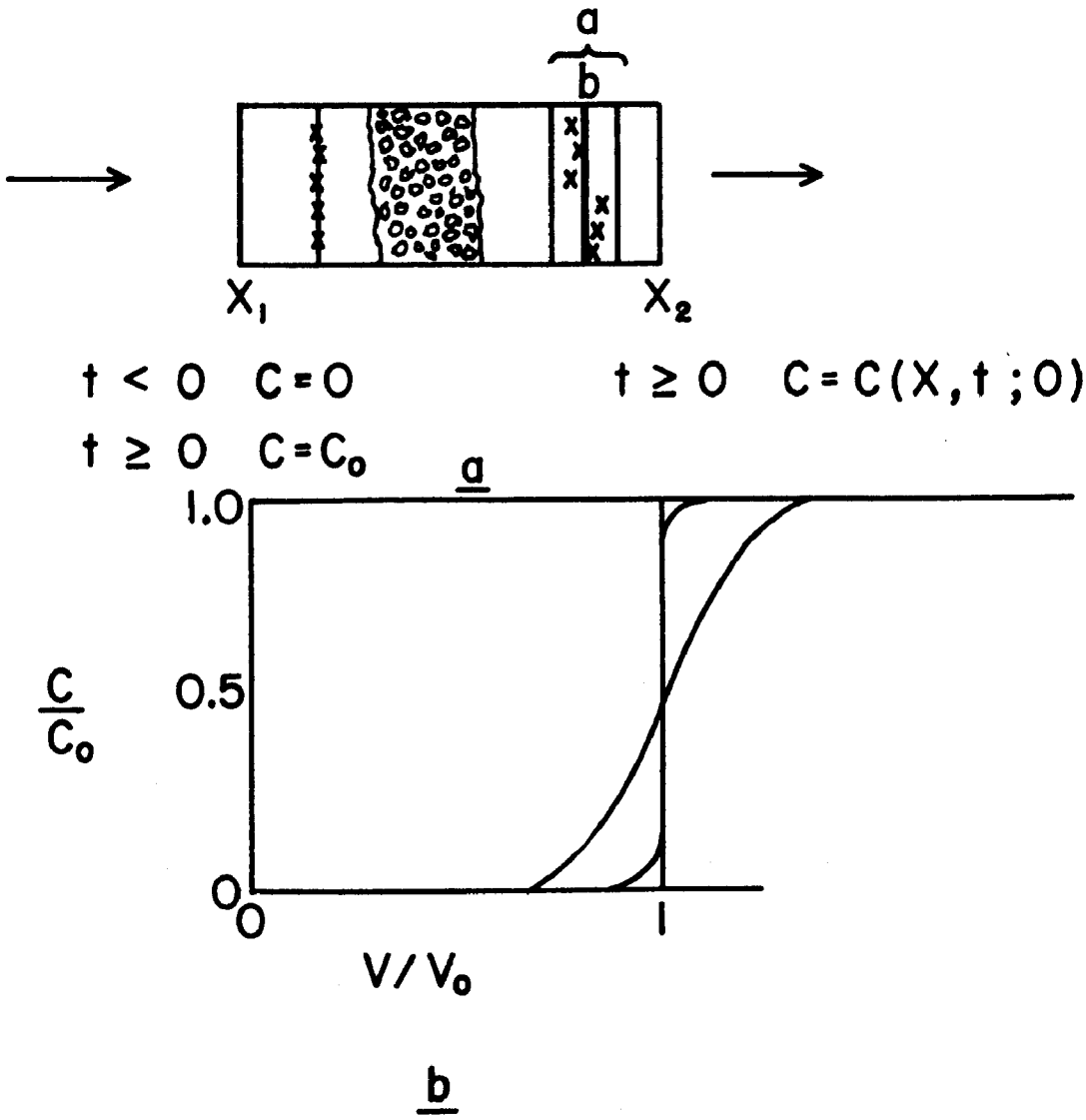


Figure 1 - Dispersion and Flow

$$D = \frac{1}{4\pi} \left. \frac{Lv_x}{\frac{\partial\, C/C_o}{\partial\, V/V_o}} \right|_{V/V_o = 1} \tag{4}$$

Thus the slope of this curve is a rough measure of the dispersion taking place in flow through the medium.

We base our definitions of heterogeneity, nonuniformity and anisotropy on the probability density distribution of permeability of random macroscopic elemental volumes selected from the medium, the permeability being expressed by the one-dimensional form of Darcy's Law, Equation (1).

By a uniform medium we mean one in which probability density function for permeability is either a Dirac $\delta$-function or a linear combination of n-functions that satisfy the relation

$$f(k) = \sum_{i=1}^{N} \zeta_i \delta \tag{5}$$

where

$$\sum_{i=1}^{N} \zeta_i = 1 \tag{6}$$

Examples of this sort of behavior are shown in Figure 2.

By nonuniform we mean a medium in which the probability density function cannot be constructed with a finite number of weighted $\delta$-functions as shown in Figure 3.

By a heterogeneous medium, we mean one in which permeability distribution is at least bimodal. Figure 2a is homogeneous and uniform and Figure 3a is homogeneous and nonuniform. Figures 2b and 2c are heterogeneous and uniform, and Figures 3b and 3c are heterogeneous and nonuniform.

By anisotropy, we mean the permeability varies with direction in an elemental volume in the medium.

The probability density function for permeability is, in general, a function of location and orientation. We can describe this function with five independent variables: the rectangular coordinates $x_i$ ($i = 1, 2, 3$) for location and the angular coordinates $\theta$ and $\psi$ for orientation:

$$P(k \leq k \leq k_2) = \int_{k_1}^{k_2} f(x_i, \theta, \psi)\, dx_i\, d\theta\, d\psi \tag{7}$$

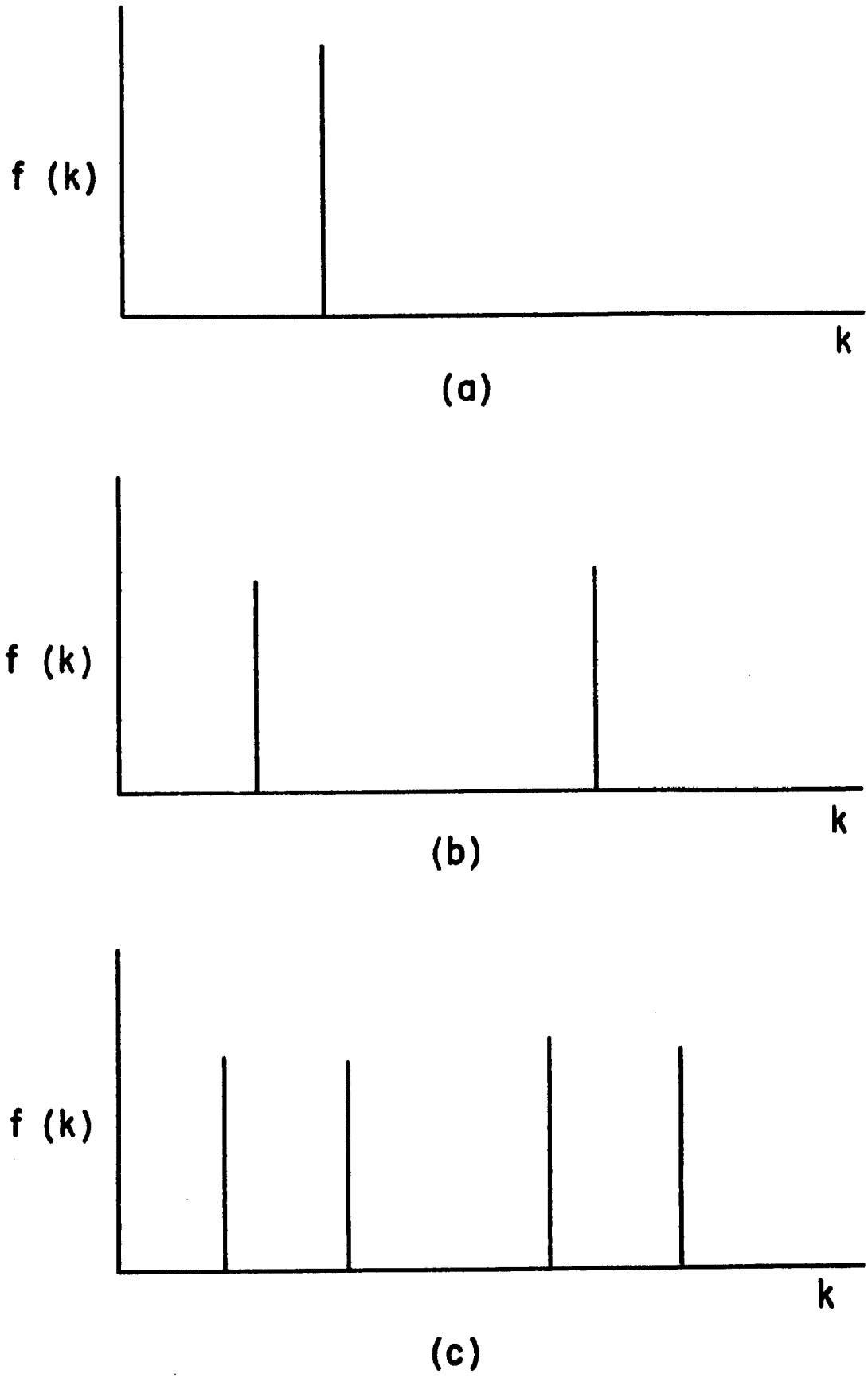


Figure 2 - Observed Permeability for Uniform Media

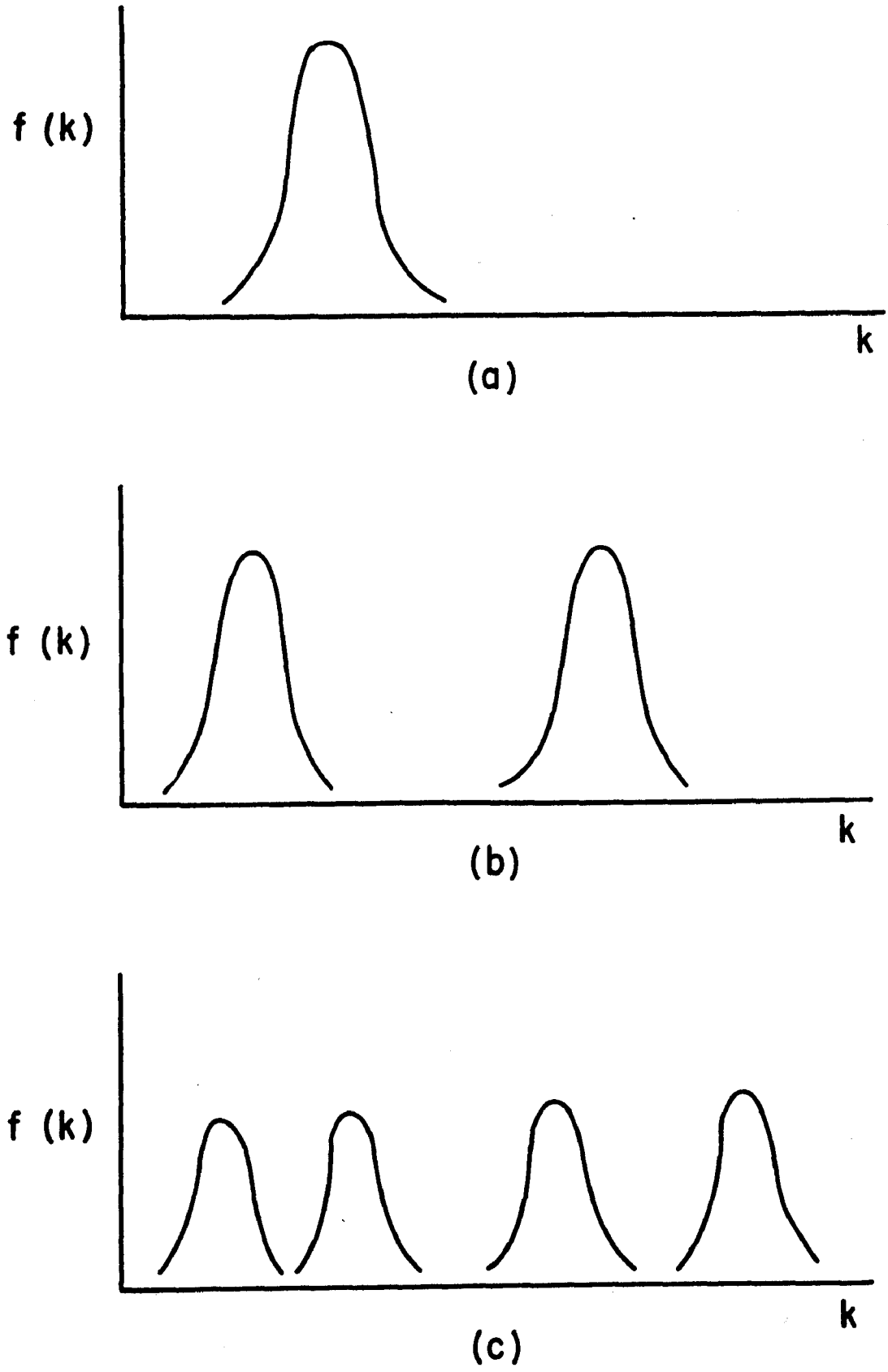


Figure 3 - Observed Permeability for Nonuniform Media

If the probability density distribution is independent of $\theta$ and $\psi$ the medium is isotropic; if the distribution is expressible by a finite linear combination of $\delta$-functions, the medium is uniform; if the distribution is monomodal, the medium is homogeneous; and if the variance of the distribution is not constant, the medium has second-order nonidealities. The second-order nonidealities may also be classified with respect to the probability density function for variance of the permeability distribution.

We have drawn the distributions in Figure 3 as if all have the same variance. We can also speak of second-order nonidealities where the variance of the permeability distribution depends on spatial location or orientation in the medium. If the variance of the distribution is not constant, the medium has second-order nonidealities. The second-order nonidealities may also be classified with respect to the probability distribution function for variance of the permeability distribution.

$$P(\mathrm{var} \leq \mathrm{var}\ k \leq \mathrm{var}_2) = \int_{\mathrm{var}_1}^{\mathrm{var}_2} g(x_i)\,dx_i \tag{7}$$

If this distribution cannot be expressed by a finite series of delta functions, the medium has a second-order nonuniformity and if this distribution is multimodal, the medium has a second-order heterogeneity. Obviously, we must consider larger elemental volumes when we are considering the variance distribution rather than the parent average distribution. These definitions could be extended to high orders, but it is not useful to do so at this point.

Literature. A knowledge of dispersion and the ability to predict dispersion is important in a broad variety of areas including: seepage of contaminants into the soil; reclamation of waste water; salt water intrusion into fresh water; movement of fluids in petroleum reservoirs; movement of fluids in packed towers and reactors; underground disposal of chemical, bacterial, and radioactive wastes; in ion exchange; filtration theory; movement of fluids in the lungs, capillaries, and other parts of living organisms; the making of paper; etc.

In the past fifteen years there has been a large amount of research directed at the problem of dispersion, mainly from three broad points of view: statistical modelling, continuum modelling, and experiment. The majority of the effort has been on modelling -- the experiments for the most part are directed at ideal media, that is, homogeneous, uniform and isotropic media.

Three review articles have appeared in the last few years which cover most of the literature and aspects of the problem. The comprehensive review by Perkins and Johnston[1] summarizes some of the mathematical treatments and discusses the effects of fluid and media properties.

The article of Chung and Wen[2] contains an extensive tabulation of experimental work, including such items as systems and range of variables studied. The more recent article of Greenkorn and Kessler[3] (This review was performed as part of this project -- a summary is attached as Appendix 1) examines dispersion in heterogeneous, nonuniform and isotropic porous media with emphasis on statistical and continuum theories which have been derived for the nonideal case.

Harleman, Melhorn, and Rumer[4] have studied to some degree the effect of heterogeneity as reflected by permeability change on dispersion in porous media. They took data on some ten different media of uniform size which had either spherical or angular shapes, and from these data developed a correlation for the dimensionless ratio of the longitudinal coefficient of dispersion to the kinetic viscosity as a function of the permeability Reynolds number. This correlation is used in a later paper by Shamir and Harleman[5] in which a specific type of heterogeneous media, that is, layered media, is studied. In this latter study they considered dispersion in flow perpendicular and parallel to layers. They determined the dispersion for the various layers from the correlation of the earlier paper of Harleman et al[4] and then calculated the resulting dispersion at the end of the column. In addition, they also took experimental data at various points along the column and showed that there was approximate agreement between the superposition of the various dispersion coefficients, the experimental data and the equivalent curve resulting from looking at the concentration output from the total length of the model.

The effect of direction on permeability, anisotropy, has been measured in a few instances and the theory of direction permeability has been worked out.

Scheidegger[6] has tested the theory on existing literature data. Greenkorn, Johnson, and Shellenberger[7] have shown the theory works on natural sandstones and they correlated various parts of the permeability tensor with measureable lithological characteristics such as grain size, grain orientation, and layering. To the authors' knowledge there are no measurements of dispersion in anisotropic media which have been interpreted as anisotropies. Shamir and Harleman[5] indicate it is conceivable to consider a layered medium as an anisotropie. However, they have done no calculations, nor have they attempted to measure dispersion in such media.

There is a vast amount of theoretical literature associated with the continuum theory of dispersion and the tensor representation of the dispersion coefficient[3]. However, this theory has not been utilized to interpret data from anisotropic porous media.

Various attempts have been made to correlate dispersion with the characteristics of porous media, but only moderate success has been achieved, probably because of the inherent difficulties in isolating

the effects of the various characteristics.[4] These characteristics can be best understood through a brief description of a porous medium. Perhaps the simplest description is: a porous medium is a solid with holes in it. But for mathematical purposes it is described as a solid containing a complex network of pore spaces or voids. Sheiddeger[8] classifies pore spaces into voids, capillaries, and pore spaces. In voids the walls have negligible effect on the hydrodynamical phenomena in their interior, while in capillaries the walls do have a significant effect. In pore spaces, the molecular structure of the fluid is a significant property. Voids can be classified further: extremely large voids are called "caverns," while extremely small ones are called "molecular interstices," the remainder being simply designated "voids." The pore space in the media used in this work fall into the void classification.

Pore spaces are also classified as to whether they are interconnected or non-interconnected. Fluid flow is possible only through interconnected pores, and this interconnected portion of the medium is called the effective pore space. Non-interconnected pores are called "dead-end pores."

Finally, the porous medium as a whole can be classified as consolidated or unconsolidated. A consolidated porous medium has a fixed structure, for example, limestone or sandstone. Unconsolidated porous media are beds made of sand, glass beads, catalyst pellets, etc., such as their effective pore space depends upon the packing procedure used in the construction of the bed. The porous media used in this work (plexiglas tubes packed with glass beads) are unconsolidated.

Permeability can be defined as a measure of the ease with which a fluid will flow through a porous medium -- the higher the permeability, the easier will be the flow. It is a statistical average of the fluid conductivities of all the flow channels in the medium, and normally considered a point property of the medium where a point is defined as a region over which Darcy's Law will hold. (A region large enough for volume averaging, see Whitaker[9]).

In all applications of Darcy's Law, whether it be in homogeneous, heterogeneous, or nonuniform porous media, it has been concluded that there is a critical seepage velocity above which the law is not valid. This critical velocity is characterized by a Reynold's number defined by

$$Re = \frac{\delta v \rho}{\mu} \tag{8}$$

where $\delta$ is the diameter associated with the porous media (average bead diameter, average pore diameter, etc.). However, investigations have been made since 1920 to determine the value of this critical Reynolds number, with the conclusion that it lies somewhere between 0.1 and 75. Sheidegger[8] explains this as due to the indeterminacy of the diameter $\delta$.

In porous media constructed of glass beads, the pore size distribution is related to the distribution of bead diameters. When a medium is packed with beads of various sizes, the small beads can rest in the interstices between the large beads. The size of the average pore space can thus be characterized by dimension smaller than the median bead size.[1]

Particle size distribution in naturally occurring, unconsolidated porous media often follows a log-normal distribution, that is, the particle size versus cumulative percent plots is merely a straight line on log probability paper. This is also often the case with commercially produced mixtures of glass beads. Raimondi, Gardner and Patrick[10] found that three mixtures of glass beads all had roughly the same permeability when their effective bead diameters crossed at approximately the bead diameter corresponding to the ten percent cumulative fraction. This effective diameter, $d_{10}$, was used for $\delta$ in calculating the Reynolds numbers for this work.

## THEORY

Dispersion coefficients are most often obtained by measuring the mixing of a trace element resulting from flow through the porous media for which the dispersion is to be estimated. Either a step input in tracer concentration or a rectangular input is utilized and the resulting breakthrough curve is analyzed with the dispersion model. When the traced solution displaces the untraced solution filling the voids of a porous medium, the concentration interface between these two solutions does not remain as a sharp plane; rather, as flow progresses, there is a gradual mixing of the traced and untraced fluid due to local velocity fluctuations. These continuous variations of velocities both in magnitude and direction throughout the tortuous path in the void space of the porous media cause mixing of the two fluids and a mixed region is formed between the traced and untraced solution. If one then collects the output of solution from such a porous media, a breakthrough curve such as is sketched in Figure 1b results, where the pore volume is the volume of the porous medium multiplied by its porosity. The problem is to describe the output tracer concentration as a function of time or pore volume. If the porous structure is assumed random a statistical model can be used to fit breakthrough curves such as Figure 1b.[11] The result for flow in the y direction as

$$C/C_o = \frac{1}{z\sqrt{\pi Dt}} \exp \left\{\frac{(L - v_x t)^2}{4Dt}\right\} \tag{9}$$

This is a solution of the diffusion equation with convection

$$\frac{\partial C}{\partial t} = D \frac{\partial^2 C}{\partial X^2} - v_x \frac{\partial C}{\partial x} \tag{10}$$

for an infinite media with a Δ-function input.

We adopt the diffusion model here but consider a step input and use the boundary conditions

$$\begin{aligned} C(0,t) &= C_o \quad ; \quad t \geq 0 \\ C(X,0) &= 0 \quad ; \quad x \geq 0 \\ C(\infty,t) &= 0 \quad ; \quad t \geq 0 \end{aligned} \tag{11}$$

The solution of Equation (10) with these boundary conditions is

$$C/C_o = \frac{1}{2} \left[\operatorname{erfc} \left\{\frac{1 - \zeta}{2\sqrt{\zeta\eta}}\right\} + \exp \left\{\frac{1}{\eta}\right\} \operatorname{erfc} \left\{\frac{1 + \zeta}{2\sqrt{\zeta\eta}}\right\}\right. \tag{12}$$

where erfc is the complementary error function, $\zeta = vt/x$ and $\eta = D/vs$, v is the Darcy velocity given by Equation (1).

Most often tracer data are interpreted with Equation (12). If $\eta$ is less than .0075, the second term may be ignored and the error will be less than 5%[12], where $\eta$ is the reciprocal of the Peclet number vL/D and therefore the Peclet number must be greater than 133 in order to drop the second term of Equation (12).

Equation (12) can be put into the form (with last term dropped)

$$C/C_o = \frac{1}{2}\left[1 - \mathrm{erf}\left\{\frac{1 - V/V_o}{2\sqrt{V/V_o\,\frac{D}{Lv_x}}}\right\}\right. \tag{13}$$

which shows that the theoretical breakthrough curve for a given medium is determined by the dimensionless Peclet number. The dispersion coefficient can be determined by taking the derivative of the breakthrough curve at the inflection point

$$D = \frac{1}{4\pi}\,\frac{Lv_x}{\left.\dfrac{\partial C/C_o}{\partial V/V_o}\right|_{V/V_o = 1}} \tag{14}$$

In using the above model we are assuming that all of the mixing is due to convective transport rather than molecular diffusion. Diffusion is not important where the Reynolds number $Re = Dv_x\rho/\mu$ is greater than $10^{-3}$.[13]

Correlation of Dispersion and Permeability. Harleman *et al*[4] have studied dispersion-permeability correlations in porous media. They correlate their data on the basis that permeability can be related to the average particle diameter by

$$k = C'd_{50}^2 \tag{15}$$

When we adopt the diffusion equation (10) and the solution (13) as a model for dispersion we have tacitly assumed calculation is directly proportional to pressure, since the fundamental equation of flow expresses flux as proportional to the gradient of a potential function. Since in Darcy's Law, equation (1), the flux is proportional to velocity we would expect the dispersion coefficient resulting from using equation (10), to be dependent on velocity. Indeed when dispersion data is investigated as a function of velocity the data follows an equation of the form:

$$D = \text{parameter (velocity)}^n \tag{16}$$

Scheidegger[8] points out when using equation (10), which is justified on statistical arguments, that there are two possible extremes for the form of the dispersion coefficient velocity dependence; the first directly proportional to velocity:

$$D = av \tag{17}$$

the second proportional to velocity squared

$$D = av^2 \tag{18}$$

Equation (17) represents the case where there is enough time for complete mixing of invading and original fluid in each pore. Equation (18) represents the case where mixing is not complete in each pore.

Relations such as Equations (16) (17) and (18) can be expressed as tensor equations and the "parameter" a becomes a fourth order tensor and the velocity dependence is represented by a dyadic product of velocity.[14] Usually in this form a linear velocity dependence is assumed and the tensor for anisotropic is reduced to a constant type of relation of a form.[15 16] (Reference 16 reports a theoretical study of the dispersion tensor referenced as part of this paper -- a summary is attached as Appendix 2).

$$D_y = \lambda\delta_{ij}v + 2\mu \frac{v_i v_j}{v} \tag{19}$$

The $\lambda$ and $\mu$ are related to the properties of the medium. For one-dimensional flow the dispersion coefficient in the direction of flow (the longitudinal coefficient) takes on the simplified form

$$D_{11} = (\lambda + 2\mu)v \tag{20}$$

which is of the form of Equation (17).

Harleman, et al[4] assume this form (Equation 17 or 20) to obtain their correlation expression from Equation (15).

$$\frac{D}{\nu} = B \frac{d_{50}v}{\nu} \tag{21}$$

and

$$\frac{D}{\nu} = \frac{B}{\sqrt{C'}} \frac{\sqrt{k}\ v}{\nu} \tag{22}$$

Poreh[17] has taken into account the possibility that mixing in the pores is not complete and he obtains constitutive type relation for the dispersion values of the form

$$\frac{D_{ij}}{D} = (\alpha_1 + \alpha_2 \frac{v^2 \ell^2}{D^2})\ \delta_{ij} + \alpha_3 \frac{\ell^2\ v_i v_j}{D^2} \tag{23}$$

which is of the form of Equation (18) for one dimensional flow.

Thus in general we would expect a combination of mechanisms in the pores depending on the velocity of flow and the properties of the media so an equation of the form of Equation (16) should represent one-dimensional experiments with the parameter a function of the media properties and the experiment dependent on velocity and media properties, since variation in pore size will cause different intersititial velocities. At very slow velocities one would expect $n \to 2$ and at relatively high velocities in a permeable media $n \to 1$.

Haring and Greenkorn[17] (This paper reports a theoretical study and was in part performed as part of this project -- a summary is attached as Appendix 3) have shown that a statistical model of a porous media with non-uniform pores predicts permeability is of the form

$$k = \phi \langle r \rangle^2 C g(\alpha,\beta) \qquad 23)$$

where $\phi$ is porosity $\langle r \rangle$ is the average pore radius, C is a numerical constant and g(a,B) is a function of the first and second moments of the pore radius distribution. We might expect the parameter C' in equation (15) to be a function of porosity and the nonuniformity of the pore size distribution. The average value to be used for comparison of data is not necessarily $d_{50}$ but the average value for the particles pore size distribution utilized. For most unconsolidated media, the distribution is skewed and a value of $d_{10}$ to $d_{20}$ must be used to obtain permeability.

Haring and Greenkorn show that the form of the dispersion coefficient in nonuniform media depends on both the values of the pore radius distribution and the pore length distribution as well as average pore length and velocities. We might expect the parameter of Equation (16) to be dependent on these distributions.

$$D = \tilde{c}g\ (\alpha,\beta)\quad f(a,b)\ \langle \ell \rangle\ vh(\ln a, b, \alpha, \beta, \langle \ell \rangle v) \tag{24}$$

In order to correlate data according to Equations (21) and (22) we must assume a uniform medium with complete mixing in the pores. With these assumptions

$$\langle r \rangle = j\ (\langle \ell \rangle) \equiv C' \langle \ell \rangle \tag{25}$$

and we can replace $\langle \ell \rangle$ in Equation (24) with $\langle r \rangle$. Combining with Equation (23) gives an equation of the form

$$D = \frac{\tilde{c}}{c' c^{1/2}} \sqrt{\frac{k}{\phi}}\ \frac{g(\alpha,B)}{\sqrt{g(\alpha,\beta)}}\ f(a,b)\ vh(\ln \{a,b,\alpha,\beta,\langle \ell \rangle\ v\}) \tag{26}$$

For uniform media $g(\alpha,\beta)$ and $t(a,b)$ are constants and $h = 1$ and

$$D = B \sqrt{\frac{k}{\phi}}\ v \tag{27}$$

or

$$\frac{D}{\nu} = \frac{B}{\sqrt{\phi}} \frac{\sqrt{k}\ v}{\nu} \tag{28}$$

which is of the form of Equation (22).

From the above we would expect if we correlate dispersion data versus permeability or grain size in the form of Equation (21) or (22) that there would be an exponent on the velocity different than 1 (but between 1 and 2) and that the porosity would be a function of the nonuniformity of the porous system. More generally we would expect to correlate

$$\frac{D}{\nu} = B\ Re_k^n \tag{29}$$

where B is a function of nonuniformity, n a function of velocity and nonuniformity.

A general form of Darcy's Law can be written

$$\underline{v} = \frac{\overline{\overline{k}}}{\mu} \underline{\nabla} p \tag{30}$$

where $k_{ij}$ is the permeability tensor. The fact that the permeability in an anisotropic porous medium has a tensorial nature leads to the following conclusions: (1) The pressure gradient and the seepage velocity in general are not parallel; (2) If the permeability tensor is symmetric, there are three orthogonal axes in space which are termed

the principal axes of the permeability tensor.

It is necessary to relate the components $k_{ij}$ of the permeability tensor to the actual measurements of the directional permeability. There are two separate cases to be considered here, which in the limit lead to the same result. The first is the case where the flow velocity is assumed parallel to the outward directed normal, (width/length of model is small) and the second case where the pressure gradient is assumed parallel to the outward directed normal n (width/length of model is large).

Consider cutting out of a porous medium a narrow tube parallel to the outward normal and measuring its permeability in the usual manner. In this case because this is a narrow pencil, the seepage velocity $v_n$ can be assumed parallel to the normal $\underline{n}$. The pressure drop along the tube, denoted by $p_n$, is then given by the following

$$p_n = \underline{n} \cdot \underline{\nabla} p = \mu[\underline{n} \cdot (\underline{\underline{k}}^{-1} \cdot n) v_n \tag{31}$$

Define a "directional permeability" $k'_N$ such that

$$k'_n = \frac{\mu v_n}{p_n} \tag{32}$$

Therefore

$$k'_n = \frac{1}{(n \cdot (\underline{\underline{k}}^{-1} \cdot \underline{n}))} \tag{33}$$

If the principal axes of the permeability tensor are chosen as coordinates and if the angle of n with the coordinate axes are called $\alpha$, $\beta$, and $\gamma$, the direction permeability $k'_N$, is given by

$$\frac{1}{k'_n} = \frac{\cos^2\alpha}{k_{11}} + \frac{\cos^2\beta}{k_{22}} + \frac{\cos^2\gamma}{k_{33}} \tag{34}$$

In two dimensions, therefore, if the square root of the directional permeability $\sqrt{k'_n}$ is plotted against the corresponding directions in an anisotropic porous medium, one obtains an ellipse. The two axes of this ellipse are in the direction of the principal axes of permeability and their length is equal to the square root of the principal values of the permeability tensor.

In the second case we choose a system in which the pressure drop is given by the boundary conditions, and we measure the component of velocity which is parallel to the pressure gradient. The directional

permeability is defined by Darcy's law from the given pressure and the velocity component parallel to it. Denoting the pressure gradient by $p_N$ in the direction of $\underline{n}$ and the velocity component parallel to $\underline{n}$ by $v_n$, then by similar derivation[6,7]

$$k''_n = k_{11} \cos^2\alpha + k_{22} \cos^2\beta + k_{33} \cos^2\gamma \tag{35}$$

Therefore, in the two-dimensional case, if the reciprocal of $\sqrt{k''_n}$ is plotted against the corresponding directions in an anisotropic porous medium, one obtains an ellipse. The axes of this ellipse are in the direction of the principal axes of permeability and their length is equal to 1 over the square root of the principal values of the permeability tensor.

Experimental data, then, are interpreted in one of the two forms, depending on which type experiment is performed. Equations (34) and (35) represent two different methods of fitting an ellipsoid to directional permeability data. The question arises as to what permeabilities we actually measure in an anisotropic laboratory model. Let's consider a model of length L and width W through which a fluid is flowing lengthwise. For W/L ratios approaching zero, the stream lines are all forced to be in the direction of the measured permeability, so Equation (34) would apply for this case. For W/L ratios approaching infinity, the pressure gradient and the measured permeability directions are parallel; the stream lines are oriented in some other direction. For this case, Equation (35) would apply. For intermediate W/L ratios, the measured permeability would fall between two limiting values $k'_N$ and $k''_N$. Scheidegger[8] has analyzed the ratios of the two limiting permeability expressions for their maximum possible deviation, and has found that the degree of anisotropy has to be appreciable before the difference becomes significant.

We have made the assumption that the permeability tensor is symmetric, that is, $k_{ij} = k_{ji}$. However, Whitaker[19], in his treatment of Darcy's law, concludes that there is no general reason to indicate the permeability tensor should be symmetric. On the other hand, Greenkorn and Kessler[20] and Guin, Kessler, and Greenkorn[21] have shown from statistical model studies that one would expect a symmetrical permeability tensor. It is certainly conceivable to imagine that in a porous medium if the interstitial velocity is such that the form drag dominates flow and further that there is a distinct particle orientation such that the form drag would be a function of direction that the permeability tensor might not be symmetric. It is not clear at what values of seepage velocity and particle size distribution this might happen.

There has been no attempt to show how one would interpret experimental data in terms of the dispersion tensor. We assume for the moment that the dispersion tensor is symmetric and thus if we select a coordinate system moving with the average velocity of the

fluid we would adopt a diffusion model for the dispersion in any porous medium. If we further assume that there is a flux relationship between the dispersion coefficient and the concentration gradient such as

$$j = D \frac{\partial c}{\partial x} \tag{36}$$

then we would have an analogous case to that of the permeability tensor as given by Darcy's Law and we would expect the same general argument might hold. That is, for the two cases, if we plotted the measured dispersion coefficient as determined from the solution of the above equation, we would plot the square root of $\sqrt{D}$ or $1/\sqrt{D}$ versus direction for the anisotropic media and expect to obtain ellipses as in the case of permeability. This of course assumes that dispersion is represented by a symmetrical tensor. We have a practical dilemma here in that we cannot obtain the dispersion coefficient by measuring the concentration change over a length and relating it to the flux; rather, we measure the concentration breakout curve and fit a solution of the diffusion equation to this breakthrough curve to obtain the parameter in the solution, the dispersion coefficient. In principle, if we maintained a constant concentration gradient across the medium (and this is concentration of marked particles resulting from flow) and measured flux we could obtain the dispersion coefficient in an analogous fashion to the permeability. Thus we are presented with an interesting dilemma -- that we must measure or obtain a measure of D by solving the second-order diffusion equation. This complicates matters, since for a radial geometry it becomes very difficult to solve this equation and in this work we resort to doing a linear analysis. Thus the measure of dispersion we utilize is not the true dispersion coefficient but rather the slope of the breakout curve which we interpret to be a relative measure of dispersion as a function of direction. We then compare plots of this coefficient versus the permeability. Similar comments as to the difference between the two limiting cases for permeability would then apply to the dispersion coefficient.

## Experimental Procedures

In order to study the effects of heterogeneity on dispersion we packed Lucite cylinders 6" long and 1-1/8" in diameter with glass beads in four ranges of spherical sizes. Figure 4 is a schematic of one of the models. Each of the models was packed with a different size of glass bead and the porosity, permeability, and dispersion of each model determined as well as the result of combining all four of these models in various arrangements to give a set of composite models that were heterogeneous by definition of Equation (7). (Note that in a realistic situation in order to obtain heterogeneity we must use bead sizes that do have a size range associated with them, so we are actually investigating the situation of Figure 3b, but our emphasis was on the effect of change in average permeability, the heterogeneity rather than variance of the permeability itself, the nonuniformity.) We used a statistical design for the permeability and dispersion measurements to investigate the effects of various parameters and the effect of replication.

The models were packed by continuously vibrating them on a shake table with a frequency of vibration of about 60 cycles per second. The beads were poured into the model slowly, taking about an hour and a half to pack a 6" model. After filling constraining screens and spacers were placed at the end of each of the models and caps screwed in place.

Porosity. The porosity of the models was determined by the liquid saturation method. Water with a very small of detergent was introduced at the bottom of the model at a very slow rate, and the air forced out of the top of the model. The detergent was added to aid in completely wetting the surface of the packing. A small amount of food coloring was added as an aid in visualizing the filling of the model. The volume of water occupied by the pore space was determined as the difference in the weight of the model before and after filling, with due regard taken to correct for water remaining in the inlet and outlet parts of the model. The porosity then was calculated as the ratio of the pore volume to the total volume of the model. Once the porosity had been determined, the model was purged with distilled water to remove soap and coloring and from that point on the model was never dried again. (In fact, we kept the models immersed in water when they were not in use and whenever they were connected or unconnected. This was done underwater to limit the air entering the models.)

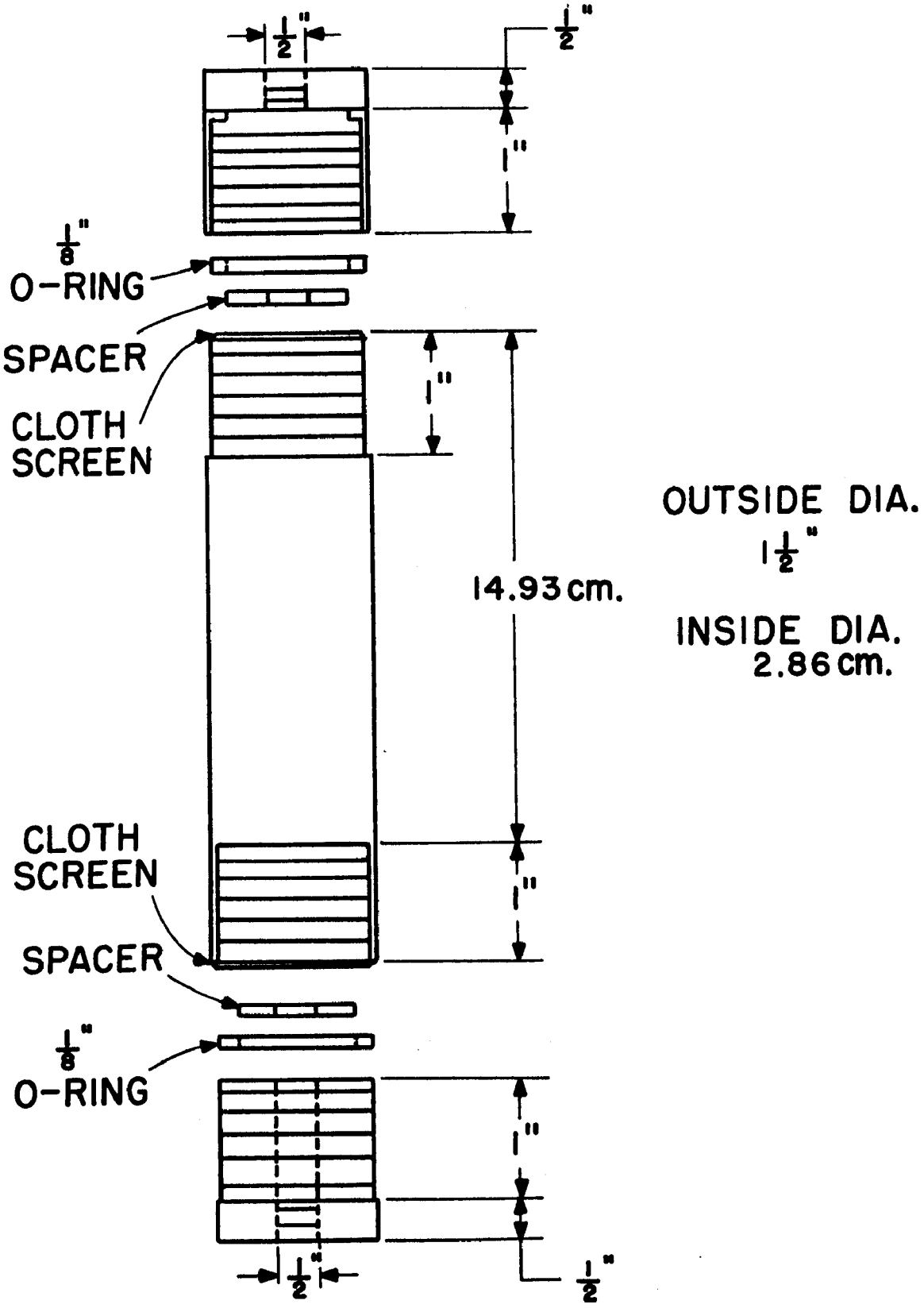


Figure 4 - Description of Model

Permeability. The permeability of each model was determined with Equation (1) in the form

$$k = \frac{\mu L}{\rho g A} \frac{Q}{\Delta h} \tag{37}$$

where Q/A is the Darcy velocity. The measurements were made in a temperature-controlled room where the temperature was held between 76-77°F. The permeabilities for the models were determined by measuring pressure drop for several flow rates for each of the models. Flow rates were measured by the amount of time for collection of a given amount of effluent. The pressure drop was measured using a Pace differential transducer, model KP-15 and a Pace transducer indicator, model CD-25. The transducers were calibrated with U-tubes and deadweight tester.

Dispersion. Breakthrough curves were determined for each model by means of an electrochemical system. Potassium chloride was used as a chemical tracer since mobilities of the potassium and chloride ions are almost the same and hence the liquid junction potential is minimized. A silver-silver chloride electrode in conjunction with a calomel reference electrode were used to determine the concentration of the chloride solution.[23] The potential was monitored on the Sargent SR balancing potentiometric recorder. (The preparation of silver-silver chloride electrodes is discussed by Schumacher and Garland.[24]) In order for the potentials of both the model fluid and the displacing fluid to be recordable on the 0-125 mv scale, the model fluid was made .02 molar KCl and the displacing fluid was .4 molar KCl. These gave potentials of approximately 80 mv and 13 mv respectively.

Permeability and dispersion were measured simultaneously, that is, the flow rate and pressure drop were monitored while the model fluid was being displaced. Figure 5 shows a schematic diagram of the equipment used.

Since there is a density difference between the .02 molar and .4 molar KCl solutions, the displacing solution was always introduced into the bottom of the model to minimize possible gravity fingering.

The actual procedure for the displacement was as follows: the model was purged with .02 KCl molar solution; the desired flow rate was obtained; the pressure drop was noted for the permeability measurement; the value controlling the .02 molar solution was shut off and the valve controlling the .4 molar solution was opened until the same pressure drop was observed on the transducer-indicator; the recorder was turned on immediately. The flow rate

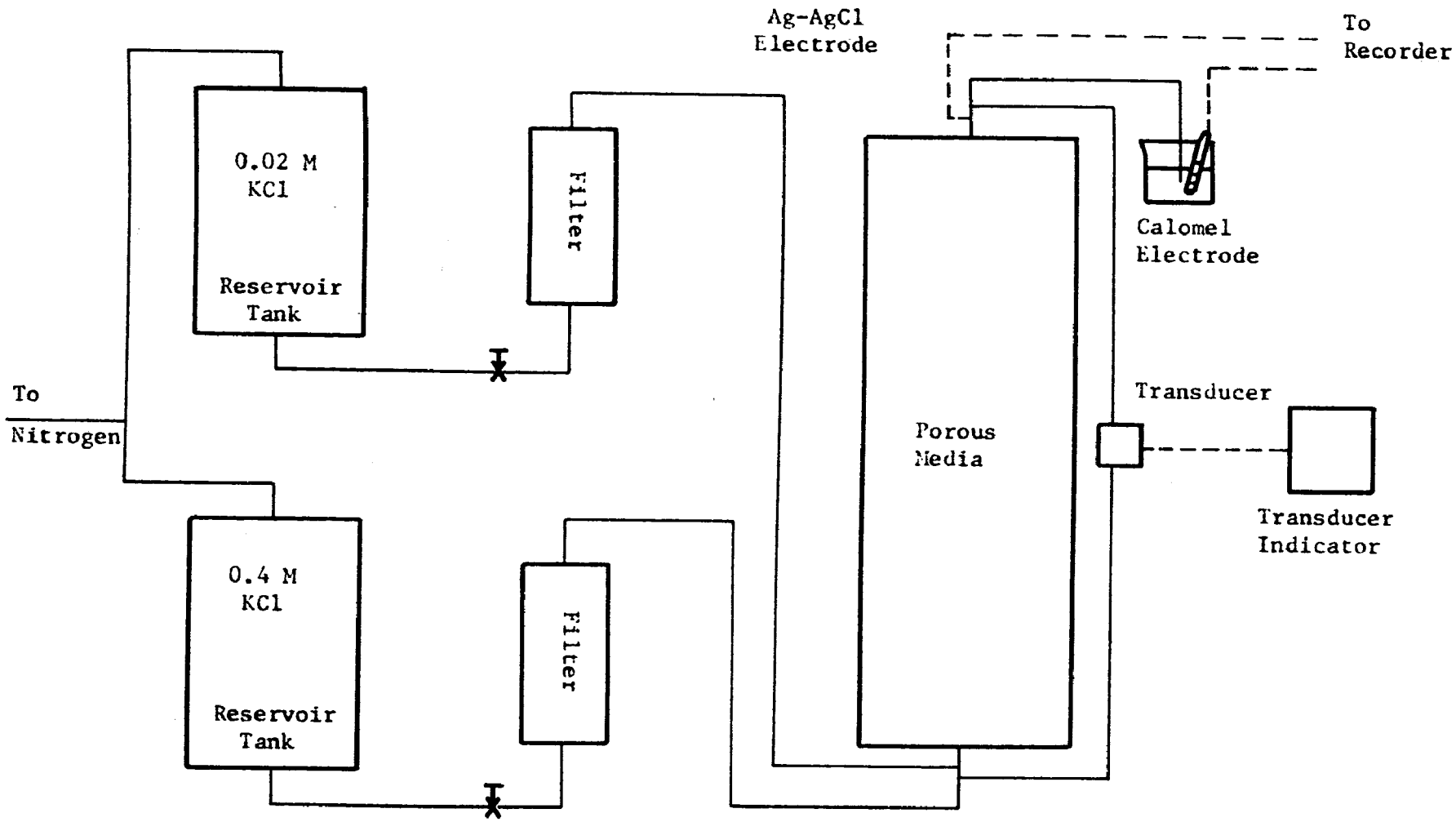


Figure 5 - Diagram of Equipment

was controlled by making sure the pressure drop remained constant throughout the displacement. After the displacement was completed, the model was purged with .02 molar KCl solution and preparation for another run.

A calibration curve was prepared from potential readings based upon the two solutions. With the calibration curve the concentrations of KCl were obtained from the recorder. A plot of dimensionless concentration versus pore volume was constructed where

$$C^* = \frac{C - .02}{.4 - .02} = \frac{C - .02}{.38} \tag{38}$$

The dispersion coefficients were obtained from these curves and Equation (4).

For each separate model, duplicates of three different velocities were used. After the 24 experiments in the individual models, the four models were screwed end-to-end in each of four arrangements and duplicates of three velocities of these composite models were run.

## Results

Table 1 shows the measurements of porosity and permeability for the single models and the measurements of permeability for three of the four composite models. The permeability was not determined for the final composite model (3412) since the results for the previous three had been so consistent.

The values of porosity are reasonable although we did not make duplicates of the porosity measurements of these particular models, since once they were saturated we did not wish to dry them, we did measure the porosity of similar models several times and the estimate of error of porosity results from these measurements.

The permeability measurements were actually made during the dispersion runs and represent a minimum of two separate measurements on each model and in some cases more. The error in the permeability measurement was about 3%. For the composite models the measurement error was much less, because we had better control of the pressure measurement across the longer model.

The permeability data are plotted in Figure 6 for the individual models (1, 2, 3, 4) according to Equation (15).

$$k = 2.52 \times 10^{-4}\, d_{50}^2 \tag{39}$$

TABLE 1 - MODEL PROPERTIES

| Model | Bead Size Range micron (cm) | Porosity* (%) | Permeability** (darcy) |
|---|---|---|---|
| 1 | 590 - 840 | 34.0 | 120 ± 2 |
| 2 | 250 - 350 | 34.0 | 35.8 ± 1.2 |
| 3 | 105 - 149 | 34.3 | 5.04 ± .06 |
| 4 | 44 - 62 | 36.5 | .487 ± .012 |
| 1234 | -- | -- | 1.82 ± .01*** |
| 4321 | -- | -- | 1.84 ± .01 |
| 2143 | -- | -- | 1.85 ± .01 |
| 3412 | -- | -- | -- |

*Measurement error ± 1% (Estimated from repeated measurements)

**2 duplicates at each of 3 velocities

***Estimated from individual model permeability - 1.75 d

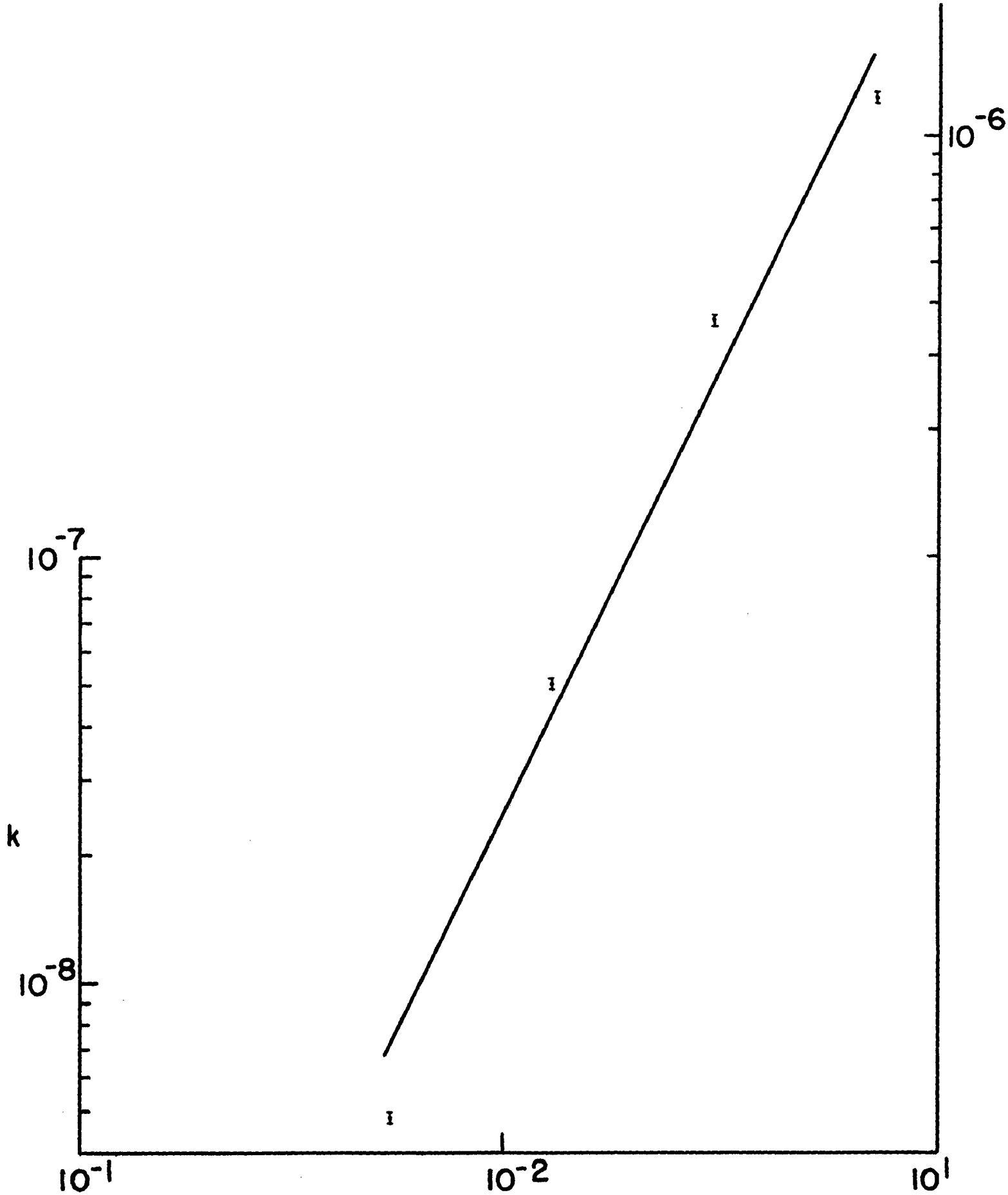


Figure 6 - k vs $d_{50}$

The data show that a straight-line relationship is a reasonable fit on log-log plot, and the slope of 2 also is a reasonable number. The value of the intercept for this relationship was lower than that predicted by Ramondi et al.[10] for spheres, and it is lower than the data given by Harleman et al.[4] also for spheres. The value of d should be the one at the correct average since the distribution of bead sizes may be skewed. The bead sizes and permeabilities reported here are less than those given by the previous authors.[4] (We may be seeing an effect due to the nonuniformity of the pack.)

The dispersion coefficients were calculated from breakthrough curves using Equation (4). Table 2 gives the dispersion coefficients calculated in this manner. For the first three models, which are the larger bead sizes, there is a distinct tail in the breakout curve. The Peclet number in all runs was greater than 133, and the Reynolds number was larger than $10^{-3}$, so the effects of asymmetry and diffusion should not be involved. Actually, the value of the dispersion coefficient is not changed if one attempts to fit the curve more exactly utilizing Equation (12). (The asymmetry may be due to entrance-exit effects though the models should be large enough considering the bead size. It may be a result of the manner in which the models were packed.)

The data for the individual models 1, 2, 3, 4 are plotted in Figure 7 as a function of velocity, and the equations representing these figures are:

Model 1: $$D = 1.0 \times 10^{-3}\, v^{1.45} \tag{40}$$

Model 2: $$D = .53 \times 10^{-3}\, v^{1.33} \tag{41}$$

Model 3: $$D = .39 \times 10^{-3}\, v^{1.25} \tag{42}$$

Model 4: $$D = .24 \times 10^{-3}\, v^{1.15} \tag{43}$$

There is a significant difference in dispersion coefficient due to the bead size or permeability. Also, there is a significant dependence on velocity above the first power. The trend shows the smaller the beads (or lower the permeability and probable higher intersitial velocity) the smaller the exponent and the intercept. These data are similar to the data of Harleman et al.[4] except they are for somewhat smaller particle sizes and indicate that the nonuniformity is having an effect.

The dispersion coefficients for the composite models are plotted as a function of velocity in Figure 7 and the Equations representing these figures are:

Arrangement 1234: $$D = 1.65 \times 10^{-3}\, v^{1.05} \tag{44}$$

Arrangement 4321: $$D = 1.50 \times 10^{-3}\, v^{1.07} \tag{45}$$

TABLE 2 - VELOCITY AND DISPERSION COEFFICIENTS

| Model | v (cm/sec) | $D \times 10^3$ ($cm^2$/sec) |
|---|---|---|
| 1 | .0420 | 3.74 |
| | .0420 | 4.40 |
| | .0580 | 5.57 |
| | .0575 | 5.85 |
| | .0750 | 10.3 |
| | .0750 | 9.08 |
| 2 | .0421 | 1.55 |
| | .0421 | 1.80 |
| | .0580 | 3.03 |
| | .0580 | 2.56 |
| | .0750 | 3.50 |
| | .0755 | 3.74 |
| 3 | .0420 | 1.36 |
| | .0417 | 1.15 |
| | .0583 | 1.65 |
| | .0583 | 2.02 |
| | .0750 | 2.29 |
| | .0750 | 3.04 |
| 4 | .0426 | .754 |
| | .0420 | .672 |
| | .0604 | 1.21 |
| | .0602 | .866 |
| | .0765 | 1.54 |
| | .0762 | 1.78 |
| 1234 | .0416 | 4.12 |
| | .0420 | 3.97 |
| | .0588 | 7.61 |
| | .0586 | 5.71 |
| | .0750 | 7.62 |
| | .0750 | 7.30 |
| 4321 | .0416 | 4.16 |
| | .0418 | 3.85 |
| | .0585 | 5.46 |
| | .0585 | 5.53 |
| | .0752 | 8.24 |
| | .0752 | 6.81 |

TABLE 2 (cont.)

| Model | v (cm/sec) | $D \times 10^3$ ($cm^2$/sec) |
|---|---|---|
| 2143 | .0416 | 3.61 |
| | .0416 | 3.11 |
| | .0585 | 5.83 |
| | .0585 | 4.28 |
| | .0750 | 6.50 |
| | .0750 | 6.59 |
| 3412 | .0416 | 3.10 |
| | .0416 | 3.34 |
| | .0586 | 4.79 |
| | .0580 | 4.73 |
| | .0752 | 6.33 |
| | .0750 | 6.13 |

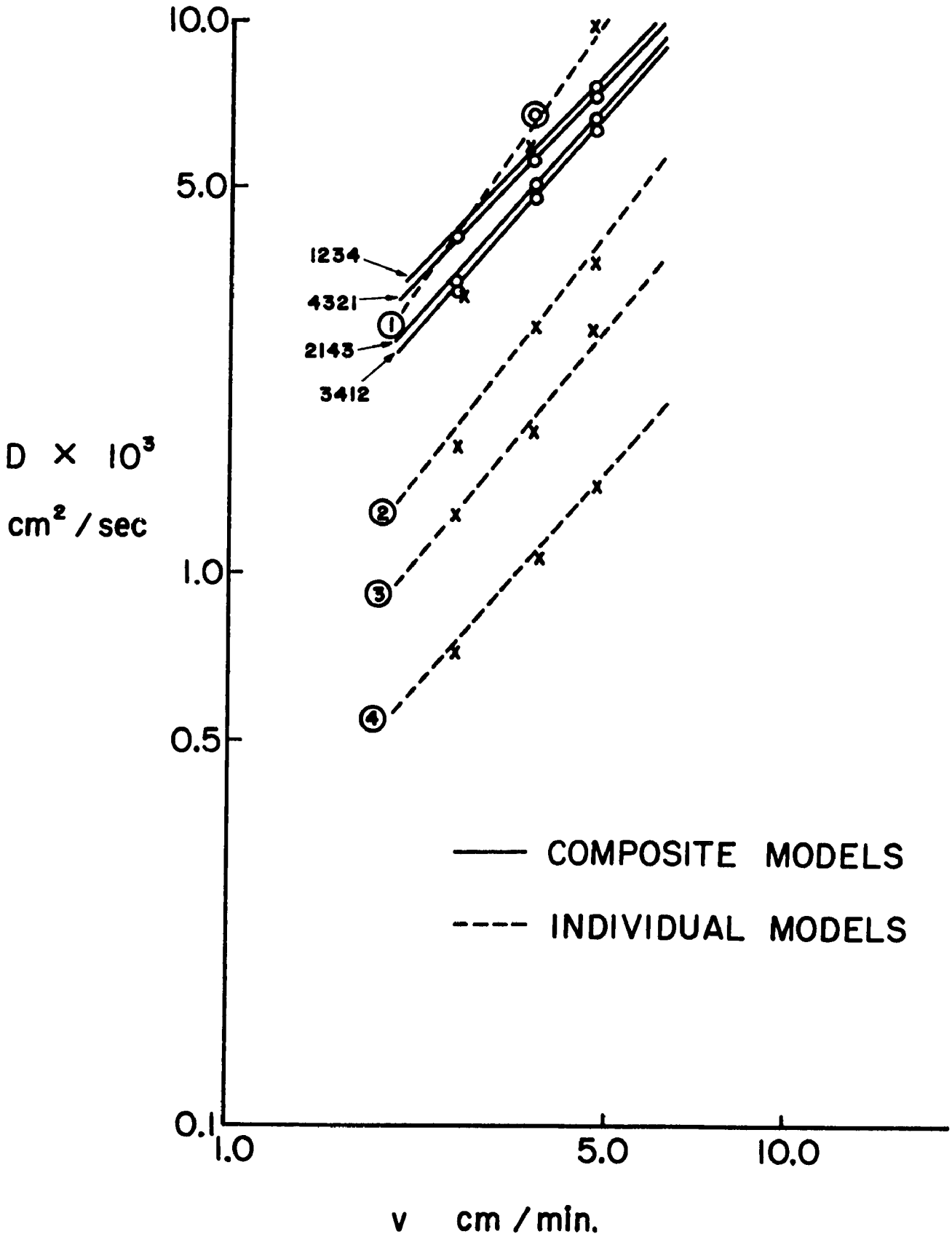


Figure 7 - Dispersion Coefficient Versus Velocity

Arrangement 2143: $D = 1.17 \times 10^{-3} v^{1.14}$ (46)

Arrangement 3412: $D = 1.10 \times 10^{-3} v^{1.15}$ (47)

There is not nearly the spread of dispersion coefficients with the composites as there is with the individual models. As can be seen, these data all fall close to that for individual model #1, the larger bead size, which indicates that the dispersion seems to be dominated by the higher-permeability material.

It is interesting to note that there is a significant difference in the results from the different arrangements. The way in which the material disperses in one permeability material has an effect on the way it disperses into the next layer. Unfortunately this seems to indicate that reciprocity does not hold in heterogeneous media, and one must preserve the location of a given level of permeability, ergo, a given dispersive media, when trying to calculate mixing during flow in such media.

The individual and composite dispersion coefficients are correlated as a function of permeability Reynolds number as given by Equation(29) in Figure (8). Equations for the data are:

Model 1: $\frac{D}{\nu} = 187\ R_k^{1.2}$ (48)

Model 2: $\frac{D}{\nu} = 215\ R_k^{1.2}$ (49)

Model 3: $\frac{D}{\nu} = 536\ R_k^{1.2}$ (50)

Model 4: $\frac{D}{\nu} = 1215\ R_k^{1.2}$ (51)

Arrangement 1234: $\frac{D}{\nu} = 3110\ R_k^{1.2}$ (52)

Arrangement 4321: $\frac{D}{\nu} = 2945\ R_k^{1.2}$ (53)

Arrangement 2143: $\frac{D}{\nu} = 2550\ R_k^{1.2}$ (54)

Arrangement 3412: $\frac{D}{\nu} = 2365\ R_k^{1.2}$ (55)

Harleman et al.[4] report

$$\frac{D}{\nu} = 54\ R_k^{1.2} \quad (56)$$

Although the power of the exponent is the same the values of the intercept are higher than Equation (56) and are definitely a function of the bead size. It may be that the nonuniformity of the bead

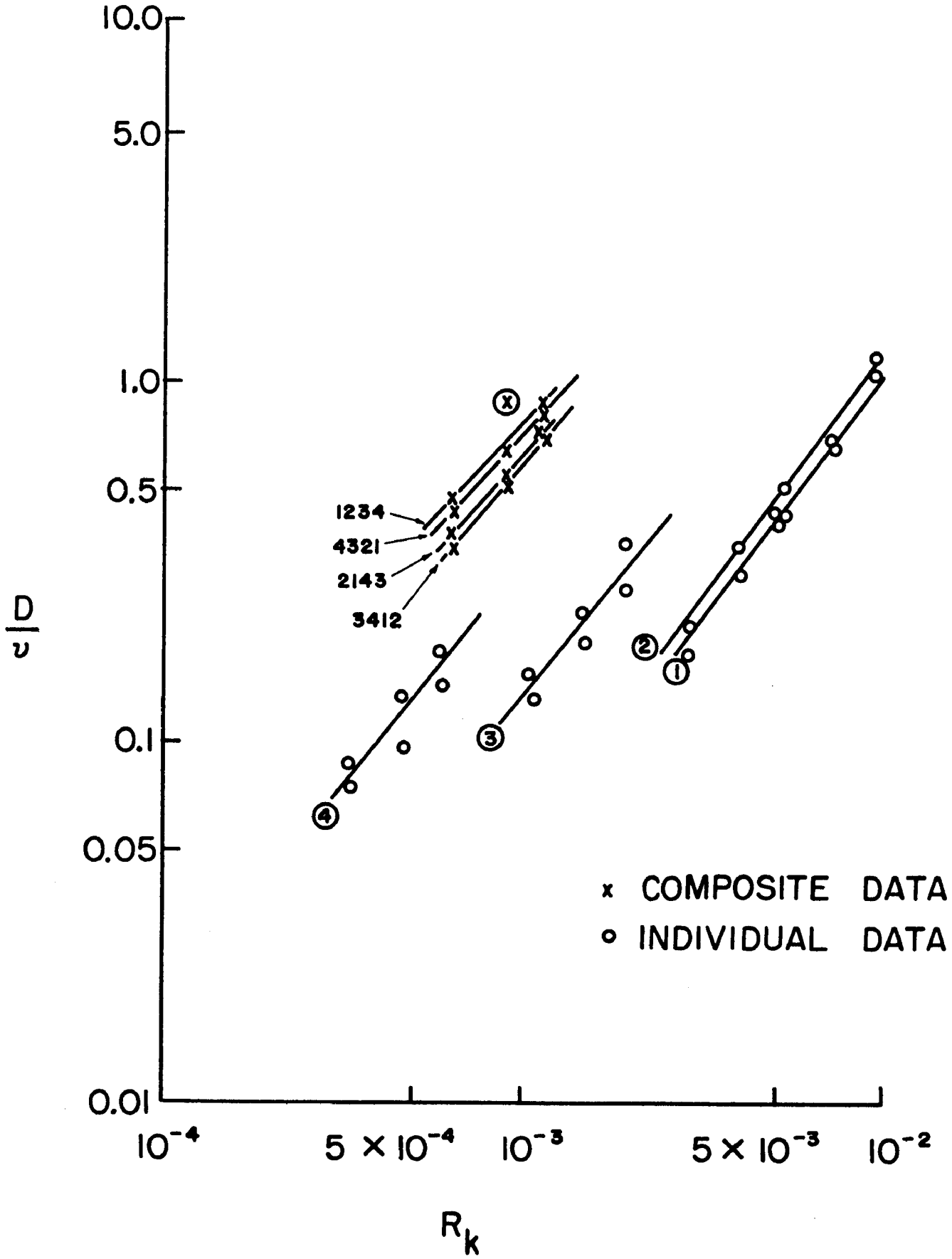


Figure 8 - $D/\nu$ vs $R_k$

size causes the intercept to change. On the other hand the heterogeneous models (the composites) also take an additive jump in intercept, although the change of intercept of Equations (52) - (55) is less drastic than the individual models Equations (48) - (51). The similar exponent is confusing at this point since the velocity dependence of the models change.

## DISPERSION DURING FLOW IN NONUNIFORM, HETEROGENEOUS POROUS MEDIA[25]

Six different porous medium models were constructed of glass beads to obtain six possible combinations of two permeabilities and three slopes (variation in permeability). The models were constructed as shown in Figure 9. Each model was run at three fluid velocities and to check the effect of packing each medium was run in both possible directions. Thus a 2 X 3 X 3 X 2 factorial design of experiments was set up without replication.

The assumption was made that the direction effect due to packing would be negligible. Then all possible combinations of the six models taken two at a time (fifteen combinations) were run at the same three velocities and the permeability and dispersion measured. Each combination was also run at both possible directions to investigate any effect due to order of models.

The distribution of bead diameters can be quantitatively described by the slope, S, of the log-normal line

$$S = \log d_{84} - \log d_{16} = \log \frac{d_{84}}{d_{16}} \tag{57}$$

where $d_{84}$ and $d_{16}$ are the bead diameters of the 84% and 16% cumulative fractions, respectively. The nonuniformity was built into the models in this study by preparing three sets each of two different size-range permeability beads where within each size range the distribution of bead diameters, that is, the slope as given by equation above changed but where the three lines crossed at $d_{10}$. This provided media which had roughly the same permeability but a different distribution of bead sizes (permeabilities) within a given bead-size range; the possibility of comparing this second-order heterogeneity; and finally the possibility of comparing the two different permeability levels (heterogeneity).

Eight replicates, randomly chosen from the 126 total experiments, were run as a measure of experimental error.

Size Distribution of Beads. To determine the size distribution of glass beads in a given mix, samples were analyzed with a photomicroscope. Bead diameters were measured off the photograph produced, and the actual bead diameters were then calculated from the value of the amount of magnification used. The number of beads appearing on a photomicrograph varied according to the mean bead diameter and the magnification used; however, 150-200 diameters were measured for each mix before the distribution was plotted on log-probability paper.

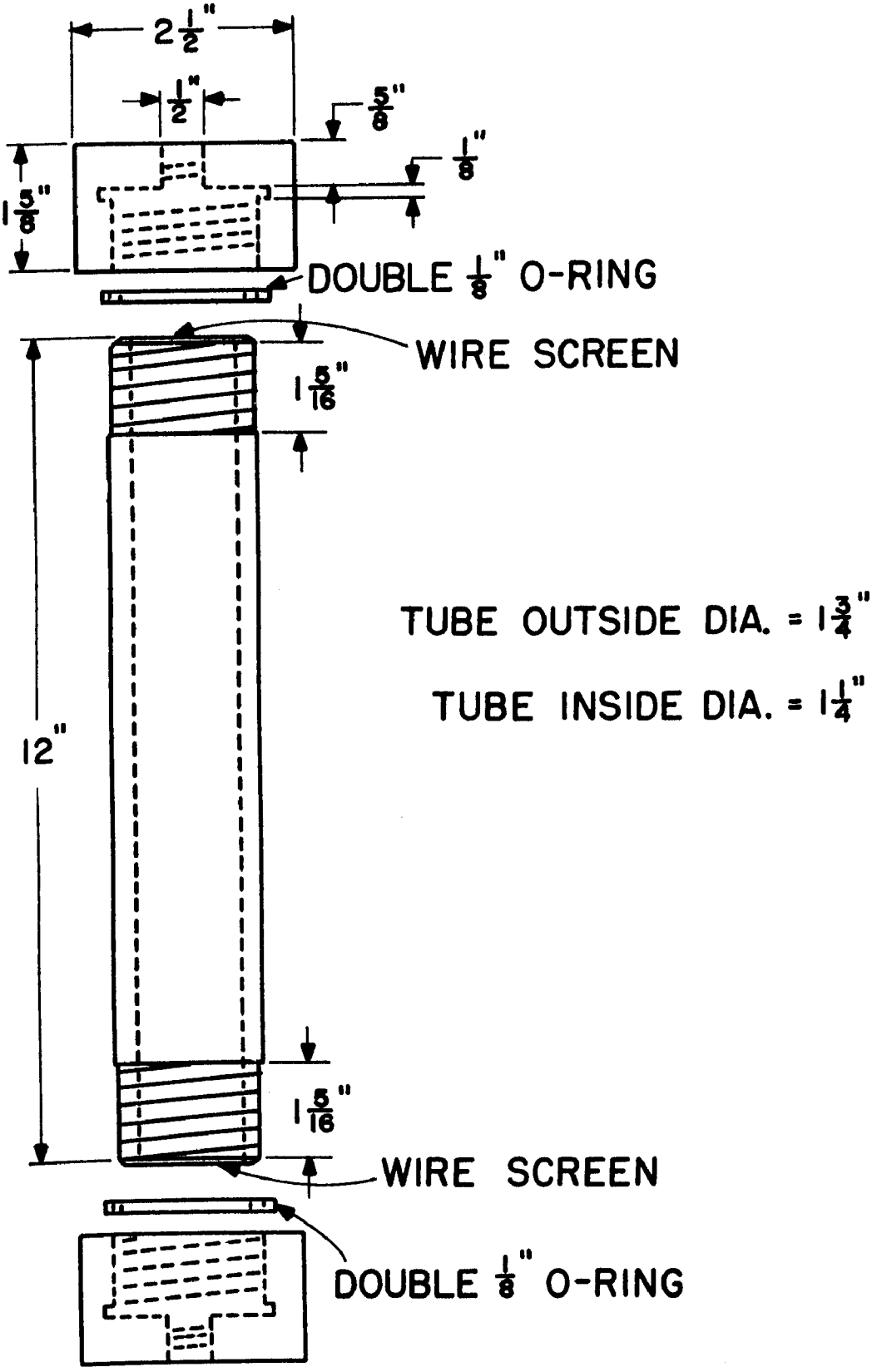


Figure 9 - Plexiglas Model - Single Tube

The mixes of beads were made up having size distributions intersecting at 10% cumulative fraction by a trial and error mixing of the available distributions from photomicrographs made of each new trail mix. The final distributions resulted from mixing various amounts of 14 different commercially available sized glass beads.

Packing Procedure. The glass beads were packed in the plexiglas tubes to give cylindrical porous media 12 inches long and approximately 1 1/4 inches in diameter. The tubes were constructed such that they could be joined end to end in order to run combined combinations of first and second order heterogeneities.

To pack a tube, beads were continuously added while the tube is vibrated on a shake table at 50-70 cycles per second. The rate of addition of the beads was held uniform throughout the packing process and it was controlled so that each of the six tubes took 45-60 minutes to fill. The vibrating was stopped with the flow of beads. Wire screens were then mounted on the models to hold the beads in place and caps were screwed on.

Porosity. The porosity was determined by saturating the porous media with distilled water, wetting the media before and after saturation. This difference in weight minus the weight of water accumulating in the fittings of the tube ends was converted to volume units and gave values of one pore volume of the porous media. Porosity was calculated as the ratio of the pore volume to the total volume.

Distilled water was used for these measurements and contained a small amount of food coloring and a very small amount of liquid detergent. The food coloring served to help visualize the saturating and help detect any air pockets, while the detergent acted as a wetting agent to help completely wet the surface of the media. With the tube in a vertical position water was introduced in the bottom, thus forcing the air out the top. The rate of water addition was varied to keep the air-water interface in the medium as flat as possible, which took about fifteen minutes. Before making permeability and dispersion measurements, each model was purged with regular distilled water to remove the food coloring and the detergent from the medium.

Permeability. Permeability was calculated from Darcy's Law using data obtained by forcing fluid through the media with a Ruska proportioning pump. Flow rates used were 224, 128, and 64 cc/hr. (Approximately 1.5, .8, and .4 cm/min.) Pressure drops were measured with a Pace differential pressure transducer and a Pace transducer indicator. Permeability was calculated from equation (37).

Dispersion. Equation (4) was used to calculate the dispersion coefficient for each run. The electrochemical system described by Koonce and Blackwell[23] was used to determine the breakthrough curves from which dispersion could be calculated. The system consisted of a

silver-silver chloride electrode in conjunction with a Calomel reference electrode and potassium chloride was used as the chemical tracer. The potential between the electrodes was a measurement of the chloride concentration in the immediate vicinity of the silver-silver chloride electrode. Figure 10 is a schematic of the experimental setup.

Throughout each experiment the electric potential was monitored on a Sargeant SR balancing potentiometric recorder, which is 0-125 millivolt range. The fluid in the model (.02 molar KCL) gave a potential reading of about 80 millivolts, while the displacing fluid (.4 molar KCl) gave a potential of about 12 millivolts. Due to the slight density difference between the two fluids, the displacing fluid was introduced into the bottom of each model to eliminate possible gravity fingering.

As a check on the electro-chemical system, a colorimetric analysis of the K in the displaced fluid was conducted on approximately 15% of the runs. For this test, a Renco automatic fraction collector was used to continuously collect 5 ml samples of the effluent stream. Two milliliter samples of this 5 ml sample was analyzed for potassium concentration by adding 25 ml of distilled water, .5 ml 1-molar sodium hydroxide at approximately .01 gm, 2, 2', 4, 4', 6, 6' hexanitrodiphenylamine. A Klett-Summerson photoelectric colorimeter with a 1 mm cell was calibrated so the readings could be easily converted to KCl concentration in the effluent stream of the model.

Dispersion and permeability measurements were made simultaneously for each run by recording the electropotential and reading the pressure drop from the transducer indicator. For each run, the model was first purged with .02 molar KCl supplied by a gravity feed tank. The proportioning pump was then set for the desired flow rate of .4 molar KCl and the pump andrecorder turned on. After completion of the displacement, the model was again purged with .02 molar KCl to prepare it for the next run.

The KCl concentration was read off the continuously recorded electrode potential at certain time intervals, and the dimensionless concentration calculated from equation (38) where C is the KCl concentration. The time was read in units of pore volume, and the plot of pore volume versus concentration is the breakthrough curve needed to calculate the dispersion.

## Results

Size distribution of the beads. The final size distribution of the bead used in packing the size porous media are shown in Figure 11. The parameter used in correlating the size distribution with the dispersion coefficient was the slope of these log-probability plots. The slopes of lines in Figure 11 are listed in Table 3.

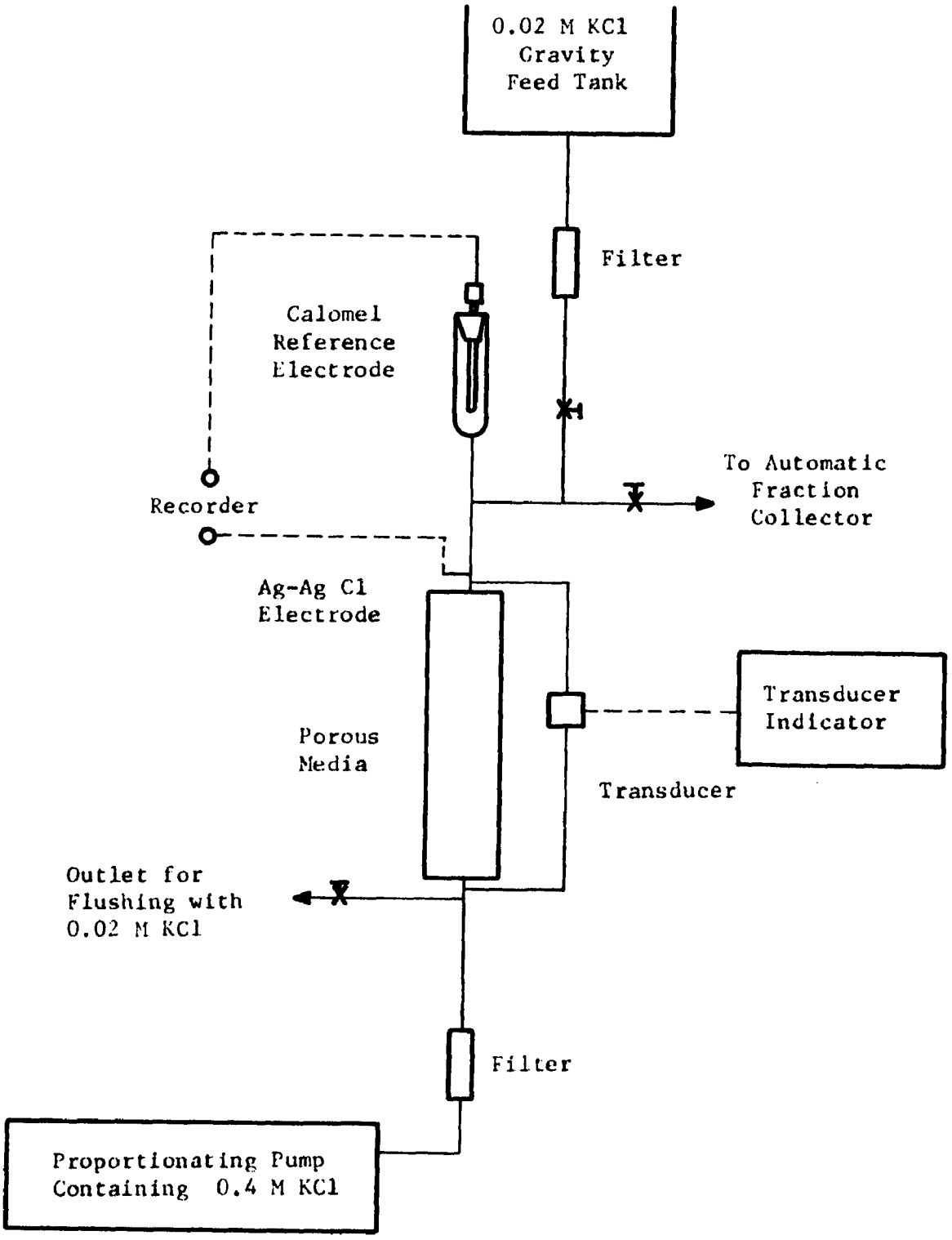


Figure 10 - Equipment Set-Up

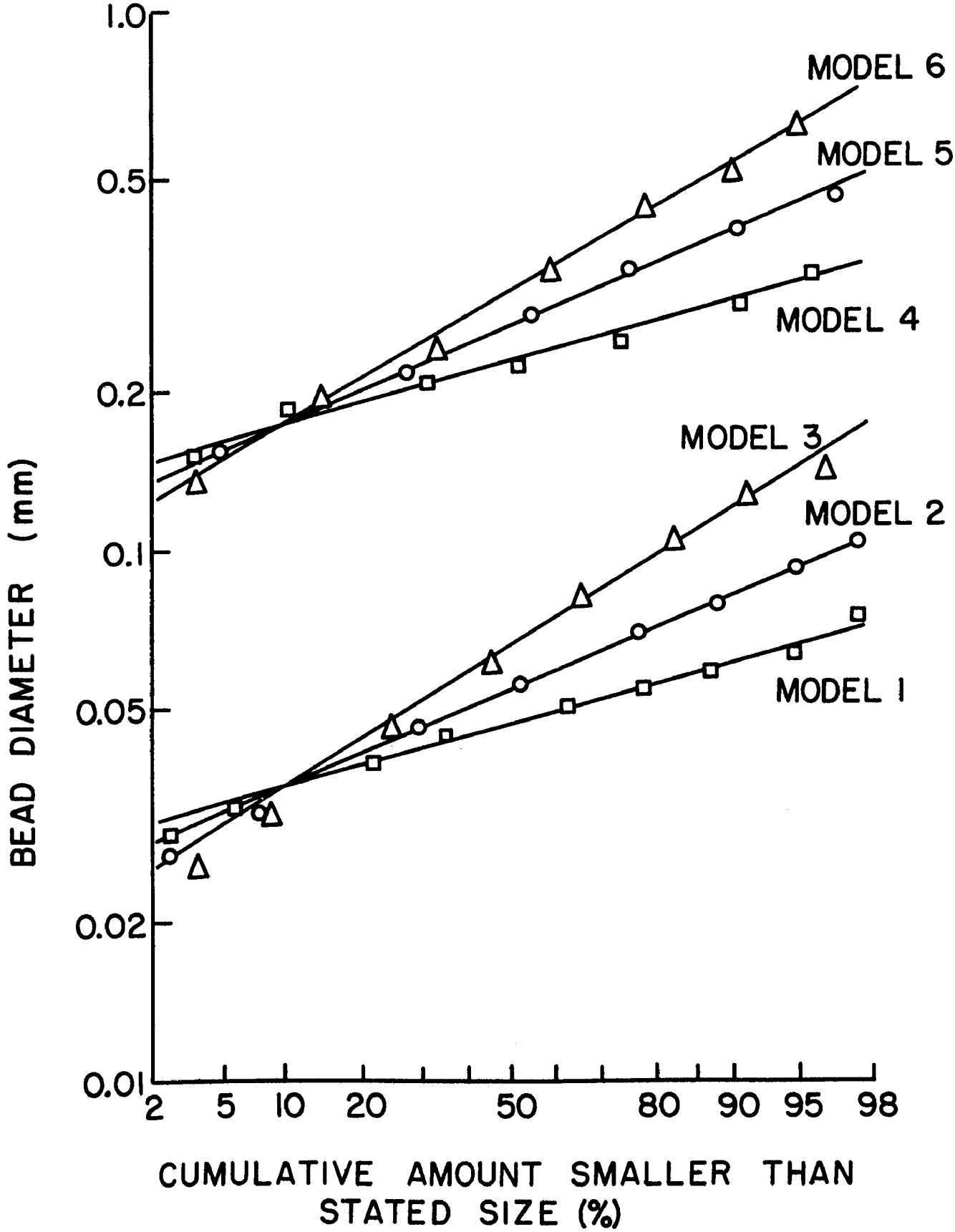


Figure 11 - Size Distribution of Beads Used in Packing Models

Table 3. Porosities and Slopes of the Bead Size Distributions for the Models.

| Model | Slope | Porosity | Description |
|---|---|---|---|
| 1 | 0.184 | 0.350 | Small beads, small spread |
| 2 | 0.280 | 0.348 | Small beads, medium spread |
| 3 | 0.389 | 0.333 | Small beads, wide spread |
| 4 | 0.182 | 0.341 | Large beads, small spread |
| 5 | 0.282 | 0.330 | Large beads, medium spread |
| 6 | 0.379 | 0.321 | Large beads, wide spread |

Porosity. The results of the porosity measurements are shown in Table 3. Although they do vary from model to model, the values are within the range expected for this kind of pack. Three porosity measurements were made on each model, and the maximum variation of porosity was 1%.

Since the vibrating time in packing each model was the same, the results indicate that porosity is decreasing as the bead diameter distribution widens or as the slope of the plots in Figure 11 increases.

When two models were joined to form a composite model, the porosity used in calculations was the arithmetic average of the two individual model porosities.

Permeability. The permeabilities were calculated from Equation (37) with the proper constants. For the nonuniform but homogeneous medium (single tubes) the permeabilities measured appear in Table 4. The permeabilities seem to decrease slightly with a decrease in velocity, and this is probably due to a small amount of air being present in the medium. Actually this change is within the error of repeated measurement, so the average permeabilities were used in the correlations. Remondi's et al[10] observations of the permeability-dependence upon $d_{10}$ would predict that models 1, 2, and 3 should have the same permeability, and likewise models 4, 5, and 6 should have the same permeability. The data in Table 4 show that this is not quite the case here, but it appears that the diameter should be greater than $d_{10}$, and probably about $d_{20}$.

For the homogeneous nonuniform models, the permeability values were correlated with Equation (39). The equations for these are

$$\text{Slope 1:} \quad k = 2.4 \times 10^{-4}\, d_{10}^{1.67} \tag{58}$$

$$\text{Slope 2:} \quad k = 2.9 \times 10^{-4}\, d_{10}^{1.64} \tag{59}$$

$$\text{Slope 3:} \quad k = 2.2 \times 10^{-4}\, d_{10}^{1.51} \tag{60}$$

In these equations we used $d_{10}$ as the average diameter rather than $d_{50}$ as did Pleshek and Greenkorn[22] and Harleman et al[4].

The permeability values for the heterogeneous porous media, that is, porous media that have first and second order heterogeneities, appear in Table 5. The predicted values of permeability are also listed in Table 5 and the average variation between measured and predicted values is about 2% of the predicted permeability.

Dispersion. The dispersion coefficient for each run was calculated from the breakout curve and Equation (4) in the manner described earlier. All the curves were roughly symmetrical. Theoretically, the

Table 4. Permeabilities of the Homogeneous Porous Media.

| Velocity (cm/min) | Model | Permeability (Darcy) | Model | Permeability (Darcy) |
|---|---|---|---|---|
| 1.42 | 1 - up | 1.98 | 1 - down | 2.00 |
| 0.81 | 1 - up | 1.96 | 1 - down | 1.98 |
| 0.40 | 1 - up | 1.94 | 1 - down | 1.93 |
| 1.42 | 2 - up | 2.78 | 2 - down | 2.89 |
| 0.81 | 2 - up | 2.81 | 2 - down | 2.85 |
| 0.41 | 2 - up | 2.73 | 2 - down | 2.77 |
| 1.49 | 3 - up | 4.70 | 3 - down | 4.76 |
| 0.85 | 3 - up | 4.65 | 3 - down | 4.68 |
| 0.43 | 3 - up | 4.40 | 3 - down | 4.54 |
| 1.46 | 4 - up | 27.6 | 4 - down | 25.4 |
| 0.83 | 4 - up | 26.3 | 4 - down | 23.3 |
| 0.41 | 4 - up | 23.1 | 4 - down | 20.2 |
| 1.50 | 5 - up | 37.2 | 5 - down | 36.8 |
| 0.86 | 5 - up | 34.6 | 5 - down | 33.4 |
| 0.43 | 5 - up | 27.0 | 5 - down | 28.5 |
| 1.55 | 6 - up | 47.0 | 6 - down | 44.6 |
| 0.88 | 6 - up | 42.1 | 6 - down | 40.2 |
| 0.44 | 6 - up | 33.5 | 6 - down | 34.7 |

Note: "up" indicates that, during the run, the model was in the same position (with respect to gravity) as when it was packed. "Down" indicates the model was in the opposite direction during the run.

Table 5. Permeabilities of the Heterogeneous Porous Media.

| Model Combination | Velocity (cm/min) | Measured Permeability (Darcy) | Predicted Permeability (Darcy) |
|---|---|---|---|
| 1 - 2 | 1.42 | 2.38 | 2.34 |
| 1 - 2 | 0.81 | 2.35 | 2.32 |
| 1 - 2 | 0.41 | 2.29 | 2.27 |
| 1 - 3 | 1.45 | 2.82 | 2.80 |
| 1 - 3 | 0.83 | 2.76 | 2.77 |
| 1 - 3 | 0.41 | 2.75 | 2.70 |
| 1 - 4 | 1.43 | 3.77 | 3.71 |
| 1 - 4 | 0.82 | 3.81 | 3.65 |
| 1 - 4 | 0.41 | 3.82 | 3.56 |
| 1 - 5 | 1.46 | 3.63 | 3.78 |
| 1 - 5 | 0.83 | 3.68 | 3.72 |
| 1 - 5 | 0.42 | 3.64 | 3.62 |
| 1 - 6 | 1.48 | 3.77 | 3.82 |
| 1 - 6 | 0.84 | 3.72 | 3.76 |
| 1 - 6 | 0.42 | 3.58 | 3.67 |
| 2 - 3 | 1.45 | 3.62 | 3.55 |
| 2 - 3 | 0.83 | 3.60 | 3.53 |
| 2 - 3 | 0.41 | 3.52 | 3.41 |
| 2 - 4 | 1.44 | 5.32 | 5.13 |
| 2 - 4 | 0.82 | 5.19 | 5.10 |
| 2 - 4 | 0.41 | 4.97 | 4.89 |
| 2 - 5 | 1.46 | 5.41 | 5.29 |
| 2 - 5 | 0.84 | 5.39 | 5.24 |
| 2 - 5 | 0.42 | 5.09 | 5.00 |
| 2 - 6 | 1.48 | 5.57 | 5.35 |
| 2 - 6 | 0.85 | 5.62 | 5.31 |
| 2 - 6 | 0.42 | 5.42 | 5.10 |

inflection point of the breakthrough curve should occur at one pore volume and a reduced concentration of .5, and the slope for Equation (4) should be calculated at this point. Experimentally, the inflection point was displaced to the right on all breakthrough curves, although it did occur at about PV = .5. This shifting of the breakthrough curve does not have any effect on the calculated dispersion coefficient and is probably a result of making errors in the pore volume calculations or in measurement of porosity. As stated earlier, not all the air can be removed from the porous media, and thus each run may carry a little bit of air, increasing the value of one pore volume and shifting the breakthrough curve to the right. The presence of dead-end pores as discussed by Coates and Smith[26] would cause a shift in the curve to the left. We would not expect a large volume of dead-end pores in an unconsolidated media. In articles by Rafai et al[11] and Harleman[4], this shifting of the breakthrough curve was not discussed.

Another possible cause of the curve shifting could be the lag time in the electrochemical measurement system. Koonce and Blackwell[23] did not note any significant lag time. The potassium analysis, which was made separate from the electrochemical analysis, agreed with the electrochemical analyses and so it is doubtful that there is a lag time in the electrochemical measurement system.

The dispersion coefficient versus velocity is plotted on a log-log scale in Figure 12. For the heterogeneous porous media, that is, first and second order heterogeneities, the plots of dispersion coefficients versus velocity are given in Figure 13.

Plots of $D/\nu$ versus $R_k$ on a log-log scale for the homogeneous nonuniform porous media are shown in Figure 14. Plots for the first and second-order heterogeneous porous media of $D/\nu$ versus $R_k$ are shown in Figure 15.

The equations for these lines in Figure 12 are

$$\frac{D}{\nu} = 297\ R_k^{1.01} \quad \text{for } d_{10} = 35_\mu \tag{61}$$

$$\frac{D}{\nu} = 1630\ R_k^{1.48} \quad \text{for } d_{10} = 170_\mu \tag{62}$$

The equations for the lines in Figure 13 are:

$$D/\nu = 534\ R_k^{.99}\ , \quad d_{10} = 36\mu \tag{63}$$

$$D/\nu = 105\ R_k^{1.39}\ , \quad \begin{cases} d_{10} = 36\mu \\ d_{10} = 170\mu \end{cases} \tag{64}$$

$$D/\nu = 985\ R_k^{1.17}\ , \quad d_{10} = 170\mu \tag{65}$$

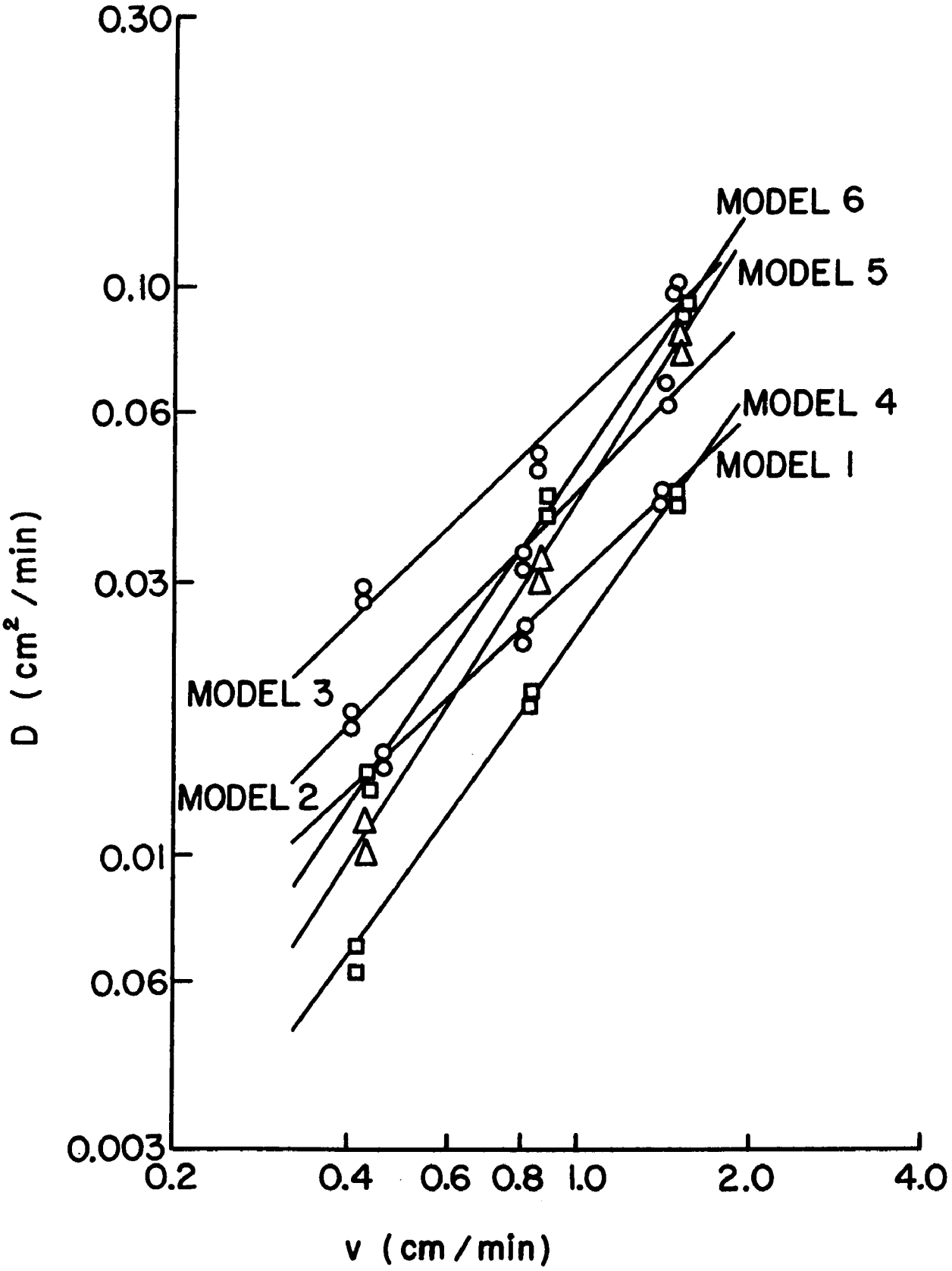


Figure 12 - Dispersion Coefficient Versus Velocity (Six Non-Uniform Models)

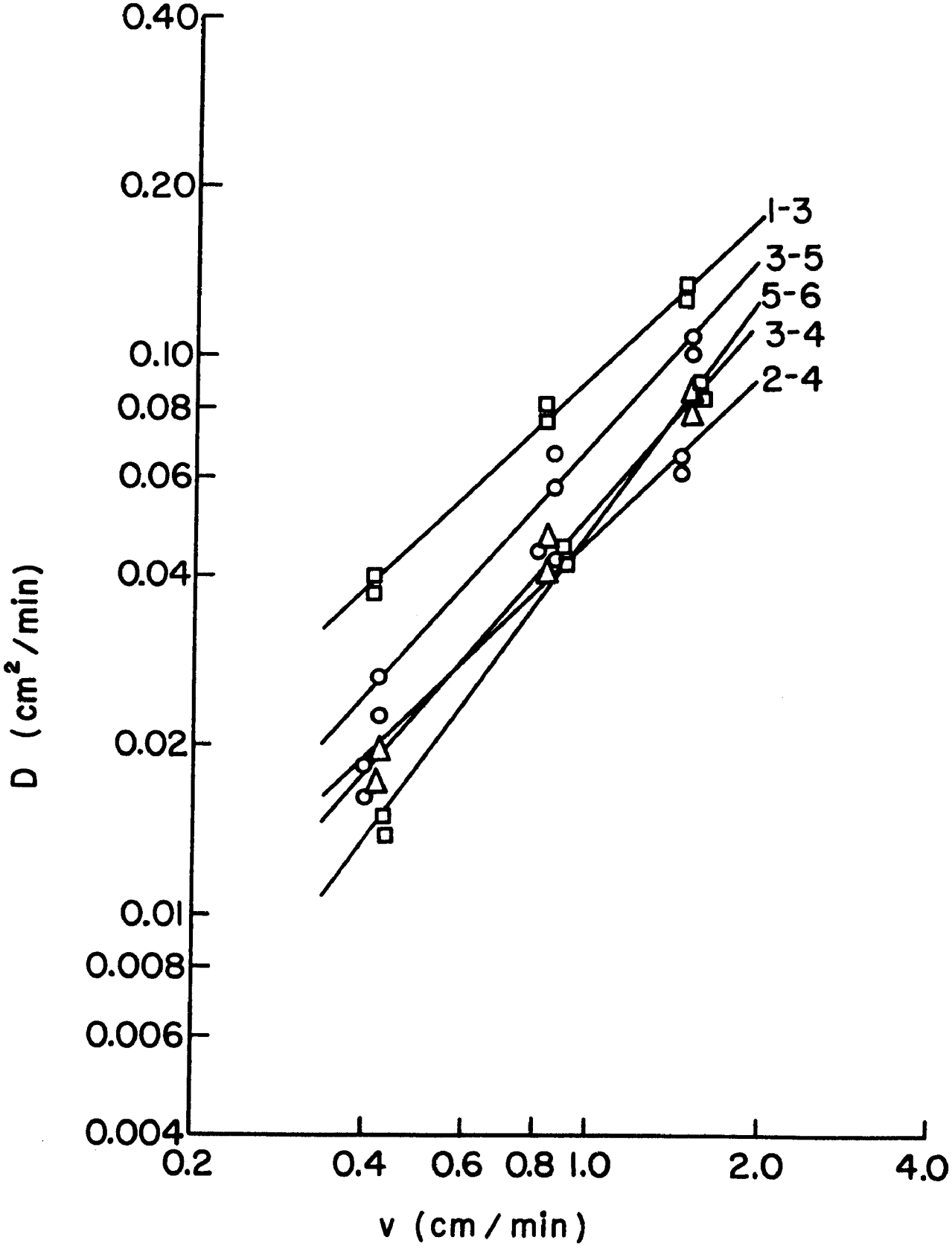


Figure 13a- Dispersion Coefficients Versus Velocity (First and Second Order Heterogeneity)

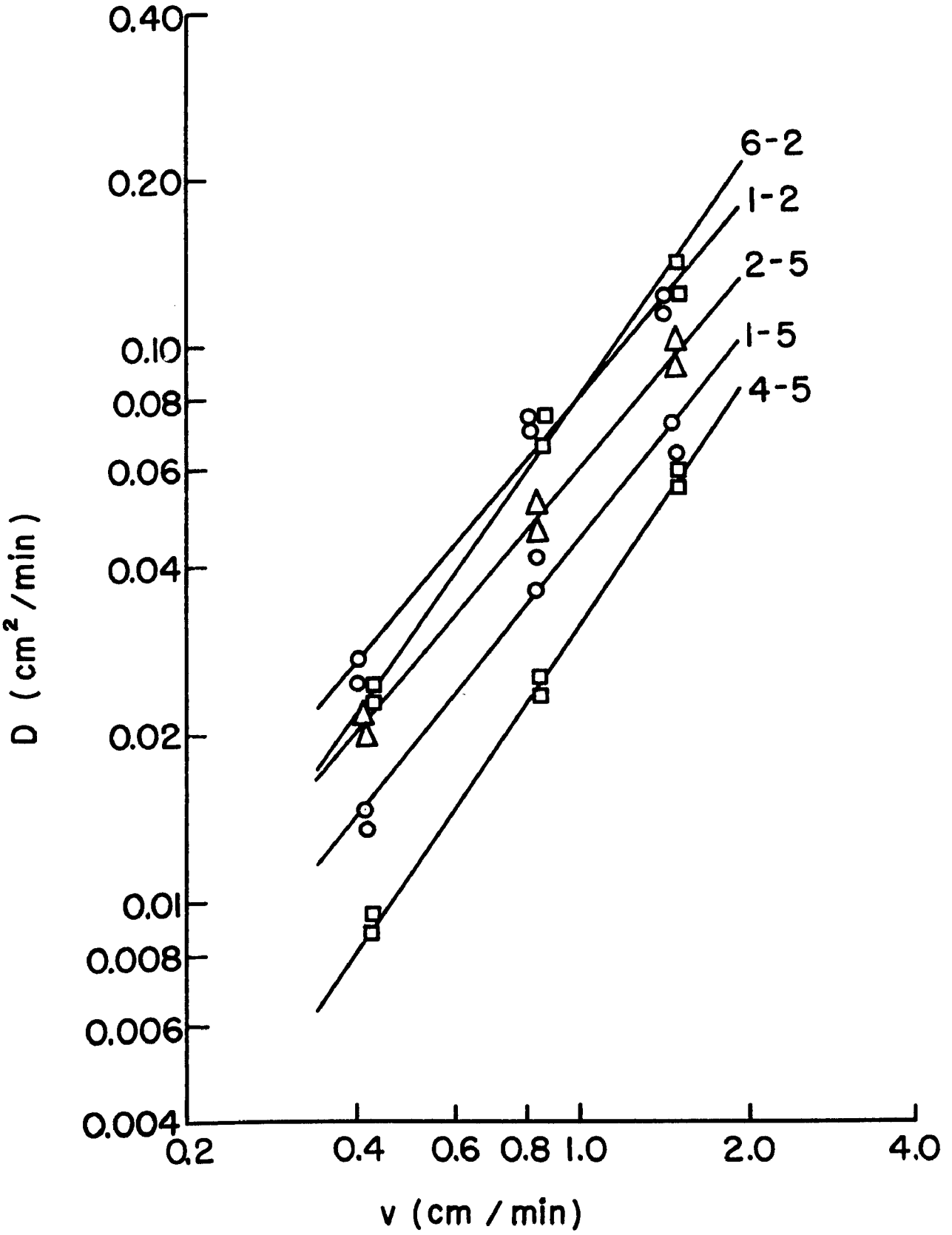


Figure 13b - Dispersion Coefficients Versus Velocity (First and Second Order Heterogeneity)

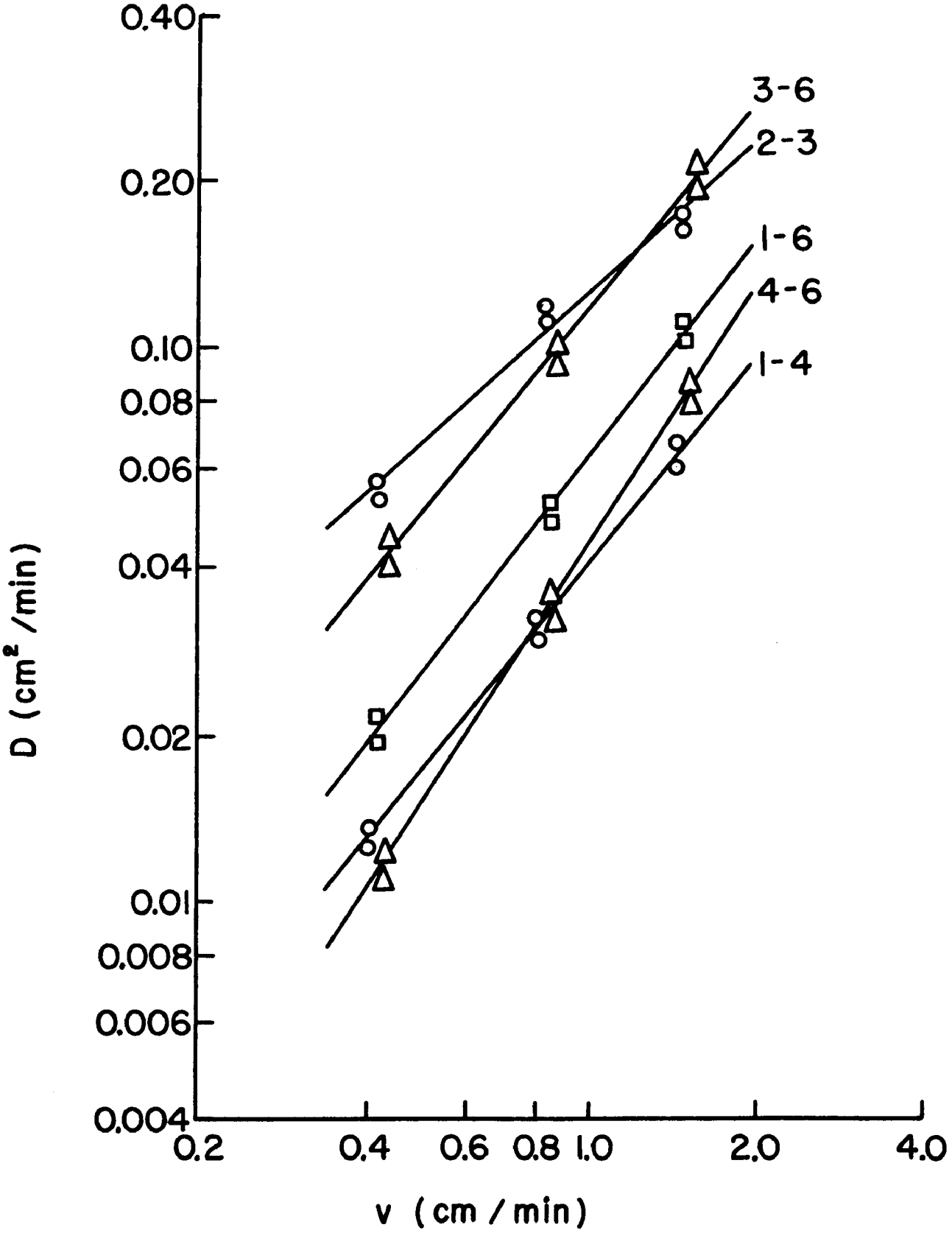


Figure 13c- Dispersion Coefficients Versus Velocity (First and Second Order Heterogeneity)

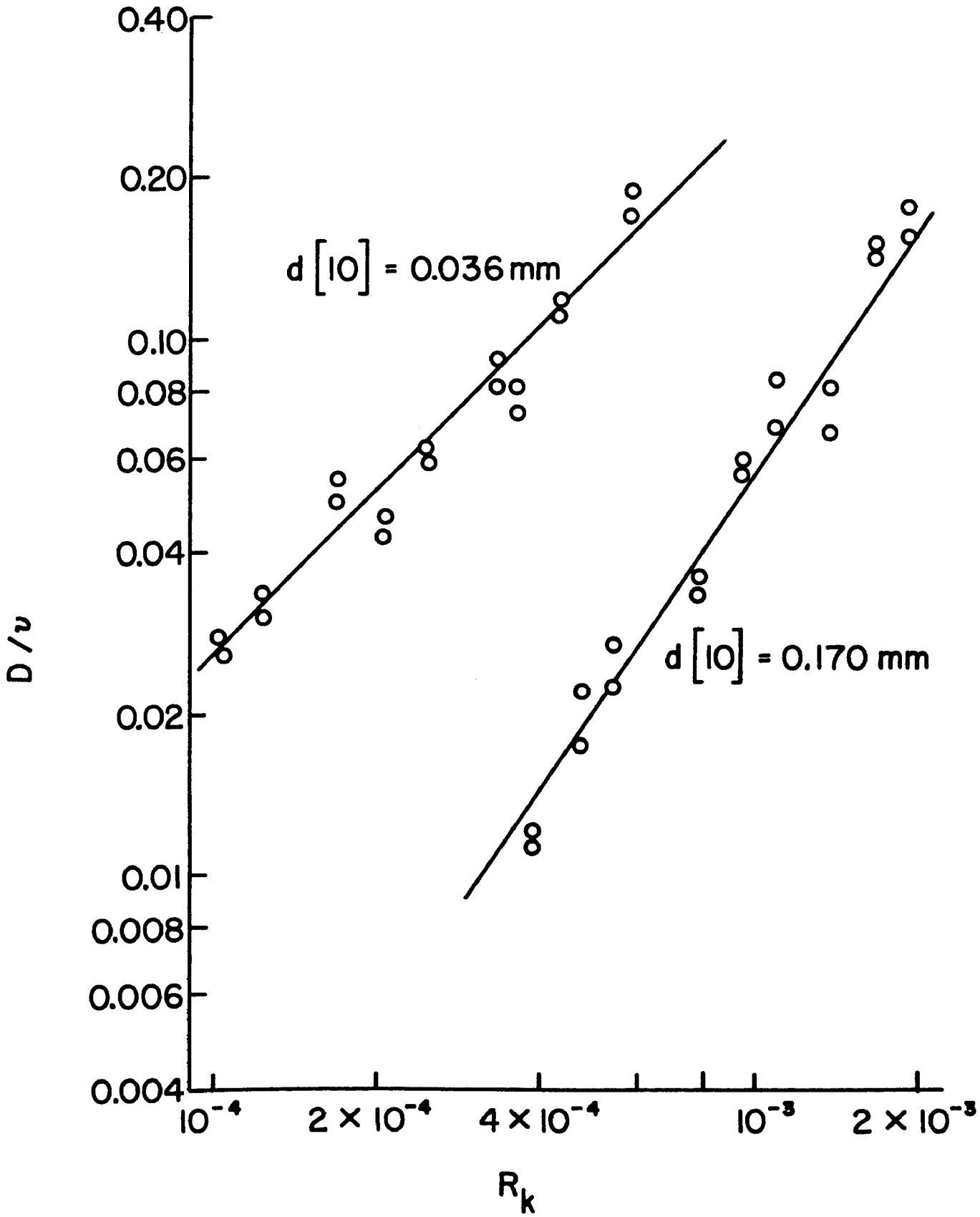


Figure 14 - D/ν vs $R_k$ (Homogeneous)

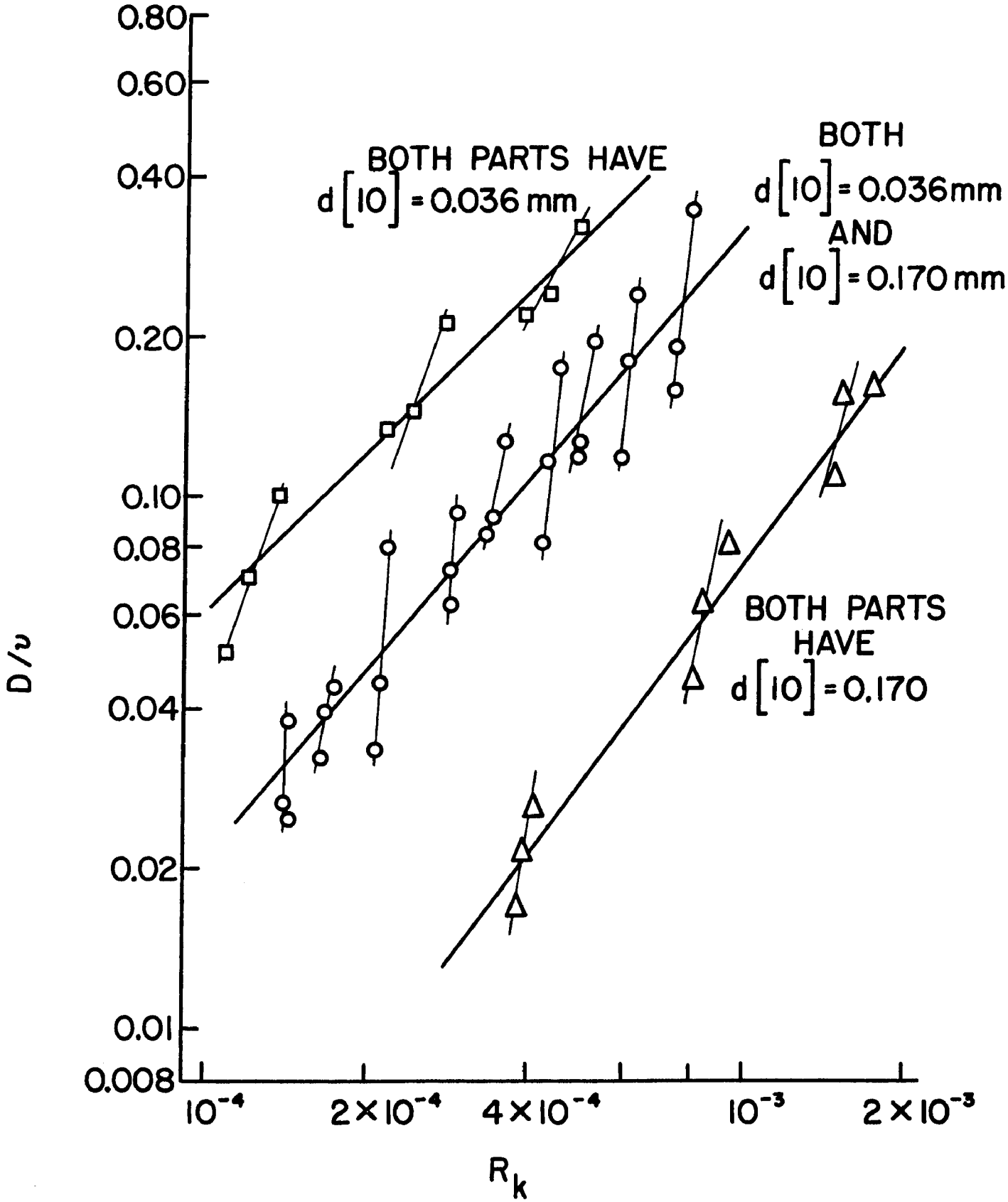


Figure 15 - D/ν vs $R_k$ (Heterogeneous)

The plots above show that not only does the dispersion coefficient vary with the level of permeability, but it does vary with the distribution of permeabilities as well as with the heterogeneity since the scatter is the outside experimental area. The magnitude of this difference suggests the existence of another factor influencing D and that we expect to be the distribution of beads sizes of permeabilities is given by the slope of the bead size distribution. To check if the slope was significant a statistical analysis of the data was performed.

Statistical analysis. The correlation developed tested was of the form

$$D = f(S, k, v, d) \tag{66}$$

An analysis of variance was performed on all the homogeneous nonuniform media data to determine which main factors and which interactions were significant. Then a regression analysis was performed to arrive at an expression for the correlation. Although a linear model of the type

$$D = bo + b_1 S + B_2 k + B_3 v + b_4 d \tag{67}$$

was investigated, greater success was achieved with a logarithmic model. This is not surprising, since the correlations compared earlier are of logarithmic form. An analysis of the variables showed that the following five variables affect the dispersion: log k, log S, log V, d, log k x log V.

The fact that d remained in the equation indicates that there is a significant effect due to the packing technique used in constructing the porous media. The regression equation derived from the analysis for the up direction is

$$D = .18 \frac{Sv^{(.7 + .54\ lvgk)}}{k^{.07}} \tag{68}$$

For the down direction the coefficient .18 becomes .2. Thus although the effect due to d is significant, it is very small. A plot of equation (68) and the data is shown in Figure 16. Thus, the slope (that is) nonuniformity is definitely affecting the value of dispersion and the scatter of Figures 14 and 15 is due to nonuniformity effects. It is also interesting to note that log permeability and log velocity gives a covariant type of effect. Again, we would expect something like this from the statistical model results of Haring and Greenkorn[18]. As with Pleshek's data, the reciprocity does not seem to hold.

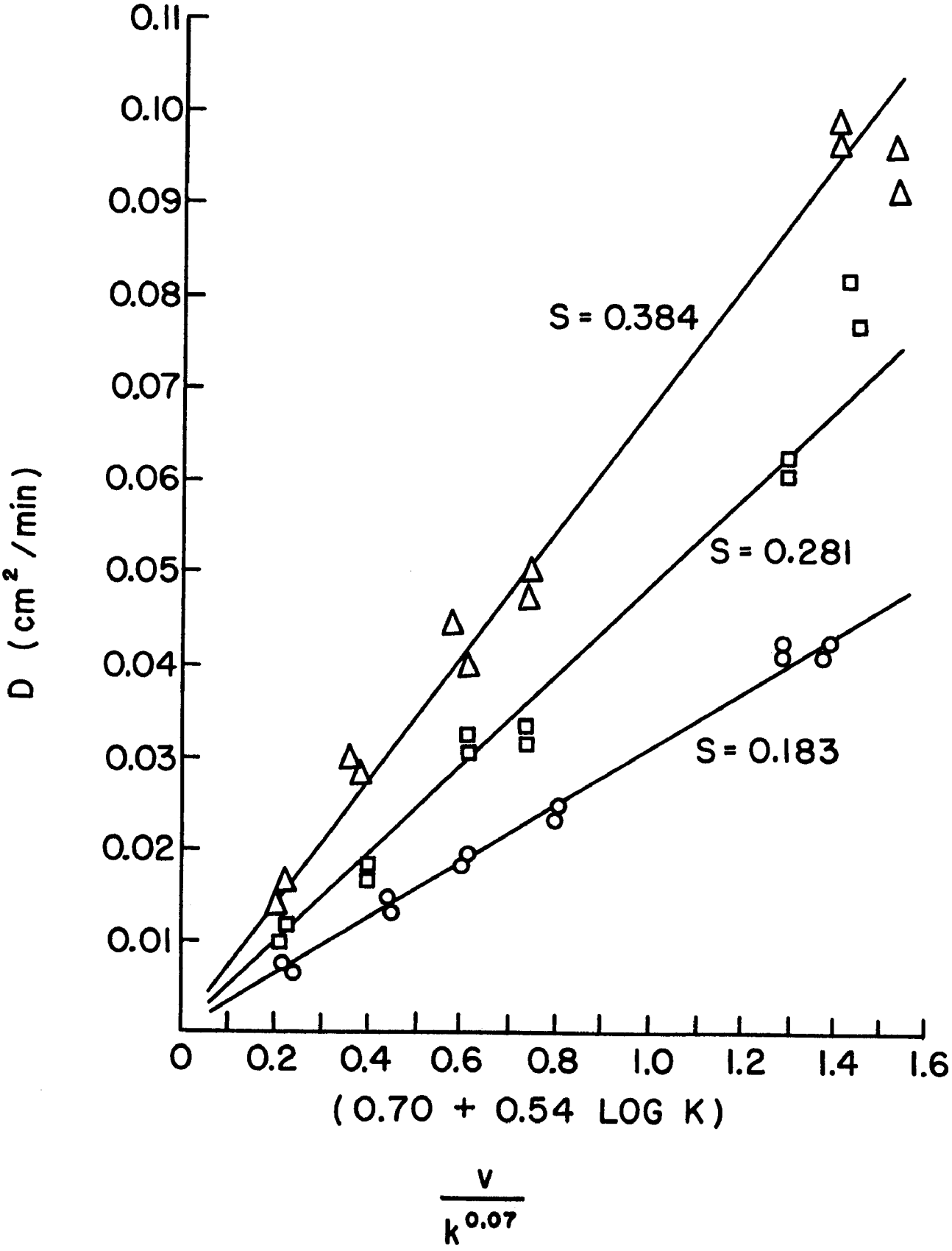


Figure 16 - D vs $\frac{v}{k}$ for Various S

## AN EXPLORATORY STUDY OF PERMEABILITY AND DISPERSION PHENOMENA IN ANISOTROPIC POROUS MEDIA[27]

Experimental Procedures. The model used is an octagonal "box" made of plexiglas and packed with alternating layers of glass beads as shown in Figure 17. The medium was made anisotropic by using glass beads of two different sizes, 590-840 μ and 105-149 μ. The anisotropy is built into the model by packing the two sizes of beads into six alternate vertical layers. A 1/2 inch hole was drilled into each lateral face of the model to permit fluid flow through the eight corresponding directions. The model had a removable plexiglas lid to allow easy packing of the beads. After packing, a rubber gasket was inserted. between the lid and the level of beads in the model, and the gasket was subjected through a hole in the center of the lid to a constant water pressure of 8 lb./in.$^2$ gauge in order to insure a tight bead pack and to minimize channeling of the fluid.

The model was packed by slowly pouring beads into their separate compartments while the model was constantly being vibrated by a mechanical oscillator. As each section was filled, the aluminum dividers were slowly removed, but a metal screen remained in place in the beads. The last packing of the beads were carefully added until the model was completely packed. Vibration was stopped immediately to prevent the possibility of the small beads sifting into the larger beads through the openings in the separation screens.

All tubing used in the experiments was 1/4 inch polyflow tubing with appropriate fittings. Other equipment consisted of a polyethylene bottle used as a constant head tank; a 0-30 lb/in.$^2$ pressure gauge to measure the pressure on the diaphragm; a simple manometer; a flow conductivity cell; and a 0.25 mv Brown-mull balancing recorder.

Porosity. The porosity of the model was determined by the displacement method. The model was weighed dry, filled with water and weighed again. The volume of the void space was determined from the weight of entrapped water. The liquid used in all experiments was distilled water which had been filtered and deaerated. In the case of the porosity measurements a small amount of detergent was added to the water to give better wetting properties and a few drops of red food coloring were added to the water to aid in visual detection of entrapped air pockets.

The model was dried by forcing hot air through the eight different directions, care being taken that the air rate was very low so that there would be no shifting of the bed. The porosity was determined as .348 and the error is estimated as + 1.1%.

Permeability. The permeability measurements were performed in a manner similar to that used by Darcy in his original experiment. The

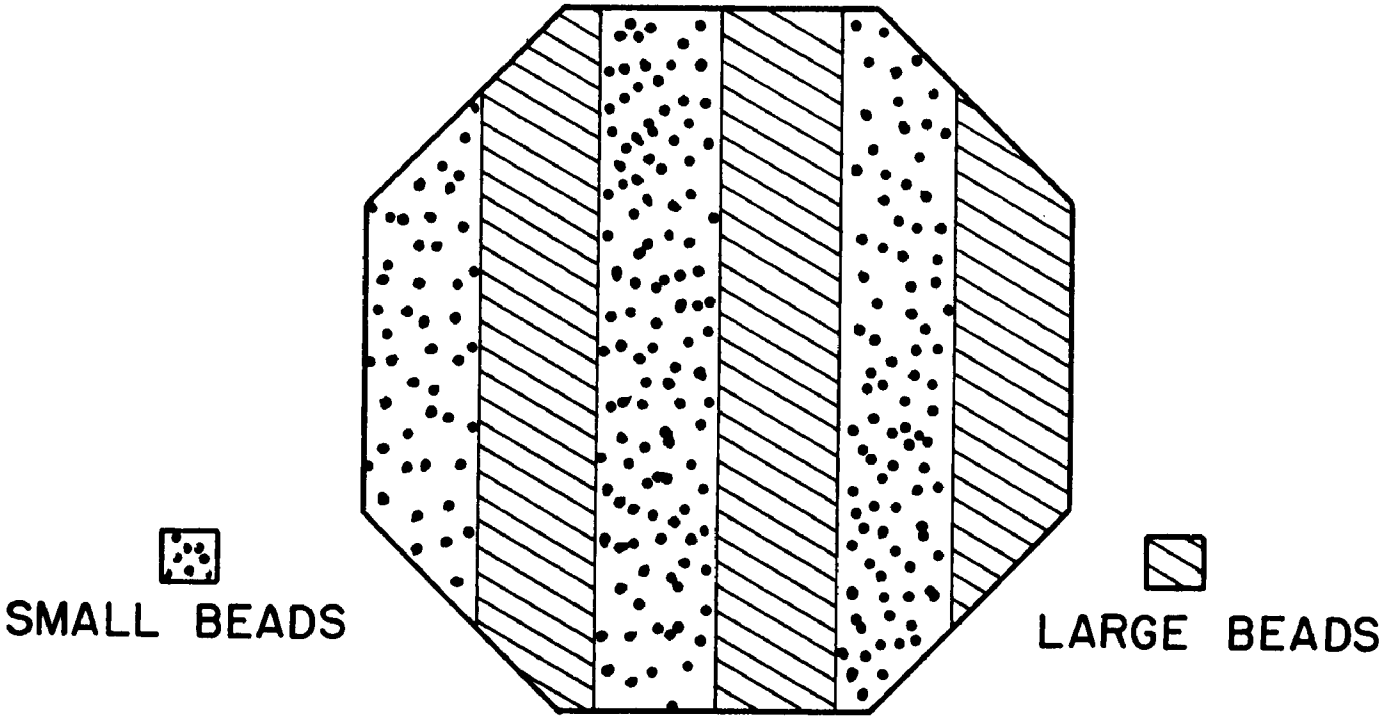


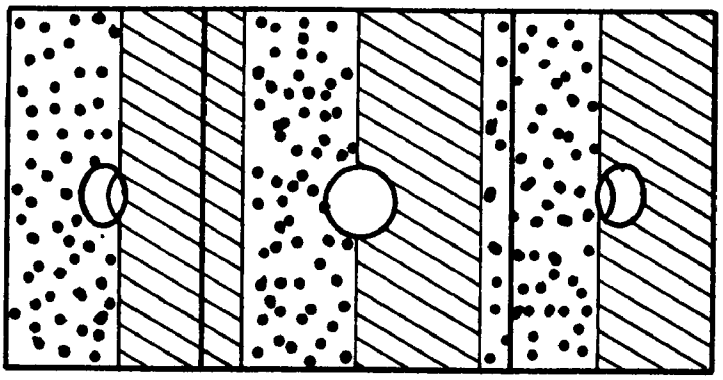

Figure 17 - Model Sketch (Double Figure)

model was placed in a vertical position with flow of distilled water provided by a variable level constant head tank. (See Figure 18 for experimental setup). After passing through the model, the water was collected in a graduated cylinder for a known period of time to determine the volumetric flow rate and the pressure drop was read from the simple manometer with one leg connected to each side of the model. The permeabilities were calculated according to Darcy's Law, Equation (37), expressed in terms of the measurable quantities. In this case, A was taken to be the area of the opening covered by the screen in each face of the model. This is the area over which the fluid pressure is distributed at the time the fluid is entering the porous medium. The laboratory was maintained at a constant temperature of 77°, so the viscosity and density of the fluids did not change during the experiment. The independent variables, therefore, in Equation (37) are Q and $\Delta h$. These are the quantities measured in each direction and in each experiment.

Dispersion. The dispersion experiments were conducted with the same equipment as was used for measuring permeability. A breakout curve was determined for each experiment at a given flow rate in a given direction, by using either a .005 molar or .02 molar solution of KCl as a displacing fluid. If the weak KCl solution was used as a tracer for the first experiment, the stronger solution was used in the second experiment, so that the two solutions were used alternatively as tracers throughout the series of experiments. The concentration was measured with a conductivity cell which was recorded on a strip chart showing the change in concentration of the effluent. The breakthrough curves for each experiment were determined from the recorder charts. In order to avoid any possible gravity effects, the experiments were always run such that the dense solution flowed from bottom to top of the model.

Sequence of Experiments. The porosity measurements were conducted first, and the permeability and tracer breakthrough experiments were run simultaneously. The flow rate and pressure drop needed for the permeability calculation were recorded during the time in which the KCl solutions were displacing one another in the model. It was assumed throughout these experiments that the density and viscosity properties of the KCl solutions were essentially the same as of water.

A total of 48 experiments was run. Three separate flow rates, 10, 15, and 22 cc/min. were run for each of the eight directions and each run was made in duplicate to provide a basis for an error estimate. This design of experiments led itself to a straightforward analysis of variance which determine the effects of flow rate and direction on the permeability and dispersion coefficients.

## Results and Discussion

Permeability. Measurements are shown in Table 6. A simple analysis of the variance was performed on these data, with results indicating

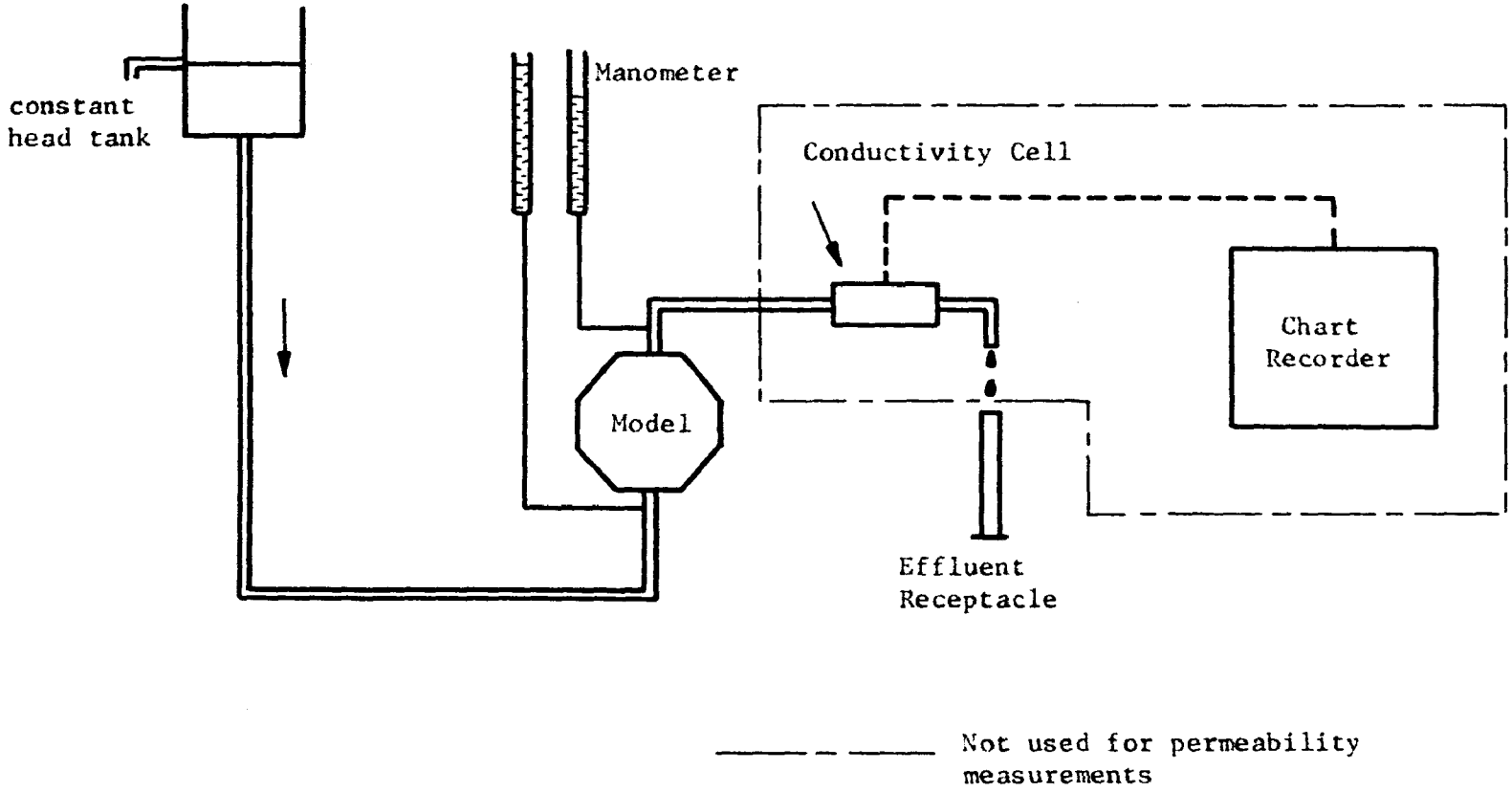


Figure 18 - Sketch of Apparatus

Table 6. Permeabilities

| | Flow rate (cc/min) | k (darcies) | Flow rate (cc/min) | k (darcies) | Flow rate (cc/min) | k (darcies) |
|---|---|---|---|---|---|---|
| Direction 1 | 9.8 | 1442 | 14.1 | 1400 | 20.75 | 1440 |
| | 9.8 | 1640 | 15.3 | 1651 | 21.0 | 1700 |
| Direction 2 | 9.33 | 907 | 15.33 | 920 | 20.33 | 851 |
| | 9.84 | 898 | 15.1 | 941 | 19.2 | 942 |
| Direction 3 | 9.5 | 178 | 14.3 | 170 | 20.33 | 175 |
| | 9.43 | 172 | 14.6 | 169 | 20.9 | 174 |
| Direction 4 | 10.5 | 945 | 16.2 | 1016 | 20.0 | 1014 |
| | 9.33 | 1030 | 14.67 | 914 | 20.3 | 1005 |
| Direction 5 | 9.2 | 1540 | 14.5 | 1530 | 21.8 | 1527 |
| | 9.5 | 1626 | 14.2 | 1533 | 20.8 | 1509 |
| Direction 6 | 10.3 | 1000 | 14.85 | 955 | 20.5 | 1002 |
| | 10.41 | 1058 | 15.8 | 1097 | 21.0 | 1052 |
| Direction 7 | 9.8 | 266 | 15.0 | 214 | 20.1 | 196 |
| | 10.1 | 196 | 15.5 | 202 | 20.5 | 196 |
| Direction 8 | 10.4 | 1011 | 13.6 | 1140 | 20.3 | 1050 |
| | 9.6 | 1110 | 15.73 | 1008 | 19.5 | 1078 |

a highly significant effect due to direction but no evidence of an effect on permeability due to flow rate or due to an interaction between the flow rate and direction.

The magnitudes of the permeabilities contained in the octagonal model are considerably higher than those values obtained for similar sized beads in linear models. This is due to the assumption of the area in the calculation of the permeability estimates. However, the results are reproducable and relative values have meaning.

It should be noted in Table 6 that the permeabilities in opposite flow directions -- for example, directions 4 and 8 -- are not identical. A possible explanation for this lack of symmetry is that the fluid sees different possible paths for flow as it enters the model. If the fluid enters in direction 4 (see Figure 17) it encounters initially a layer of small beads, whereas the fluid entering in direction 8 encounters a layer of large beads which offers less resistance to flow. These paths of greater and lesser resistances are presumed to be the reason for lack of agreement between the permeabilities measured in opposite directions although in general the difference between opposite direction permeabilities is not large.

The permeability data obtained from the octagonal model was tested according to the theory of directional permeability as shown earlier. For the particular geometry of the model used here, one should use the second case where the velocity is not parallel to the pressure gradient; thus,

$$k''_n = k_{11} \cos^2\alpha + k_{22} \cos^2\beta \tag{69}$$

If the reciprocal of the square root of each permeability is plotted against its corresponding direction, an ellipse should be obtained. In Figure 19 this curve has been plotted and it resembles an ellipse, although it is not symmetric for the reasons discussed above. The results indicated, as expected, that the flow rate vector is not in the same direction as the pressure gradient.

Dispersion. Two separate methods of calculating $C/C_o$ were used in order to obtain similar curves for those experiments in which the weak KCl solution was used as the tracer and in the experiments where the stronger KCl solution was used as the tracer. The breakthrough curves corresponding to the directions of highest permeability are the steepest and those corresponding to the directions of lowest permeability are the flattest. The dimensionless concentrations approached 1 after about 1-1/2 to 2 pore volumes for experiments in all directions except the directions 1 and 5 (those with the highest permeability). In those directions the breakthrough curves do not approach 1 until 3 or 4 pore volumes of fluid were discharged. For directions 1 and 5 the curve rises

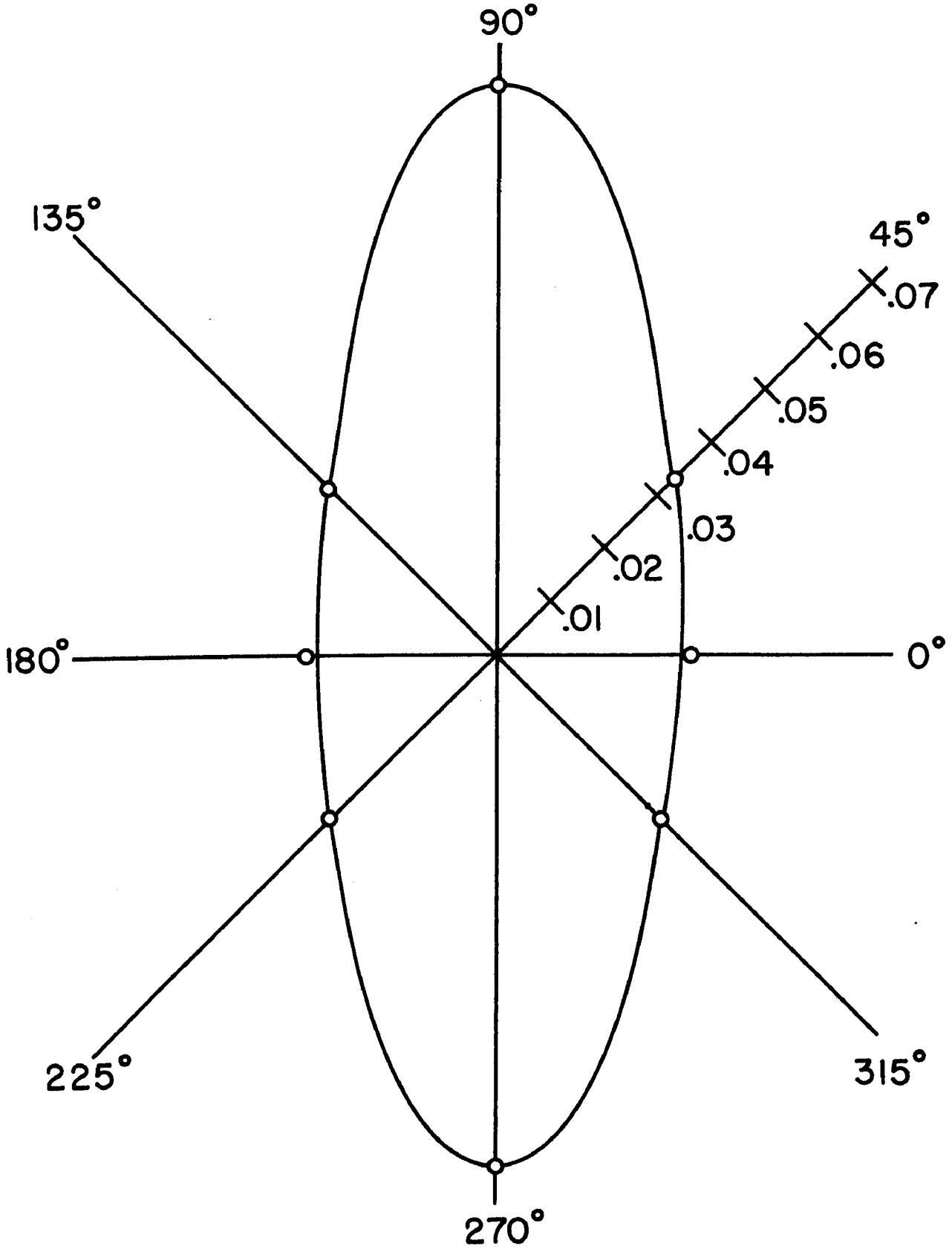


Figure 19 - $\frac{1}{\sqrt{k}}$ vs angle

rapidly at first and then levels off and rises very slowly. An explanation for this may be that tracer fluid travels rapidly through the layer of large beads until the curve reaches a value of .6 or .7. Then the fluid in the layers on either side of the large bead layer begins to be displaced. It is the displaced fluid from these adjacent layers which causes the curve to rise so slowly for the remainder of the experiment.

In order to compare the breakthrough curves with the permeability, we decided to calculate the dispersion coefficient in the normal fashion for a linear porous medium using Equation (4). Although these data would not correctly describe the exact mixing in this type of model, they are an approximation and also we should be able to compare the relative values in such a way that we can determine whether or not there is a directional dependence on the dispersion and further, if this directional dependence has any relation to permeability. Thus calculating the dispersion by Equation (4) is shown in Table 7 as a function of flow rate and direction. An analysis of variance of these data shows the effects of both direction and flow rate are highly significant and that the interaction between flow rate and direction is slightly significant.

Since dispersion is a tensor it is assumed that it appears in the flux equation in a form analogous to the appearance of the permeability tensor K in Darcy's law. Therefore with the boundary conditions for the octagonal model we plotted the reciprocal of the square root of the dispersion coefficient versus direction and as a function of velocity. Figure (20) is a plot of this data. A comparison of Figures (19) and (20) shows that the principal directions of these two ellipses correlate but are oriented 90° apart from each other. This indicates the dispersion coefficient increases in the direction of decreasing permeability. It is interesting to note that the two ellipses are geometrically similar; the ratio of the major permeability axis to the minor axis is 1.3 and the ratio for the dispersion ellipse is 1.38. This fact indicates the anisotropy of the model effects permeabilities and dispersion coefficients to a similar extent. The fact that the major directions are orthogonal is disturbing since we would assume that the dispersion would increase directly with permeability according to the correlations of Harleman *et al*[4].

Table 7. Dispersion Coefficients

| | Flow rate (cc/min) | D (x $10^3$) ($cm^2$/sec) | Flow rate (cc/min) | D (x $10^3$) $cm^2$/sec) | Flow rate (cc/min) | D (x $10^3$) ($cm^2$/sec) |
|---|---|---|---|---|---|---|
| Direction 1 | 9.8 | 9.78 | 14.1 | 14.4 | 20.75 | 36.8 |
| | 9.8 | 7.12 | 15.3 | 19.4 | 21.0 | 21.1 |
| Direction 2 | 9.33 | 39.4 | 15.33 | 74.9 | 20.33 | 98.2 |
| | 9.84 | 25.5 | 15.1 | 76.4 | 19.2 | 70.0 |
| Direction 3 | 9.5 | 90.1 | 14.3 | 107 | 20.33 | 185 |
| | 9.43 | 57.2 | 14.6 | 241 | 20.9 | 283 |
| Direction 4 | 10.5 | 66.1 | 16.2 | 89.0 | 20.0 | 113 |
| | 9.33 | 34.3 | 14.67 | 80.0 | 20.3 | 118 |
| Direction 5 | 9.2 | 7.07 | 14.5 | 7.22 | 21.8 | 19.9 |
| | 9.5 | 8.22 | 14.2 | 8.21 | 20.8 | 20.9 |
| Direction 6 | 10.3 | 51.7 | 14.85 | 60.0 | 20.5 | 97.9 |
| | 10.41 | 38.7 | 15.8 | 78.0 | 21.0 | 129 |
| Direction 7 | 9.8 | 130 | 15.0 | 158 | 20.1 | 245 |
| | 10.1 | 95.0 | 15.5 | 202 | 20.5 | 251 |
| Direction 8 | 10.4 | 46.1 | 13.6 | 66.4 | 20.3 | 83.3 |
| | 9.6 | 46.7 | 15.73 | 81.4 | 19.5 | 107 |

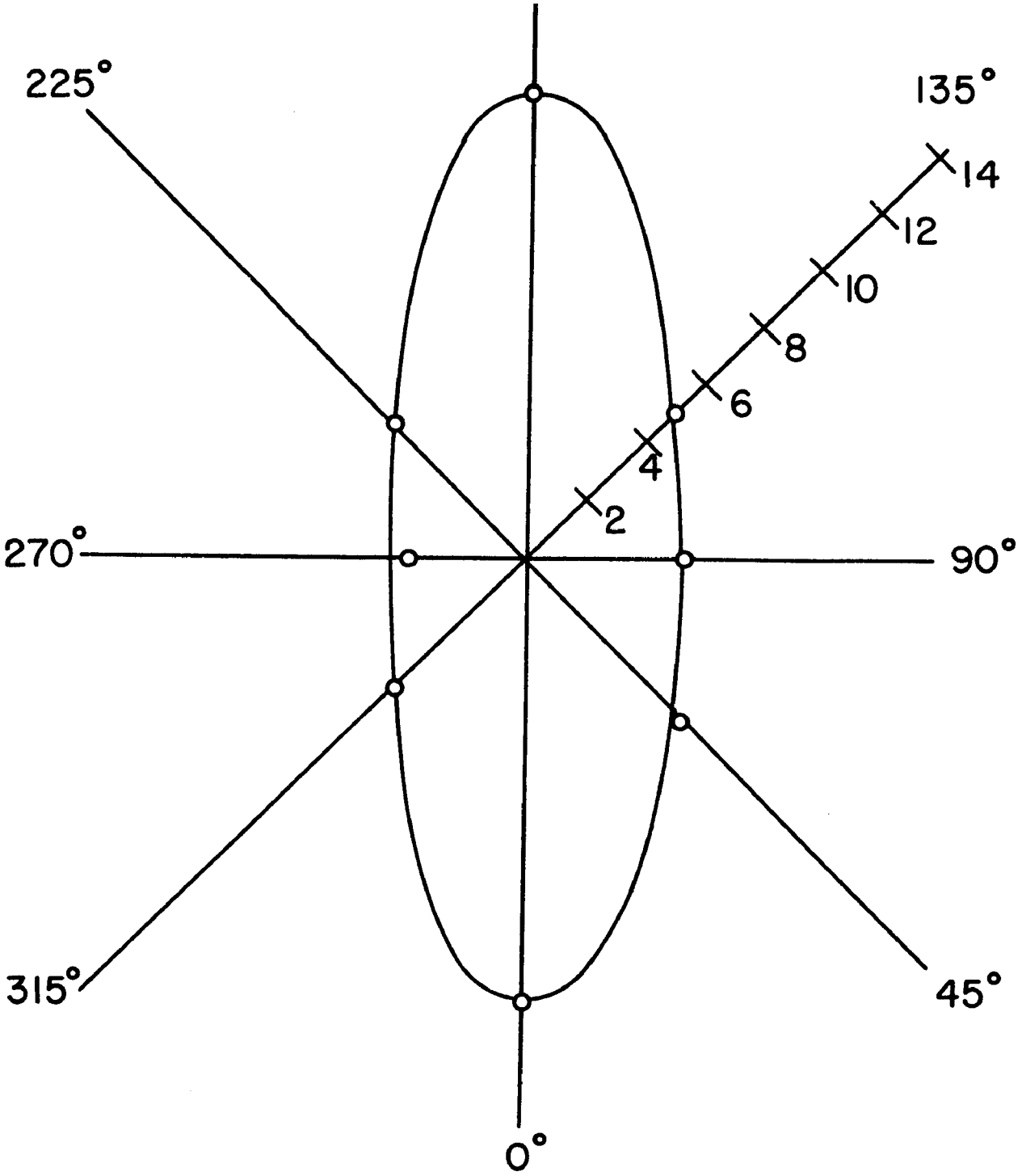


Figure 20 - $1/\sqrt{D}$ vs angle

## PERMEABILITY AND DISPERSION DURING FLOW IN LINEAR HETEROGENEOUS ANISOTROPIC POROUS MEDIA[28]

### Experimental Procedures

Figure 17 depicts the porous medium used by Lenth and Greenkorn[27]. The medium is made up of alternating 1-inch thick layers of large (590-840 μ) and small (105-149 μ) glass beads. The porous media models that would result from coring the medium in Figure 17 at 45° intervals represents the porous media modelled in this work. The result of this envisioned coring operation is shown in Figure 21. It can be see that, depending on flow directions through each medium, model 1 represents two angles (90° and 270°) of flow through the bed. Model 3 represents two angles (0, 180°). Because of the symmetry of Lenth's model, model 2 includes four angles (45, 135, 225, 315°). Figure 22 shows the details of the Lucite tube for making the models and the details of the packing arrangement.

In order to maintain heterogeneity of the beds the two sizes of beads were kept segregated by screens. Once the dividers were in place, the models were packed by adding beads slowly while the model was continuously vibrated on a Centron vibrating table. Beads were packed through the ends of the model where possible, or by small access holes on the side of the models.

Porosity. The liquid-saturation method was used to determine the porosity of the models. The models were weighed and then filled with distilled water which contained small amounts of food coloring and detergent (two to three drops per liter of water). The difference between the wet and dry weights, with corrections for fittings and entrance sections, allowed the void volume to be determined. When the tubes were filled initially with water almost no air was observed to be trapped on the inside tube wall. However, when repeated measurements were attempted by draining, drying, and refilling, air bubbles were visible on the tube walls. Therefore, the models were filled initially and maintained full of water. Before further measurements were made the food coloring and detergent were removed by flushing with several volumes of distilled water.

Permeability. The permeability measurements were made by forcing fluid, (.4 M KCl) through the porous media with a Ruska proportioning pump. Various constant flow rates were available from the positive displacement pump. The pressure drop was measured with a water manometer.

Permeability was determined at three fluid flow rates (130, 263, 453 cc/hr). The corresponding frontal velocities were about .9, 1.8, and 3.1 cm/min. Room temperature was held constant at 76°F during all runs; thus the fluid properties remained constant. The permeability was determined with Equation (37). Replicates were run at all flow rates in order to determine experimental error.

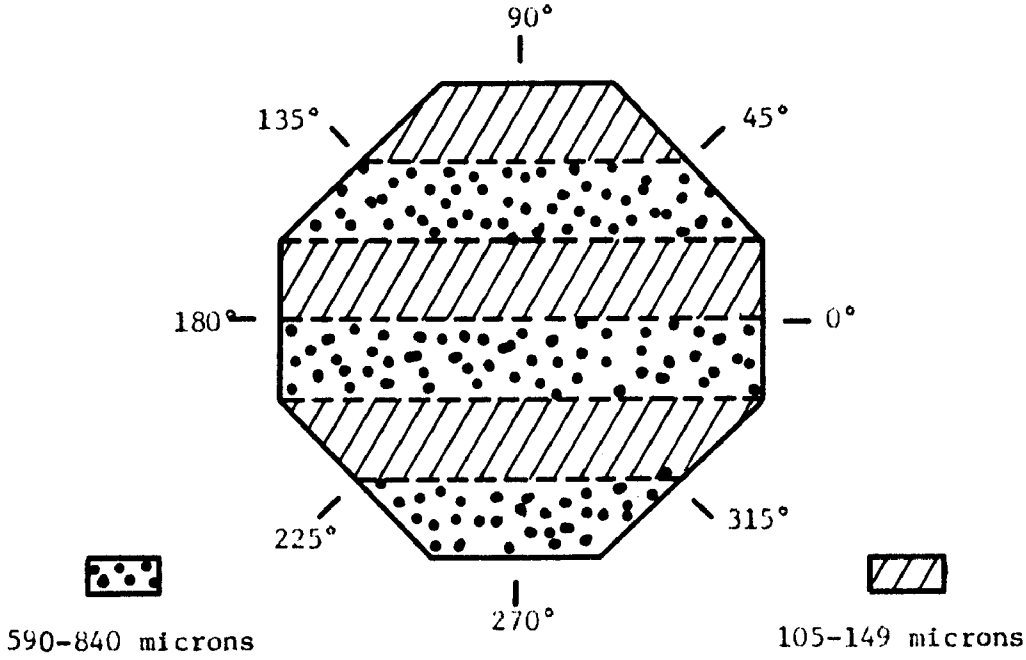


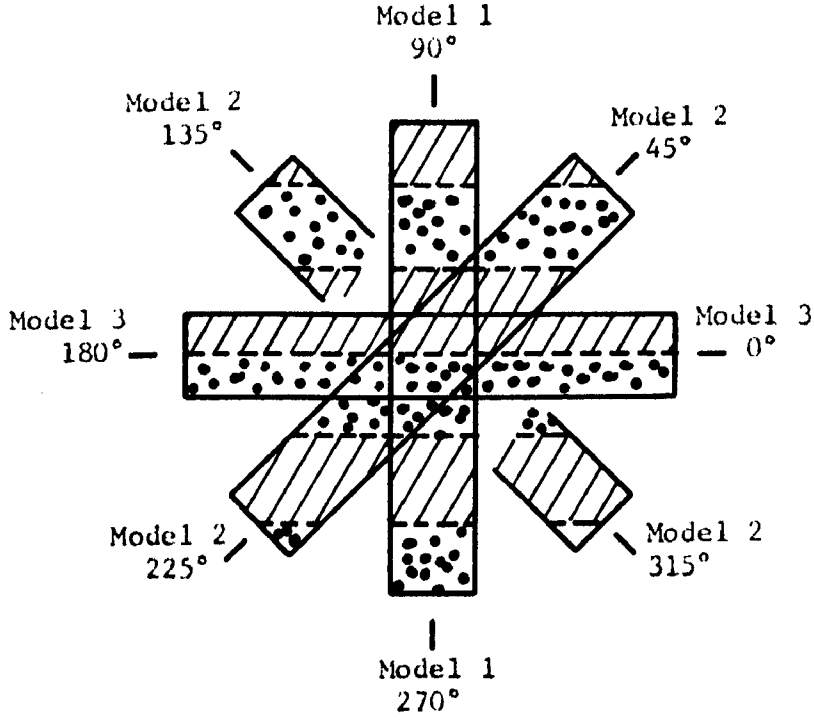


Figure 21 - Lenth Apparatus Cored at 45° Intervals

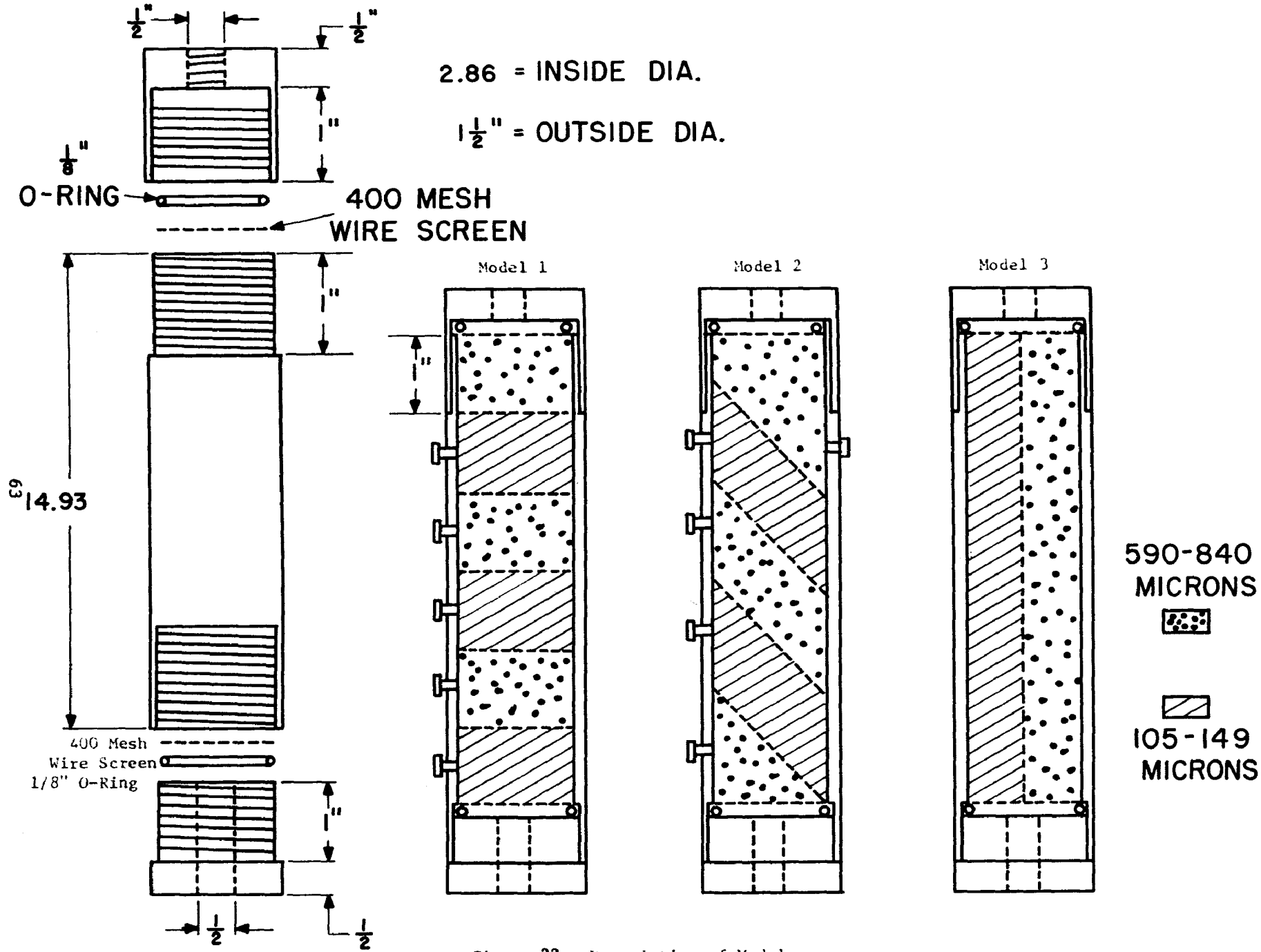


Figure 22 - Description of Models

Dispersion. Potassium chloride was used as a chemical tracer to determine the breakthrough curves for each porous medium. A silver-silver chloride electrode was used in conjunction with a Calomel reference electrode[23] was used to monitor chloride concentrations at the outlet of each model. The potential developed by the electrode system was monitored with a Sargeant SR balancing potentiometric recorder. The recorder range was 0-100 mv.

A .4 M KCl solution was used to displace a .02 molar KCl solution. The two solutions gave potential readings of about 3 and 74 mv respectively. When a run was completed, the model was backflushed with .02 M KCl solution in preparation for the next run. The models were positioned vertically and the .4 M solution was always introduced at the bottom of the tube. Figure 23 is a diagram of the equipment.

The data (time, millivolts, calibration equation, physical properties) were punched on computer cards. A CDC 6500 computer was used to determine the dispersion coefficients. The computer is programmed to first calculate dimensionless concentration with a space for $C_1$ as initial KCl concentration, $C_o$ as the tracer solution concentrations, and C is the KCl concentration of fluid leaving the model. About 16 data points were used for each dispersion run.

The dispersion coefficient was then determined by iteration with equation (12). The standard deviation between the data and the values were predicted by Equation (12) and calculated. Minimization of this quantity by least sequence was the basis for curve-fitting the data. The experimental and theoretical breakthrough curves were plotted automatically (See Figure 24 for an example).

Equation (13), the truncated form of Equation (12) was also used to calculate dispersion coefficients. In most runs the Peclet number was less than 133; therefore an error of greater than 5% was expected in dispersion coefficients calculated by Equation (13).

## Results and Discussion

Porosity. The porosities of the three models are 1 - .376, 2 - .372 and 3 - .388. The values vary only slightly from model to model, and the error in the porosity is estimated less than + .01.

Permeability. The permeability values determined as described by Pleshek and Greenkorn[22]. The permeability of models 1 and 3 were estimated as 10 and 62.5 Darcys respectively. Model 2 should fall between these two values. The permeabilities are summarized as a function of flow rate in Figure 25. The values given here are in good agreement with the predicted values, although they were slightly low. (This slight difference was due to the fact that the values of Pleshek contained silk-cloth containers at the end of the models and thus his values are just slightly low.)

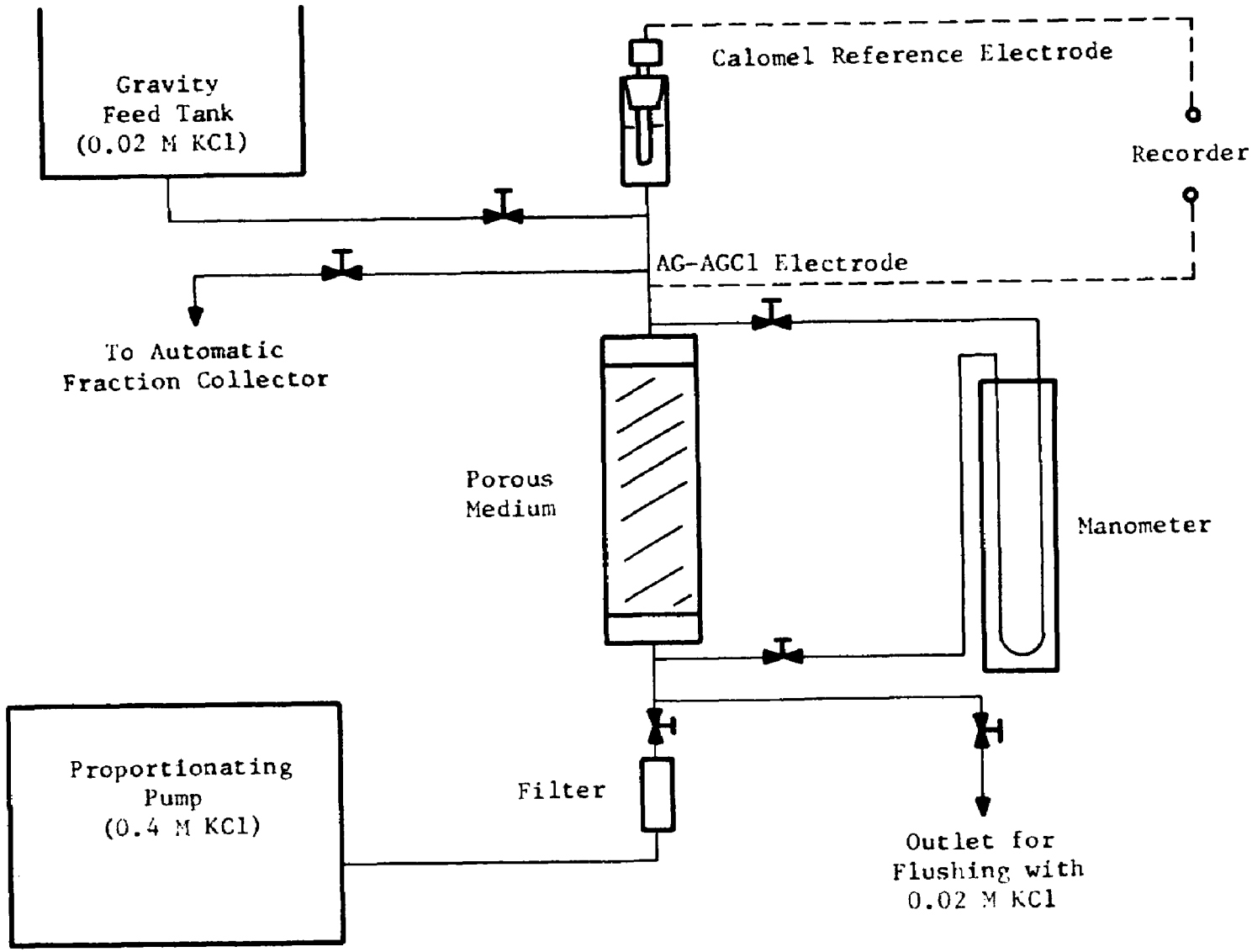


Figure 23 - Equipment Diagram

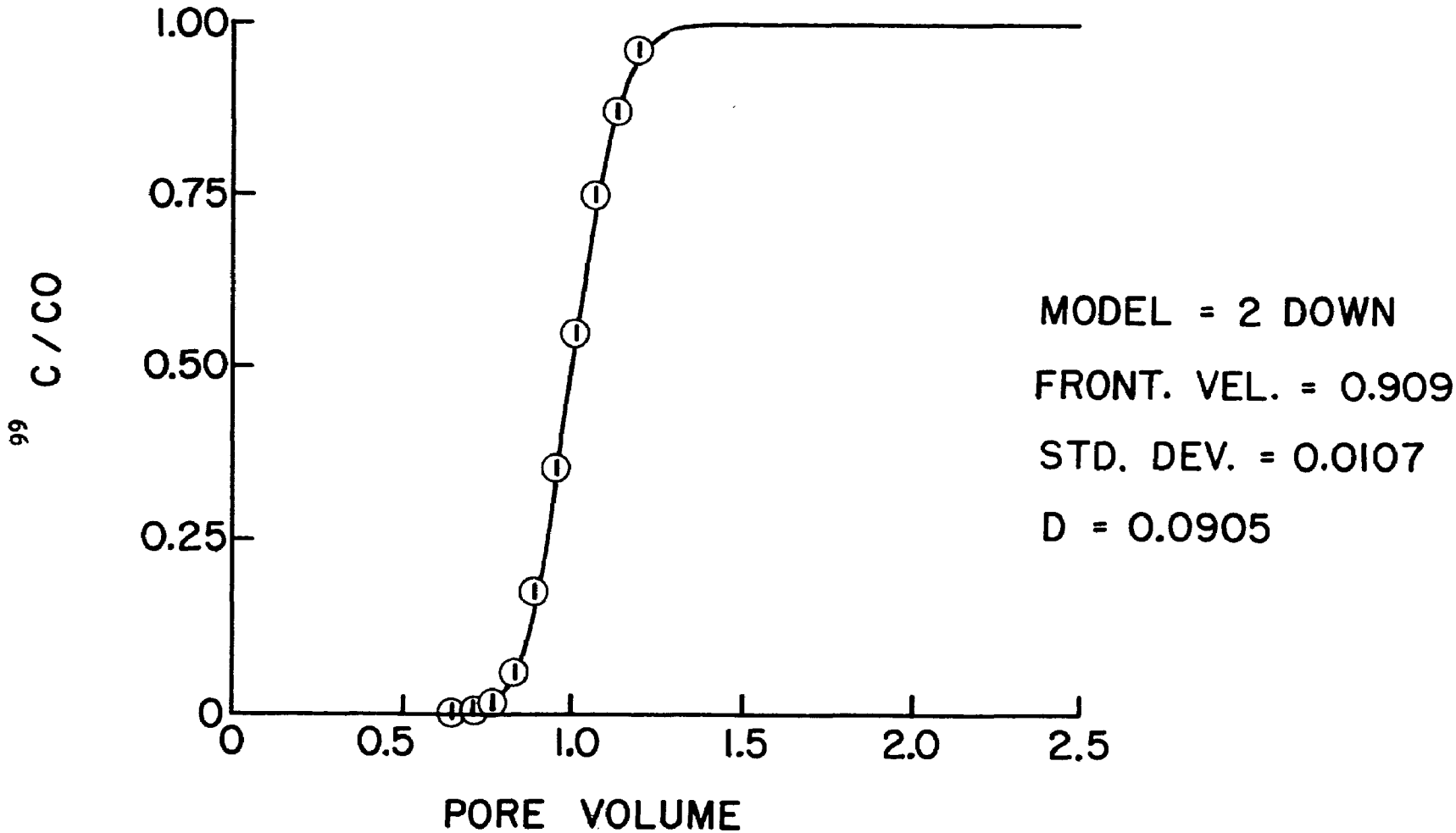


Figure 24 - Breakthrough Curve

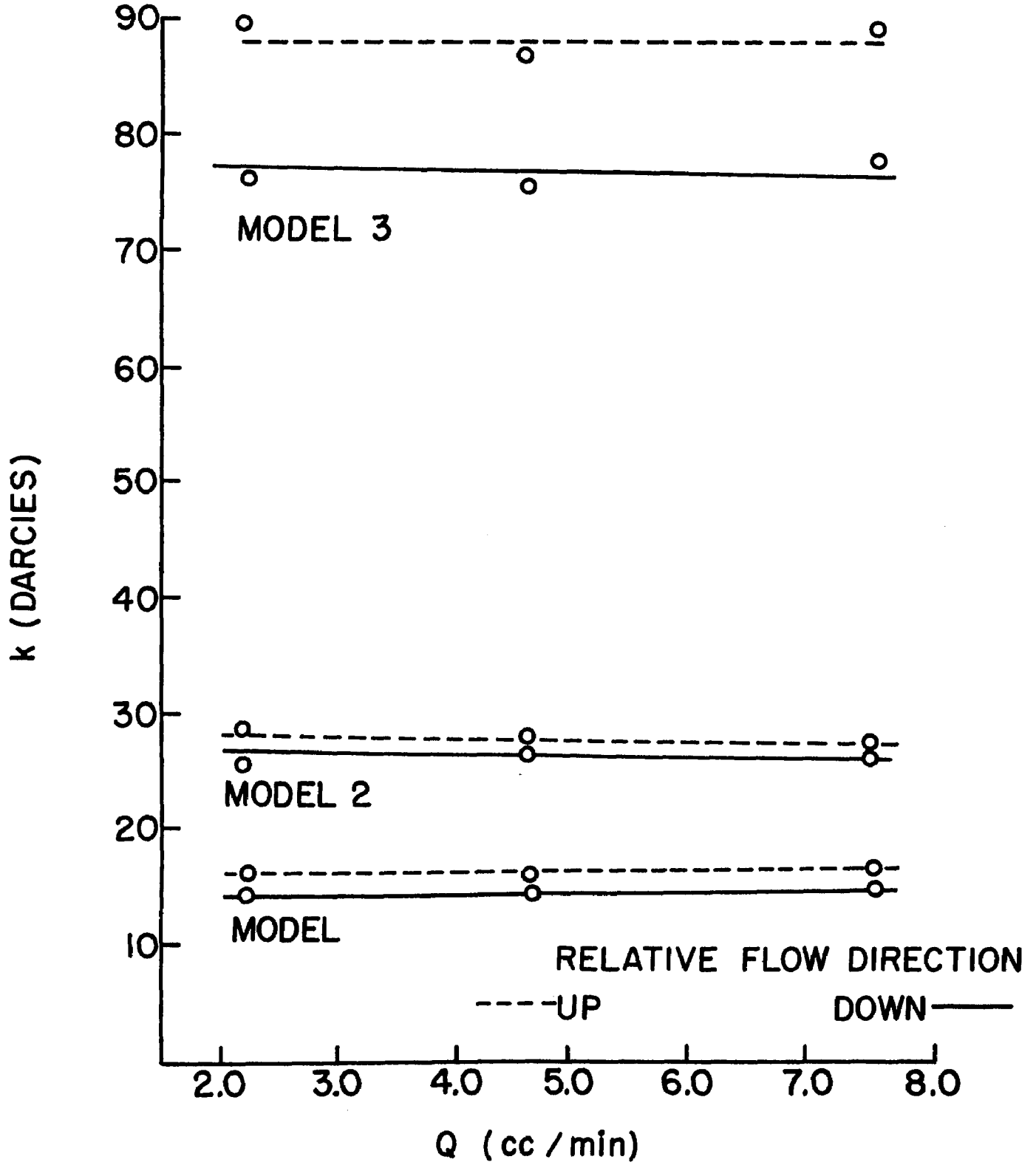


Figure 25 - Average Permeability Versus Flow Rate

An analysis of variance was performed to determine the effect of flow rate and flow direction on each tube. The mean squares for flow rate and direction for each tube were compared with the best estimate of the experimental error. It was found that the effect of flow rate was not significant for any of the models. However, reversing the direction of flow was significant in model 1 and highly significant in model 3. Flow direction reversal was not significant in model 2. The explanation of the symmetry of permeability in model 2 and the asymmetry in models 1 and 3 is not apparent. Evaluation of the packing procedure gives no indication that this result should be expected. Lenth and Greenkorn[27] found that in general permeabilities in opposite flow directions were not the same.

The data collected for permeability in this experiment are most closely represented by the first case of the tensor theory of permeability and thus one would expect the plot of the square root of permeability as a function of angle to give an ellipse. The results of such a plot for the data for these models are shown in Figure 26. The ellipse is a least squares fit determined by the method utilized by Greenkorn et al.[7]

Lenth and Greenkorn[27] choice of area term used in Darcy's Law resulted in much larger values of permeability than were found in this study. However, the directions and relative magnitudes of the major and minor axes of the permeability found in this work agree with the results of Lenth and Greenkorn.[27]

Dispersion. The dispersion coefficient was determined from Equation (12) by a least-squares curve fitting technique using the computer. The raw data were fed directly into the computer program and the best fit in dispersion coefficient was determined in this form.

The results of the dispersion coefficient calculations, standard deviations, and Peclet numbers are shown in Table 8. There was a slight shift in the breakout curves such that the value for $C/C_o$ to .5 did not always occur at one pore volume. In these cases a slight shift of the breakout curve was made to correct for a probable error in the porosity measurements.

The asymmetry that was observed in some of the curves in this study was considerably more than Equation (12) could predict. For the late portions of the breakthrough curve the $C/C_o$ measured was always below the theoretical value. This tail-off has been observed by others in studies of both homogeneous and heterogeneous porous media. As mentioned previously this tail-off has been attributed to dead-end pores in the media. The magnitude of the tail-off observed here is more than could be realistically attributed to dead-end pores. The tail-off in general gets more exaggerated as the fluid velocity increased. The least of this effect was seen in the volumes of the displaced fluid are left behind. In time, this trapped fluid with both diffuse out into the main stream and be displaced by a slow convective mixing which occurs in these semi-dead regions. The results was the tail-off or exaggerated

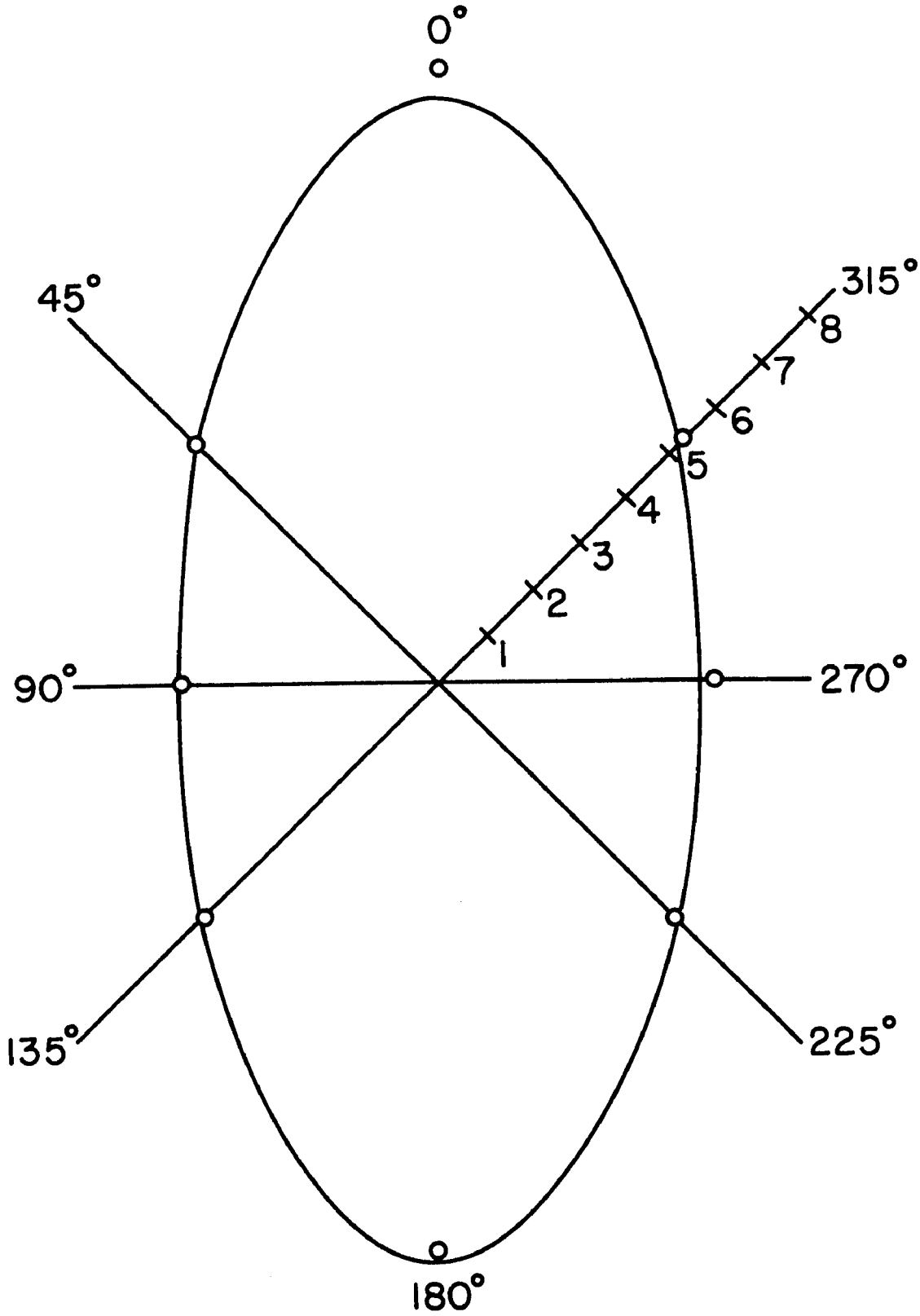


Figure 26 - $\sqrt{k}$ vs angle

Table 8. Dispersion Coefficients for Model with Screen Dividers

| Model-Position | Velocity (cm/min) | D ($cm^2$/min) Computer Least-Squares-Fit | By Slope Method | (Standard Dev.) from Dispersion Eq. | Peclet No. |
|---|---|---|---|---|---|
| 1-down | 3.128 | 0.9445 | 0.450 | 0.1169 | 49.44 |
| 1-down | 1.814 | 0.2412 | 0.194 | 0.0878 | 112.30 |
| 1-down | 0.899 | 0.0500 | 0.038 | 0.0729 | 268.58 |
| 1-up | 3.128 | 0.9174 | 0.645 | 0.0921 | 50.90 |
| 1-up | 1.814 | 0.3258 | 0.347 | 0.0853 | 83.15 |
| 1-up | 1.814 | 0.2810 | 0.281 | 0.0752 | 96.40 |
| 1-up | 0.899 | 0.0743 | 0.111 | 0.0520 | 180.75 |
| 2-up | 3.161 | 0.8251 | 0.822 | 0.1069 | 57.21 |
| 2-up | 1.834 | 0.4243 | 0.396 | 0.0798 | 64.53 |
| 2-up | 0.911 | 0.2152 | 0.170 | 0.0667 | 63.24 |
| 2-down | 3.161 | 1.1032 | 0.838 | 0.0921 | 42.78 |
| 2-down | 3.161 | 1.6597 | 1.77 | 0.0633 | 28.44 |
| 2-down | 1.834 | 0.7336 | 0.865 | 0.0728 | 37.32 |
| 2-down | 0.909 | 0.0905 | 0.108 | 0.0107 | 149.91 |
| 3-down | 3.031 | 1.3428 | 0.957 | 0.0375 | 33.70 |
| 3-down | 1.758 | 0.8336 | 0.912 | 0.0588 | 31.49 |
| 3-down | 0.871 | 0.6446 | 0.423 | 0.1194 | 20.18 |
| 3-up | 3.031 | 2.3489 | 1.50 | 0.0959 | 19.26 |
| 3-up | 3.031 | 1.8228 | 2.08 | 0.0625 | 24.83 |
| 3-up | 1.758 | 0.8519 | 1.07 | 0.0826 | 30.82 |
| 3-up | 1.758 | 0.8434 | 1.07 | 0.0470 | 31.13 |
| 3-up | 0.871 | 0.3939 | 0.294 | 0.0707 | 33.02 |

asymmetry observed in this work.

The flow in the model 2 is envisioned to look as in Figure 27 with the flow taking the path of least resistance. For an elemental volume of fluid, this path consists of the longest possible time spend in the high permeability sections and the shortest time spend in the low permeability sections. A stream line directly along the wall represents the highest resistance path available for the flow in the tube that is, the longest possible path in the low permeabilities and the shortest path through the high permeabilities. This gives rise to "semi-dead" regions near the wall in each section of the medium especially in model 2. The areas outside of the depicted flow path in Figure 27 show these slow displacement regions. Again, the result is the asymmetric concentration distributions observed.

The majority of the flow model 3 will take place through the high permeability section with a ratio of frontal velocities ($V_1$ to $V_2$) equal to the ratio of permeabilities of two sections, about 25 to 1. Assuming no cross-flow between sections, when the tracer front has traversed the length of the tube in the high permeability section, it will have gone about 1/25th of the model 1 (90°), with slightly more tail-off appearing in model 2 (45°) and more yet in model 3 (0°).

The breakthrough curves obtained in this work and in Lenth and Greenkorn[27] appear to be inherent in this approach to anisotropic porous media, for example, packed beds layered at various angles. The diffusion model with one parameter, D, simply will not predict the observed asymmetry. The two bead sizes used here have permeabilities of 120 and 5 Darcys ($k_1 : k_2 = 25$). As the degree of heterogeneity decreases, the degree of asymmetry decreases and at some point nearing a homogeneous bed ($k_1 : k_2 = 1$). The application of the diffusion model to dispersion would describe the observed concentration distribution satisfactorily.

In addition, in model 1 the five circular dividers between the bead sections probably caused a slight restriction at each divider, thus causing an orifice effect in the data as shown in Figure 27.

The results of the computer calculations of dispersion coefficients were tested against the correlations described previously.

The correlation expressed by Equation (29) was tested. The equations for the data are:

1) $D/\nu = 6.7 \times 10^5 \, R_k^{2.14}$ (70)

2) $D/\nu = 2.5 \times 10^6 \, R_k^{3.5}$ (71)

3) $D/\nu = 1.0 \times 10^3 \, R_k^{1.26}$ (72)

Model 3 is in reasonably good agreement with previous workers for the same reasons discussed above. Models 2 and 3 have greater intercepts

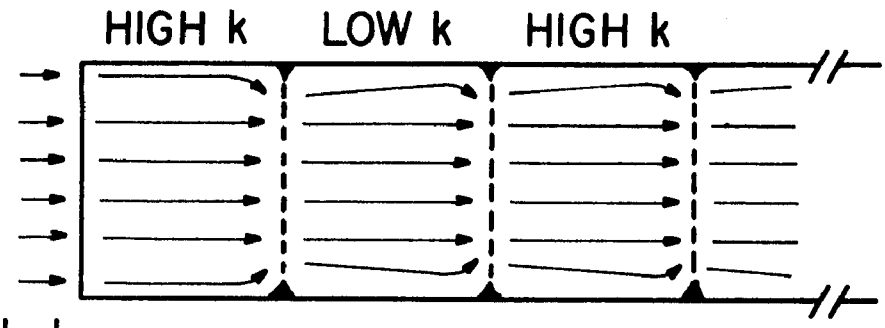


a. MODEL 1

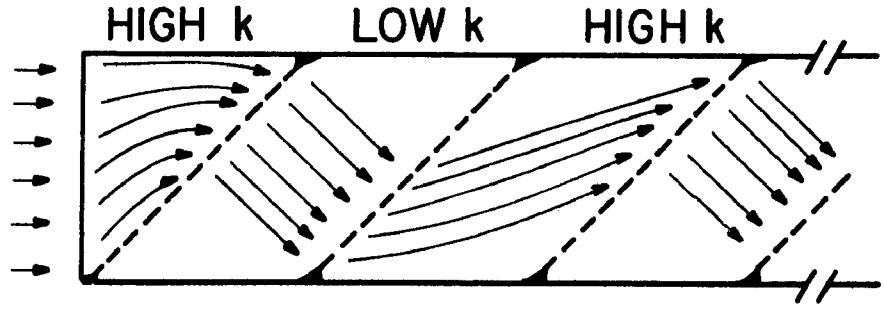


b. MODEL 2

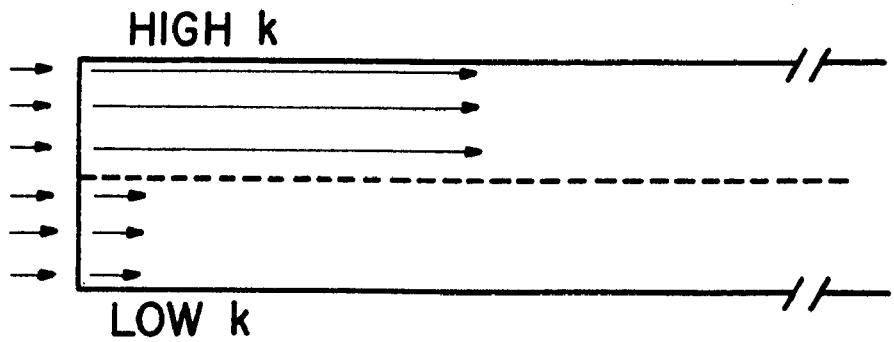


c. MODEL 3

Figure 27 - Flow Pattern in Model

and exponents.

We realize that the correlations used for comparison above were not necessarily intended for extension to porous media of the type used in this study. The comparison was meant to indicate the results to be expected when these correlations are applied to heterogeneous, anisotropic porous media. It is acknowledged that the observed dispersion would decrease to values predictable by the correlations of previous workers as the degree of heterogeneity decreases to approach a homogeneous system.

The correlations developed in this study may be used to predict dispersion in heterogeneous anisotropic porous media with the realization that only one ratio of section to section permeability was investigated (25 to 1).

In testing the tensorial properties of dispersion Lenth and Greenkorn[27] found for the octagonal model that $1/\sqrt{D}$ plotted against direction yielded an ellipse. This form ($1/\sqrt{k}$ vs. direction) which Lenth and Greenkorn used for permeability. The axes for dispersion and permeability were found to be 90° apart.

In this study the square root of the measured dispersion coefficient is plotted against the packing angle for all flow rates studied and is shown in Figure 28. Ellipses shown were calculated by least-squares fit. Since the dispersion increases with velocity, the ellipses of course get larger as the velocity increases. The major and minor axes of the dispersion coincide with the axes of permeability, Figure 26.

The ratio of major to minor axes ($\lambda_1/\lambda_2$) for the ellipses in Figure 28 are 4.83, 2.10, 1.40 as velocity change from 2.17 cc/min to 4.38 to 7.55. The ratio is roughly inversely proportional to flow rate. The equation relating $\lambda_1/\lambda_2$ to flow rate is

$$\frac{\lambda_1}{\lambda_2} = T\,\frac{1}{Q} \tag{73}$$

where T is a constant of about 10. These results indicate that the anisotropy would not appear in these models at a flow rate of about 10 cc/min., and that $\sqrt{D}$ versus packing yield angle should yield a circle. It should be noted that 10 cc/min. would give a Reynolds number of .65, which should still be in the Darcy flow regime. It is interesting to note that as we increase the flow rate more, the ratio of major to minor axes reverses, and we do get the major and minor axes not in the same direction as the permeability ellipse such as reported by Lenth and Greenkorn[27]. Please note, this statement is based on an extrapolation of the data with Equation (73).

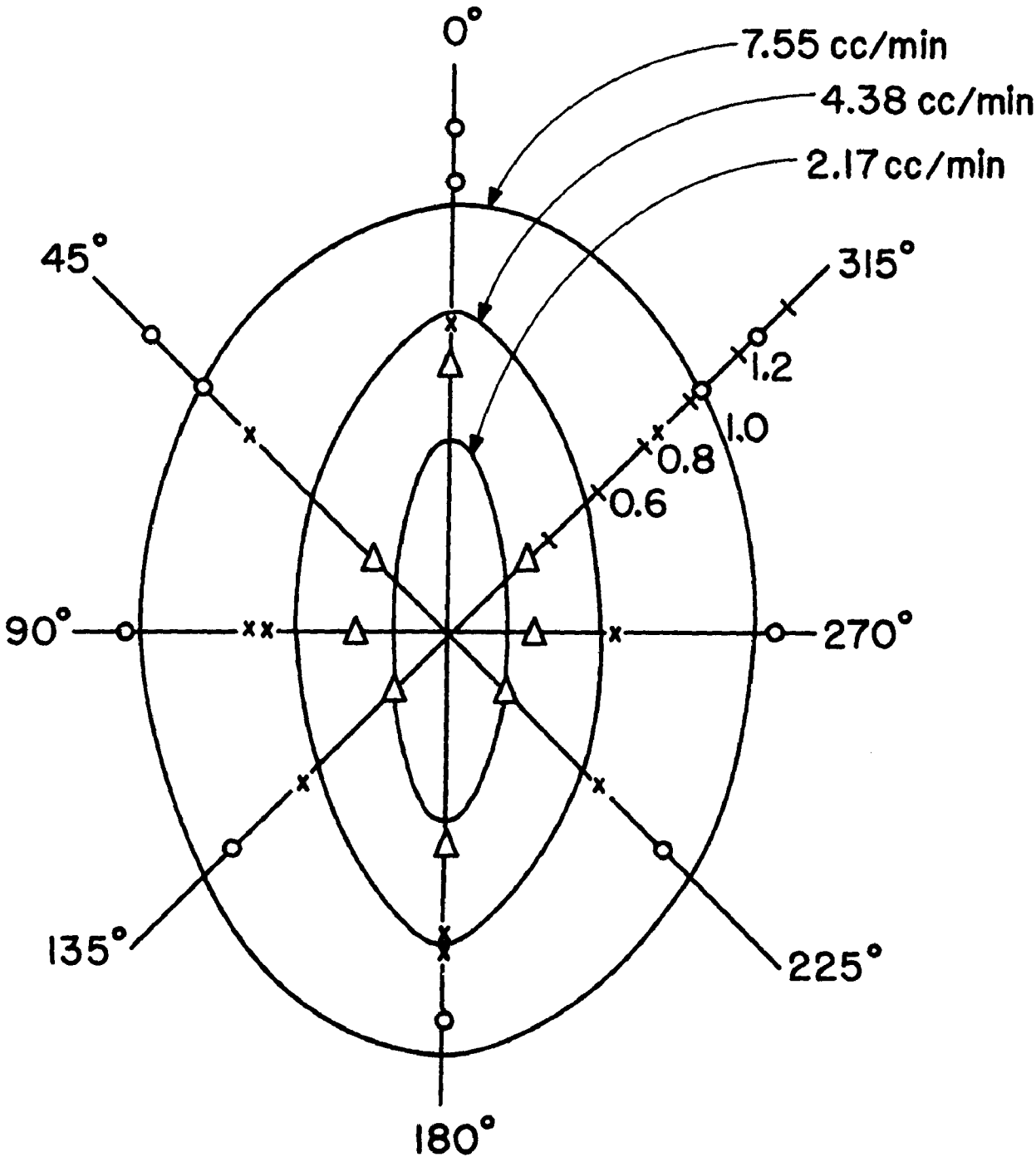


Figure 28 - $\sqrt{D}$ vs angle

## REFERENCES


1. Perkins, T. K., and Johnston, O. C., "A Review of Diffusion and Dispersion in Porous Media," Pet. Trans. AIME 228, SPEJ 70 (1963).

2. Chung, S. F., and Wen, C. Y., "Longitudinal Dispersion of Liquid Flowing Through Fixed and Fluidized Beds," AIChE J 14, 857 (1968).

3. Greenkorn, R. A., and Kessler, D. P., "Dispersion in Heterogeneous Nonuniform Anisotropic Porous Media," Ind. Eng. Chem. 61 #9, 14 (1969).

4. Harleman, D. R. F., Melhorn, P. F., and Rumer, Jr., R. R., "Dispersion-Permeability Correlation in Porous Media," J. Hydraul. Div.: Proc. Am. Soc. Civil Eng. 89 HY2, 67 (1963).

5. Shamir, V. Y., and Harleman, D. R. F., "Dispersion in Liquid Porous Media," J. Hydraul Div. : Proc. Am. Soc. Civ. Eng. HY5, 237 (1967).

6. Schiedegger, A. E., "Directional Permeability of Porous Media to Homogeneous Fluids," Geofis Pura Appl. 28, 75 (1954).

7. Greenkorn,R. A., Johnson, C. R., and Shallenberger, L. K., "Directional Permeability of Heterogeneous Anisotropic Porous Media," Pet. Trans. AIME 231, SPEJ 124 (1964).

8. Schiedegger, A. E., "Physics of Flow Through Porous Media," MacMillan New York (1957).

9. Whitaker, S., "Diffusion and Dispersion in Porous Media," AIChE J. 13, 420 (1967).

10. Ramondi, P., Gardner, G. H. F., and Petrick, C. B., "Effect of Pore Structure and Molecular Diffusion on the Mixing of Miscible Liquids Flowing in Porous Media," Reprint 43 AIChE-SPE Joint Symposium, San Francisco (December, 1959).

11. Rifai, M. N. E., Kaufman, W. J., and Todd, D. K., "Dispersion Phenomena in Laminar Flow through Porous Media," Report #3, Sanitary Engineering Research Laboratory, Univ. of California, Berkeley, (July, 1956).

12. Ogata, A., and Banks, R., "A Solution to the Differential Equation of Longitudinal Dispersion in Porous Media," U. S. Geologie Survey Prof. Paper 411-A, U. S. Govt. Post Office, Washington (1961).

13. Harleman, D. R. F., and Rumer, R. R., "Longitudinal and Latual Dispersion in an Isotropic Porous Medium," J. Fld. Mech. 16 #3, 385 (1963).

14. DeJosselin DeJong, G., and Bossen, M. S., "Discussion of paper

by Jacob Bear, on the Tensor Form of Dispersion in Porous Media," J. Geophys. Res. 66 (10), 3623 (1961).

15. Bachmat, Y., and Bear, J., "The General Equations of Hydrodynamic Dispersion in Homogeneous, Isotropic, Porous Mediums," J. Geophys. Res. 69 (12), 2561 (1964).

16. Patel, R. D., and Greenkorn, R. A., "On Dispersion in Laminar Flow Through Porous Media," AIChE J. 16, 332 (1970).

17. Poreh, M., "The Dispersivity Tensor in Isotropic and Anisotropic Porous Mediums," J. Geophys. Res. 70 (16), 3609 (1965).

18. Haring, R. E., and Greenkorn, R. A., "A Statistical Model of a Porous Medium With Nonuniform Pores," AIChE J. 16 477, (1970).

19. Whitaker, S., "The Equations of Motion in Porous Media," Chem. Eng. Sci. 21, 291 (1966).

20. Greenkorn, R. A., and Kessler, D. P., "A Statistical Model for Flow in Nonuniform Anisotropic Porous Media," Proc. ASCE-EMD Specialty Conference on Probablistic Concepts and Methods, (November, 1969).

21. Guin, J. A., Kessler, D. P., and Greenkorn, R. A., "On the Permeability Tensor for Anisotropic Nonuniform Porous Media," Submitted to Chem. Eng. Sci. May, (1970).

22. Pleshek, R. C., and Greenkorn, R. A., "Dispersion During Flow in Linear Heterogeneous Porous Media," To be submitted to Water Resources Res. (1970).

23. Koonce, K. T., and Blackwell, R. J., "Single-Probe Method for Measuring Cl-Concentration in a Flowing Fluid," Private Commonwealth (1967).

24. Shoemaker, D. P., and Garland, C. W., "Experiments in Physical Chemistry," McGraw-Hill (1962).

25. Niemann, E. H., Greenkorn, R. A., and Eckert, R. E., "Dispersion During Flow in Nonuniform, Heterogeneous Porous Media," To be submitted to Water Resources Res. (1970).

26. Coats, K. H., and Smith, B. D., "Dead-End Pore Volume and Dispersion in Porous Media," Pet Trans AIME 231, SPEJ 73 (1964).

27. Lenth, E. G., and Greenkorn, R. A., "An Exploratory Study of Permeability and Dispersion Phenomena in Anisotropic Porous Media," To be submitted to Water Resources Res. (1970).

28. Goad, T. L., and Greenkorn, R. A., "Permeability and Dispersion During Flow in Linear Heterogeneous Anisotropic Porous Media," To be submitted to Water Resources Res. (1970).

## ACKNOWLEDGMENT

The support for this project was provided by the Federal Water Pollution Control Administration. However a large amount of supplementary work was directly or indirectly supported by the Petroleum Research Fund of the American Chemical Society, the Purdue Research Foundation, the National Science Foundation, and the Esso Production Research Company. Special thanks is due to these organizations for their help.

## APPENDIX 1 - Summary of Dispersion in Heterogeneous Nonuniform Anisotropic Porous Media[3]

This is a state-of-the-art review of dispersion in real porous media to examine present knowledge and to indicate research directions.

We limited the discussion to macroscopic mixing caused by uneven cocurrent laminar flow exemplified by flow of petroleum in reservoirs, movement of fresh water and waste fluids in aquifers, and flow of fluids in fixed beds. Countercurrent gas-liquid, liquid-liquid, and fluidized systems are not considered. Further, the discussion is directed at dispersion in nonideal media.

We do not pretend to be exhaustive in this review - rather, we attempt to cover selected papers which illustrate the major directions of research. The interested reader can find more material in the bibliography than can be given fair treatment within the scope of this paper.

We start with definitions of dispersion and of the three nonidealities, heterogeneity, nonuniformity, and anisotropy. After a brief general introduction, we consider statistical models of dispersion, continuum models of dispersion, and data which apply to systems containing nonidealities.

In general, the most effort for real media seems to be in the continuum theories. There is relatively less on the statistical models reported, and meager amounts of data are interpreted in nonideal media.

If one accepts the form of Equation 31, the effect of heterogeneity can be incorporated by defining $D_{ik}$ as a function of position. Any useful predicted results will probably have to be made using numerical techniques for solving Equation 31.

The effect of nonuniformity is incorporated in the form of dispersion tensor and is summarized in terms of the ratio of the longitudinal to transverse dispersion coefficients for one-dimensional flow in Table 9.

These models and the data can be made to agree, except in the case of Whitaker's results which seem to show that for the assumptions made to get to a comparable result we must assume the medium to be uniform. Otherwise, the form of the ratio from Whitaker is a complex function of several tensors.

Table 9. Ratio of Longitudinal to Transverse Dispersion Coefficients Effect of Nonuniformity

Experimental data

$$3 \leq \frac{D_L}{D_T} \leq f$$

Statistical model

Haring and Greenkorn

$$\frac{D_L}{D_T} = \frac{4}{95} \ln \left[\frac{27(a + b + 2)^2}{2(a + 1)\ J^2} \frac{vT}{\langle l \rangle}\right]$$

Continuum models

Nikolaevskii

$$\frac{D_L}{D_T} = \frac{\lambda_1}{\lambda_2}$$

Bear, Scheidegger, de Josselin de Jong

$$\frac{D_L}{D_T} = \frac{A_I}{A_{II}}$$

Bachmat and Bear

$$\frac{D_L}{D_T} = \frac{\lambda + 2\mu}{\lambda}$$

Poreh

$$\frac{D_L}{D_T} = \frac{\alpha_1 + (\alpha_2 + \alpha_3) \frac{|^2 v_1{}^2}{D_0^2}}{\alpha_1 + \alpha_2 \frac{|^2 v l^2}{D_0{}^2}}$$

Whitaker

$$\frac{D_L}{D_T} = 3$$

To attack anisotropy, we need more experimental data, extension of the statistical model for this case, and further investigation of the forms of the dispersion tensor. Empirically, it is appealing to adopt Bachmat and Bear's model of the tensor and find $\lambda$ and $\mu$ as functions of angle.

There are three major questions to be answered after we get a meaningful amount of data and interpretation for nonideal system.

(1) What is the "correct" model for flow in porous media in the sense of giving sufficient accuracy? Do we need anything in addition to curve fitting using the normal distribution (error function) of Equation 2 and empirical corrections to it?

(2) Can one characterize a porous medium with a reasonable number of parameters - i.e., at what level do heterogeneity, nonuniformity, and anisotropy become important?

(3) What is the limiting step in our analysis of the problem: the mathematical model, the computing techniques, or the experimental data?

## APPENDIX 2 - Summary of

## On Dispersion in Laminar Flow Through Porous Media[16]

Dispersion of a tracer in fluid flow through a porous medium has been extensively studied. The present communication seeks to relate the recent work of Whitaker[9] to the traditional treatment of the dispersion equation. Some anomalies in Whitaker's results are revealed and discussed.

1. Whitaker's analysis of dispersion in porous media results in an equation identical to the usual dispersion equation.

2. For anisotropic media, the dispersion tensor is related to the fluid velocity through a tensor of third order as well as one of fourth order. For isotropic materials, only the fourth-order tensor is to be retained. However, Whitaker's analysis indicates (contrary to previous work) that this fourth-order tensor has only one distinct component for such isotropic media.

3. Whitaker's analysis leads to predicting that the longitudinal dispersion coefficient is three times the value of the transverse dispersion coefficient for uniform flow in isotropic materials.

## APPENDIX 3 - Summary of

## A Statistical Model of a Porous Medium with Nonuniform Pores[18]

A random network model of a porous medium with nonuniform pores has been constructed. Nonuniformity is achieved by assigning two-parameter distributions to pore radius and pore length. Statistical derivations result in expressions for bulk model properties which are consistent with known empirical behavior of porous media such as capillary pressure, hydraulic permeability, and longitudinal and transverse dispersion. A series of experiments is suggested whereby the parameters of porous media structure may be determined from observed macroscopic behavior by using the expressions developed in this paper.

A statistical model of a porous medium with nonuniform pores has been constructed which matches experimental capillary pressure, permeability, and dispersion data. Several interesting properties are predicted from such a model. As one might expect, saturation is a function of capillary pressure and the parameters of flow radius distribution. The permeability-porosity ratio is a function of the average radius squared and the pore radius distribution. Thus, the permeability-porosity ratio causes dissipation due to entrance-exit effects. The dispersion coefficient is dependent on the parameters of both the pore radius and length distribution. Therefore, one would expect dispersion to change as a function of nonuniformity of the medium, even though the average resistance and tortuosity are constant. Furthermore, given a pore length distribution, the tortuosity is constant. Finally, for a nonuniform medium, a particle following the most probable path is transported through the medium at a velocity different from the Darcy velocity by a factor which is a function of the flow radius distribution.